

Remarks on non-invertible symmetries on a tensor product Hilbert space in 1+1 dimensions

Kansei Inamura^{1,2,*}

¹*Mathematical Institute, University of Oxford,
Andrew Wiles Building, Woodstock Road, Oxford, OX2 6GG, UK*
²*Rudolf Peierls Centre for Theoretical Physics,
University of Oxford, Parks Road, Oxford, OX1 3PU, UK*

We propose an index of non-invertible symmetry operators in 1+1 dimensions and discuss its relation to the realizability of non-invertible symmetries on the tensor product of finite dimensional on-site Hilbert spaces on the lattice. Our index generalizes the Gross-Nesme-Vogts-Werner index of invertible symmetry operators represented by quantum cellular automata (QCAs). Assuming that all fusion channels of symmetry operators have the same index, we show that the fusion rules of finitely many symmetry operators on a tensor product Hilbert space can agree, up to QCAs, only with those of weakly integral fusion categories. We also discuss an attempt to establish an index theory for non-invertible symmetries within the framework of tensor networks. To this end, we first propose a general class of matrix product operators (MPOs) that describe non-invertible symmetries on a tensor product Hilbert space. These MPOs, which we refer to as topological injective MPOs, include all invertible symmetries, non-anomalous fusion category symmetries, and the Kramers-Wannier symmetries for finite abelian groups. For topological injective MPOs, we construct the defect Hilbert spaces and the corresponding sequential quantum circuit representations. We also show that all fusion channels of topological injective MPOs have the same index if there exist fusion and splitting tensors that satisfy appropriate conditions. The existence of such fusion and splitting tensors has not been proven in general, although we construct them explicitly for all examples of topological injective MPOs listed above.

CONTENTS

I. Introduction	2
A. Physical assumptions	4
II. Non-invertible symmetries without mixing with QCAs	6
A. Left and right dimensions	6
B. Exact fusion rules imply integrality	8
III. Non-invertible symmetries mixed with QCAs	9
A. Lattice quantum dimension and index	9
B. Homogeneity of the index	11
C. Homogeneity of the index implies weak integrality	12
D. A comment on the case without tensor product decomposition	13
IV. Tensor network formulation of non-invertible symmetries	15
A. Preliminaries	16

* kansei.inamura@physics.ox.ac.uk

B. Definitions	17
1. General case	18
2. Example: invertible symmetries	20
C. Topological injective MPOs	21
D. Defect Hilbert spaces and movement operators	24
E. Relation to sequential quantum circuits	27
F. Properties of dimensions	31
 V. Sufficient conditions for the homogeneity of the index	 33
A. Fusion and splitting tensors	34
B. Broken zipper condition and two-sided zipper condition	34
C. Consequences	36
1. Fusion channels are topological	36
2. The left and right dimensions obey the fusion rules	37
3. The index is homogeneous	38
 VI. Examples	 39
A. Invertible symmetries	39
B. Non-anomalous fusion category symmetries	43
C. Kramers-Wannier symmetry for \mathbb{Z}_2 gauging	47
D. Kramers-Wannier symmetry for \mathbb{Z}_N gauging	53
 VII. Summary and outlook	 58
 Acknowledgments	 59
A. Choice of Λ^l and Λ^r in Definition IV.1	60
B. Equivalence of Definitions IV.1 and IV.2	61
C. Determination of $\delta_l(\mathcal{O})$ and $\delta_r(\mathcal{O})$ in Definition IV.2	62
D. Derivation of (VI.28)	62
 References	 63

I. INTRODUCTION

Symmetry is one of the guiding principles in theoretical physics. In the last decade, the notion of symmetry has been generalized in various ways. Prominent examples of generalized symmetries are those generated by non-invertible conserved operators. Such symmetries are called non-invertible symmetries; see [1–8] for reviews. Given the generalizations of the notion of symmetry, it is natural to ask what kinds of mathematical structures symmetries of quantum many-body systems generally have.

In relativistic quantum field theories (QFTs), symmetry operators/defects are defined by topological operators/defects [9]. Based on this definition, it is expected that finite internal non-invertible symmetries in 1+1 dimensions are generally described by fusion categories [10–12]. There are many

examples of non-invertible symmetries in 1+1d, such as the Kramers-Wannier duality symmetry of the Ising CFT and more general symmetries generated by the Verlinde lines of diagonal rational conformal field theories [11, 13–19]. Notably, it is known that any fusion category can be realized as the symmetry of a topological QFT [12, 20–22].

On the lattice, however, the problem is more subtle. This is because the symmetry structure on the lattice is strongly constrained by the fact that the state space is given by the tensor product of finite dimensional local Hilbert spaces.¹ Indeed, it was recently shown in [26] that a fusion category \mathcal{C} can be realized as the symmetry on a tensor product Hilbert space if and only if \mathcal{C} is integral, i.e., all objects of \mathcal{C} have integral quantum dimensions. Nevertheless, even if \mathcal{C} is not integral, it sometimes admits a slightly modified realization on a tensor product Hilbert space. For example, as clarified in [27, 28], the fusion rules of the Ising fusion category, which is an example of a non-integral fusion category, can be realized on a tensor product Hilbert space of qubits if we allow mixing with the lattice translation. More specifically, the Kramers-Wannier duality operator D_{KW} on the lattice obeys the fusion rule [27, 28]

$$D_{\text{KW}} D_{\text{KW}} = T(1 + U), \quad (\text{I.1})$$

where T is the lattice translation by one site and U is the spin-flip operator generating the \mathbb{Z}_2 symmetry of the Ising model. More general examples of this type of realization were studied recently in [29].

The above example suggests that the fusion rules of some non-integral fusion categories can be realized on a tensor product Hilbert space if we allow mixing with lattice translations or more general quantum cellular automata (QCAs).² Based on this observation, it is natural to ask which class of fusion categories admits such a realization.

A recent conjecture proposed in [32, 33] states that a fusion category symmetry \mathcal{C} can be realized on a tensor product Hilbert space if we allow mixing with QCAs only when \mathcal{C} is weakly integral, i.e., the total dimension of \mathcal{C} is an integer.³ To prove or disprove this conjecture, it would be inevitable to have a precise definition of non-invertible symmetries on a tensor product Hilbert space. However, such a definition is still lacking, despite recent remarkable observations on general properties of non-invertible symmetries [35–39].

In this paper, we provide two complementary approaches to the conjecture mentioned above. In the first approach, without specifying a precise definition of symmetry operators, we postulate several physical assumptions on the corresponding defect Hilbert spaces. Based on these assumptions, we study the constraints on possible fusion rules of symmetry operators on a tensor product Hilbert space. As a key quantity, we introduce an index of non-invertible symmetry operators, generalizing the Gross-Nesme-Vogts-Werner (GNVW) index of QCAs [40]. We show that as long as all fusion channels of two symmetry operators have the same index, the symmetry operators on a tensor product Hilbert space can only realize the fusion rules of a weakly integral fusion category, even if we allow mixing with QCAs. This result provides a connection between the conjecture in [32, 33] and the yet-to-be-established index theory of non-invertible symmetries.

As another approach, we also discuss the above problem within the framework of tensor networks. Specifically, we first propose a general class of tensor network operators that we consider to be

¹ There are also lattice models, such as the anyon chain models [23–25], whose state space does not admit a tensor product decomposition. We will not consider such models in this paper, except for Section III D. We will also not consider the case where the local Hilbert space has an infinite dimension.

² A QCA is a unitary operator that preserves the locality; see, e.g., [30, 31] for reviews.

³ Equivalently, the quantum dimension of every simple object of \mathcal{C} is a square root of an integer [34, Proposition 9.6.9].

indecomposable symmetry operators on a tensor product Hilbert space. These are matrix product operators (MPOs) with some special properties, and are referred to as topological injective MPOs.⁴ For these MPOs, we define an index, which agrees with the one mentioned in the previous paragraph, and write down sufficient conditions for all fusion channels to have the same index. As a corollary, it follows that topological injective MPOs satisfying these sufficient conditions can only realize the fusion rules of a weakly integral fusion category, even if we allow mixing with QCAs. We note that the sufficient conditions have not been proven yet in the general setting. Nevertheless, we will show that all examples of topological injective MPOs discussed in this paper satisfy the sufficient conditions.

We emphasize that general properties of the index of non-invertible symmetry operators have not been fully understood. In particular, it has not been proven that every fusion channel of two non-invertible symmetry operators has the same index. As such, the conjecture in [32, 33] is still open.

Structure of the paper. This paper is organized as follows. In Section II, we discuss non-invertible symmetries realized on a tensor product Hilbert space without mixing with QCAs. Based on the physical assumptions spelled out in Section IA, we show that the fusion rules of a unitary fusion category \mathcal{C} can be realized exactly on a tensor product Hilbert space only when \mathcal{C} is integral, recovering the mathematical result in [26]. In Section III, we generalize this result to the case when the fusion rules mix with QCAs. Assuming that every fusion channel of two symmetry operators has the same index, we show that the fusion rules of \mathcal{C} can be realized up to QCAs on a tensor product Hilbert space only when \mathcal{C} is weakly integral. As in Section II, the discussions in Section III are based on the physical assumptions in Section IA. In Section IV, we provide a tensor network formulation of non-invertible symmetry operators on a tensor product Hilbert space. More specifically, we introduce topological injective MPOs and construct the associated defect Hilbert spaces. We also show that topological injective MPOs admit sequential quantum circuit representations. In Section V, we give sufficient conditions for every fusion channel of two topological injective MPOs to have the same index. In Section VI, we discuss various examples of topological injective MPOs, including all invertible symmetry operators and the Kramers-Wannier duality operator. We will see that all of these examples satisfy the sufficient conditions given in Section V. In Section VII, we conclude with a more detailed summary of the results and a brief outlook. Several technical details are relegated to appendices.

Conventions. The vector spaces and fusion categories considered in this paper are defined over \mathbb{C} . In particular, the fusion categories are always supposed to be unitary. The on-site Hilbert space, denoted by \mathcal{H}_o , is supposed to be finite-dimensional. All QCAs and MPOs considered in this paper are translationally invariant. The fixed point of the transfer matrix of an injective MPO always refers to the eigenvector with the largest eigenvalue, even if the eigenvalue is not normalized to 1.

A. Physical assumptions

Before moving on to the main text, we first specify the physical assumptions on which the discussions in Sections II and III rely. The discussions from Section IV onwards do not rely on these assumptions.

⁴ We refer the reader to, e.g., [41–44] for various MPO representations of non-invertible symmetries.



FIG. 1. A schematic picture of defect Hilbert spaces $\mathcal{H}_{D_X}^l$ (left) and $\mathcal{H}_{D_X}^r$ (right).

Assumption 1 (Existence of defect Hilbert spaces). *For every (possibly non-invertible) symmetry operator D_X , there exist defect Hilbert spaces $\mathcal{H}_{D_X}^l$ and $\mathcal{H}_{D_X}^r$, which are obtained by modifying the original Hilbert space \mathcal{H} locally around the defect locus. Physically, $\mathcal{H}_{D_X}^l$ is the Hilbert space in the presence of a defect X oriented upwards, while $\mathcal{H}_{D_X}^r$ is the Hilbert space in the presence of a defect X oriented downwards; see Figure 1. We assume that the defect X can be moved by unitary operators. In particular, the defect Hilbert spaces do not depend on the position of a defect up to isomorphism.*

Assumption 2 (Product of symmetry operators). *For every pair of (possibly non-invertible) symmetry operators D_X and D_Y , the product $D_X D_Y$ is also a symmetry operator. The defect Hilbert spaces associated with $D_X D_Y$ are isomorphic to the Hilbert spaces in the presence of two defects X and Y apart from each other.*⁵

Assumption 3 (Sum of symmetry operators). *For every pair of (possibly non-invertible) symmetry operators D_X and D_Y , the sum $D_X + D_Y$ is also a symmetry operator. The defect Hilbert spaces associated with $D_X + D_Y$ are isomorphic to the direct sum of the defect Hilbert spaces associated with each summand, i.e., $\mathcal{H}_{D_X+D_Y}^l \cong \mathcal{H}_{D_X}^l \oplus \mathcal{H}_{D_Y}^l$ and $\mathcal{H}_{D_X+D_Y}^r \cong \mathcal{H}_{D_X}^r \oplus \mathcal{H}_{D_Y}^r$.*

Assumption 4 (Compatibility with the unitary structure). *For every (possibly non-invertible) symmetry operator D_X , its Hermitian conjugate D_X^\dagger is also a symmetry operator. The defect Hilbert spaces associated with D_X^\dagger are isomorphic to those associated with D_X with the opposite orientation, i.e., $\mathcal{H}_{D_X^\dagger}^l \cong \mathcal{H}_{D_X}^r$ and $\mathcal{H}_{D_X^\dagger}^r \cong \mathcal{H}_{D_X}^l$.*

Throughout the paper, except for Section III D, we assume that any defect Hilbert space is given by the tensor product of finite dimensional Hilbert spaces on a one-dimensional chain. In particular, the original Hilbert space without a defect is given by

$$\mathcal{H} = \bigotimes_{i=1,2,\dots,N} \mathcal{H}_o^{(i)}, \quad (\text{I.2})$$

where N is the number of sites and $\mathcal{H}_o^{(i)}$ is a finite dimensional Hilbert space on site i . For simplicity, in what follows, we assume that $\mathcal{H}_o^{(i)}$ is independent of site i . Accordingly, the on-site Hilbert space will be denoted simply by \mathcal{H}_o . We also assume that the symmetry operators are translationally invariant, which implies that the local modification around the defect does not depend on the position of the defect.

Due to Assumption 1, the defect Hilbert spaces $\mathcal{H}_{D_X}^l$ and $\mathcal{H}_{D_X}^r$ are obtained by modifying the original Hilbert space \mathcal{H} locally around the defect. Since \mathcal{H} is supposed to have the tensor product

⁵ Since the insertion of a defect is a local modification due to Assumption 1, the Hilbert space in the presence of two defects is well-defined as long as the distance between the defects is sufficiently large.

decomposition as in (I.2), the local modification amounts to replacing the Hilbert space on a finite region around the defect with another Hilbert space. Therefore, the defect Hilbert spaces can be generally written as

$$\mathcal{H}_{D_X}^l \cong L_X \otimes \mathcal{H}_o^{\otimes N - n_X^l}, \quad \mathcal{H}_{D_X}^r \cong R_X \otimes \mathcal{H}_o^{\otimes N - n_X^r}, \quad (\text{I.3})$$

where n_X^l and n_X^r are positive integers and L_X and R_X are finite dimensional Hilbert spaces. We note that n_X^l , n_X^r , L_X , and R_X are independent of the position of the defect because of the translational invariance. We also note that these quantities are independent of the system size N because the modification is assumed to be local. Equation (I.3) means that $\mathcal{H}_{D_X}^l$ is obtained by replacing the Hilbert space on n_X^l sites with L_X , and $\mathcal{H}_{D_X}^r$ is obtained by replacing the Hilbert space on n_X^r sites with R_X . In the case of invertible symmetries represented by QCAs, a general construction of defect Hilbert spaces is given in [45].

II. NON-INVERTIBLE SYMMETRIES WITHOUT MIXING WITH QCAS

In this section, we consider non-invertible symmetries in 1+1d that do not mix with QCAs. Based on the physical assumptions stated in Section IA, we will show that a unitary fusion category symmetry \mathcal{C} can be realized without mixing with QCAs on a tensor product Hilbert space only when \mathcal{C} is integral, i.e., only when every object of \mathcal{C} has an integral quantum dimension. This statement and its converse were recently proved rigorously in [26] by a different method. Throughout this section, we use the notations introduced in Section IA.

A. Left and right dimensions

Following [28], we first introduce key quantities that we will call the left and right dimensions.

Definition II.1. *For each symmetry operator D_X on a tensor product Hilbert space, we define the left and right dimensions of D_X by the ratios*

$$\text{ldim}(D_X) := \frac{\dim(\mathcal{H}_{D_X}^l)}{\dim(\mathcal{H})}, \quad \text{rdim}(D_X) := \frac{\dim(\mathcal{H}_{D_X}^r)}{\dim(\mathcal{H})}, \quad (\text{II.1})$$

where $\mathcal{H}_{D_X}^l$ and $\mathcal{H}_{D_X}^r$ are the defect Hilbert spaces and \mathcal{H} is the Hilbert space without a defect.

In [28], the above quantities are called lattice quantum dimensions. However, in this paper, we reserve the term “lattice quantum dimension” for another quantity that we will define in Section III A.

The left and right dimensions are well-defined because the dimensions of the defect Hilbert spaces do not depend on the position of the defect due to Assumption 1. Based on the general form (I.3) of the defect Hilbert spaces, the left and right dimensions can also be written in terms of local quantities as

$$\text{ldim}(D_X) = \frac{\dim(L_X)}{\dim(\mathcal{H}_o)^{n_X^l}}, \quad \text{rdim}(D_X) = \frac{\dim(R_X)}{\dim(\mathcal{H}_o)^{n_X^r}}. \quad (\text{II.2})$$

We note that both $\text{ldim}(\mathbf{D}_X)$ and $\text{rdim}(\mathbf{D}_X)$ are positive rational numbers by definition. Furthermore, they are independent of the system size N because n_X^l , n_X^r , L_X , and R_X are independent of N as mentioned in Section IA. We also note that due to Assumption 4, the left and right dimensions of \mathbf{D}_X and \mathbf{D}_X^\dagger are related by $\text{ldim}(\mathbf{D}_X^\dagger) = \text{rdim}(\mathbf{D}_X)$ and $\text{rdim}(\mathbf{D}_X^\dagger) = \text{ldim}(\mathbf{D}_X)$.

Multiplicativity and additivity. Due to Assumption 2, we can show that the left and right dimensions are multiplicative under the composition of symmetry operators, that is,

$$\text{ldim}(\mathbf{D}_X \mathbf{D}_Y) = \text{ldim}(\mathbf{D}_X) \text{ldim}(\mathbf{D}_Y), \quad \text{rdim}(\mathbf{D}_X \mathbf{D}_Y) = \text{rdim}(\mathbf{D}_X) \text{rdim}(\mathbf{D}_Y). \quad (\text{II.3})$$

To show the above equation, we note that Assumption 2 implies that the defect Hilbert spaces associated with the composite operator $\mathbf{D}_X \mathbf{D}_Y$ are given by

$$\mathcal{H}_{\mathbf{D}_X \mathbf{D}_Y}^l \cong L_X \otimes L_Y \otimes \mathcal{H}_o^{\otimes N - n_X^l - n_Y^l}, \quad \mathcal{H}_{\mathbf{D}_X \mathbf{D}_Y}^r \cong R_X \otimes R_Y \otimes \mathcal{H}_o^{\otimes N - n_X^r - n_Y^r}. \quad (\text{II.4})$$

Therefore, the left and right dimensions of $\mathbf{D}_X \mathbf{D}_Y$ can be computed as

$$\begin{aligned} \text{ldim}(\mathbf{D}_X \mathbf{D}_Y) &= \frac{\dim(L_X \otimes L_Y)}{\dim(\mathcal{H}_o)^{n_X^l + n_Y^l}} = \text{ldim}(\mathbf{D}_X) \text{ldim}(\mathbf{D}_Y), \\ \text{rdim}(\mathbf{D}_X \mathbf{D}_Y) &= \frac{\dim(R_X \otimes R_Y)}{\dim(\mathcal{H}_o)^{n_X^r + n_Y^r}} = \text{rdim}(\mathbf{D}_X) \text{rdim}(\mathbf{D}_Y), \end{aligned} \quad (\text{II.5})$$

which shows (II.3). Furthermore, due to Assumption 3, the left and right dimensions are additive under the sum of symmetry operators, that is,

$$\text{ldim}(\mathbf{D}_X + \mathbf{D}_Y) = \text{ldim}(\mathbf{D}_X) + \text{ldim}(\mathbf{D}_Y), \quad \text{rdim}(\mathbf{D}_X + \mathbf{D}_Y) = \text{rdim}(\mathbf{D}_X) + \text{rdim}(\mathbf{D}_Y). \quad (\text{II.6})$$

This immediately follows from isomorphisms $\mathcal{H}_{\mathbf{D}_X + \mathbf{D}_Y}^l \cong \mathcal{H}_{\mathbf{D}_X}^l \oplus \mathcal{H}_{\mathbf{D}_Y}^l$ and $\mathcal{H}_{\mathbf{D}_X + \mathbf{D}_Y}^r \cong \mathcal{H}_{\mathbf{D}_X}^r \oplus \mathcal{H}_{\mathbf{D}_Y}^r$.

Fusion rules. As a consequence of the multiplicativity (II.3) and additivity (II.6), it follows that the left and right dimensions are one-dimensional representations of the fusion rules of the symmetry operators on the lattice. To see this, we consider symmetry operators that obey the following fusion rules:

$$\mathbf{D}_X \mathbf{D}_Y = \sum_{Z \in S_{XY}} \mathbf{D}_Z. \quad (\text{II.7})$$

Here, S_{XY} is the set of fusion channels, which may contain a single label Z multiple times, meaning that the fusion multiplicity can be greater than one. Since the left and right dimensions are multiplicative (II.3) and additive (II.6), the fusion rules (II.7) imply

$$\text{ldim}(\mathbf{D}_X) \text{ldim}(\mathbf{D}_Y) = \sum_{Z \in S_{XY}} \text{ldim}(\mathbf{D}_Z), \quad \text{rdim}(\mathbf{D}_X) \text{rdim}(\mathbf{D}_Y) = \sum_{Z \in S_{XY}} \text{rdim}(\mathbf{D}_Z). \quad (\text{II.8})$$

Thus, as pointed out in [28], the left and right dimensions are one-dimensional representations of the fusion rules of the symmetry operators. We emphasize that these one-dimensional representations are positive and rational by definition. As we will see in the next subsection, this fact imposes

a strong constraint on the possible symmetry structure that can be realized exactly on a tensor product Hilbert space.

The case of invertible symmetries. As an example, let us consider the case of invertible symmetries, whose symmetry operators are represented by QCAs. For any QCA U , the multiplicativity (II.3) of the left and right dimensions imply

$$\text{ldim}(U)\text{ldim}(U^\dagger) = \text{rdim}(U)\text{rdim}(U^\dagger) = 1. \quad (\text{II.9})$$

On the other hand, due to Assumption 4, the left and right dimensions of U and U^\dagger are related by $\text{ldim}(U^\dagger) = \text{rdim}(U)$ and $\text{rdim}(U^\dagger) = \text{ldim}(U)$. Therefore, the above equation implies

$$\text{ldim}(U)\text{rdim}(U) = 1. \quad (\text{II.10})$$

Namely, the left dimension of a QCA is the inverse of its right dimension. For instance, when U is the lattice translation operator by one site, the left and right dimensions are given by $\dim(\mathcal{H}_o)$ and $\dim(\mathcal{H}_o)^{-1}$, respectively [28, 45]. More generally, as we will discuss in Section IV B 2, the left and right dimensions of a general QCA are given by its GNVW index and its inverse.

B. Exact fusion rules imply integrality

In this subsection, based on the physical assumptions in Section IA, we show that a unitary fusion category symmetry \mathcal{C} in 1+1d can be realized exactly on a tensor product Hilbert space only when \mathcal{C} is integral. This result agrees with the mathematical result in [26]. To make the statement more precise, let us suppose that there exists a finite set of symmetry operators $\{\mathsf{D}_X \mid X \in \text{Irr}(\mathcal{C})\}$ whose fusion rules are exactly given by those of \mathcal{C} , i.e.,

$$\mathsf{D}_X \mathsf{D}_Y = \sum_{Z \in X \otimes Y} \mathsf{D}_Z. \quad (\text{II.11})$$

Here, $\text{Irr}(\mathcal{C})$ denotes the set of (isomorphism classes of) simple objects of \mathcal{C} , and \otimes denotes the tensor product in \mathcal{C} . The summation on the right-hand side of (II.11) is taken over all fusion channels, including the fusion multiplicities. In what follows, we will show that \mathcal{C} must be an integral fusion category, i.e., a fusion category in which all objects have integral quantum dimensions.

To show the above statement, we first recall that the left and right dimensions defined by (II.1) are positive one-dimensional representations of the fusion rules of the symmetry operators, cf. (II.8). Thus, equation (II.11) implies that the left and right dimensions are positive one-dimensional representations of the fusion rules of \mathcal{C} . It is known that a positive one-dimensional representation of the fusion rules of any unitary fusion category \mathcal{C} is unique and is given by the quantum dimension [34, Proposition 3.3.6]. Therefore, both the left and right dimensions of D_X agree with the quantum dimension of X , i.e.,

$$\text{ldim}(\mathsf{D}_X) = \text{rdim}(\mathsf{D}_X) = \text{qdim}_{\mathcal{C}}(X), \quad (\text{II.12})$$

where $\text{qdim}_{\mathcal{C}}(X)$ denotes the quantum dimension of $X \in \text{Irr}(\mathcal{C})$. Since the left and right dimensions are rational numbers by definition, the above equation implies that the quantum dimension of any simple object of \mathcal{C} is a rational number. On the other hand, the quantum dimension of any object

of a unitary fusion category is known to be an algebraic integer [34, Proposition 3.3.4]. Hence, it follows that $\text{qdim}_{\mathcal{C}}(X)$ is a rational algebraic integer for all $X \in \text{Irr}(\mathcal{C})$. Since any rational algebraic integer must be an integer (see, e.g., [46, Chapter 2]), we conclude that \mathcal{C} is integral.

Remark. The above proof does not guarantee that the fusion rules of all integral unitary fusion categories can be realized exactly on a tensor product Hilbert space. Nevertheless, it was recently shown in [26] that any integral fusion category can indeed be realized as a symmetry on a tensor product Hilbert space.⁶ Basic examples of integral unitary fusion categories are non-anomalous fusion categories [11, 12], i.e., those that admit a fiber functor [12]. Physically, non-anomalous fusion categories describe the symmetries that admit a symmetry protected topological phase [12], i.e., a symmetric gapped phase with a unique ground state on a circle. It is known that any non-anomalous unitary fusion category is equivalent to the category of representations of a finite dimensional semisimple Hopf algebra [34]. Concrete realizations of this class of fusion category symmetries on a tensor product Hilbert space are given in [22, 41, 47].

III. NON-INVERTIBLE SYMMETRIES MIXED WITH QCAS

In this section, we discuss non-invertible symmetries in 1+1d that mix with non-trivial QCAs. We first define the lattice quantum dimension and the index of non-invertible symmetry operators using the left and right dimensions defined in Section II A. We then show that the lattice quantum dimension is a positive one-dimensional representation of the fusion rules if and only if all fusion channels of two indecomposable symmetry operators have the same index. When all fusion channels have the same index, we say that the index is homogeneous. As a corollary, we show that if the index is homogeneous, the fusion rules of the symmetry operators on a tensor product Hilbert space can agree, up to QCAs, with those of a unitary fusion category \mathcal{C} only when \mathcal{C} is weakly integral. We will also comment on the case where the Hilbert space does not admit a tensor product decomposition, and discuss why the above constraint does not apply to such a case.

A. Lattice quantum dimension and index

Let us begin with the definitions of the lattice quantum dimension and the index.

Definition III.1. *For each symmetry operator D_X , we define the lattice quantum dimension and the index of D_X by*

$$\text{qdim}_{\text{lat}}(D_X) := \sqrt{\text{ldim}(D_X)\text{rdim}(D_X)}, \quad \text{ind}(D_X) := \sqrt{\frac{\text{ldim}(D_X)}{\text{rdim}(D_X)}}, \quad (\text{III.1})$$

where $\text{ldim}(D_X)$ and $\text{rdim}(D_X)$ are the left and right dimensions defined by (II.1).

For the symmetry operators whose fusion rules agree exactly with those of a unitary fusion category \mathcal{C} , we have $\text{qdim}_{\text{lat}}(D_X) = \text{qdim}_{\mathcal{C}}(X)$ and $\text{ind}(D_X) = 1$ due to (II.12). On the other hand, for the lattice translation operator T , we have $\text{qdim}_{\text{lat}}(T) = 1$ and $\text{ind}(T) = \dim(\mathcal{H}_o)$ because

⁶ More precisely, in [26], Evans and Jones constructed a symmetry action of an arbitrary integral fusion category on a tensor product quasi-local algebra on an infinite chain.

$\text{ldim}(T) = \dim(\mathcal{H}_o)$ and $\text{rdim}(T) = \dim(\mathcal{H}_o)^{-1}$ as mentioned below (II.10). More generally, for any QCA, the lattice quantum dimension is equal to one due to (II.10) and the index agrees with the GNVW index; see Section IV B 2 for more details. In particular, our index generalizes the GNVW index to non-invertible symmetry operators.⁷

Due to the multiplicativity (II.3) of the left and right dimensions, the lattice quantum dimension and the index are also multiplicative in the sense that

$$\text{qdim}_{\text{lat}}(\mathsf{D}_X \mathsf{D}_Y) = \text{qdim}_{\text{lat}}(\mathsf{D}_X) \text{qdim}_{\text{lat}}(\mathsf{D}_Y), \quad (\text{III.2})$$

$$\text{ind}(\mathsf{D}_X \mathsf{D}_Y) = \text{ind}(\mathsf{D}_X) \text{ind}(\mathsf{D}_Y). \quad (\text{III.3})$$

On the other hand, the lattice quantum dimension and the index are not additive in general. Indeed, as we will see below, the lattice quantum dimension is additive only for symmetry operators with the same index. Namely, for any positive integer n , we have

$$\text{qdim}_{\text{lat}}\left(\sum_{i=1}^n \mathsf{D}_{X_i}\right) = \sum_{i=1}^n \text{qdim}_{\text{lat}}(\mathsf{D}_{X_i}) \Leftrightarrow \text{ind}(\mathsf{D}_{X_i}) = \text{ind}(\mathsf{D}_{X_j}), \quad \forall i, j = 1, 2, \dots, n. \quad (\text{III.4})$$

Furthermore, one can also show that the index is invariant under the addition of symmetry operators if and only if they have the same index, i.e.,

$$\text{ind}(\mathsf{D}_X + \mathsf{D}_Y) = \text{ind}(\mathsf{D}_X) \Leftrightarrow \text{ind}(\mathsf{D}_X) = \text{ind}(\mathsf{D}_Y). \quad (\text{III.5})$$

In the remainder of this subsection, we will show (III.4) and (III.5).

To show (III.4), we notice that the additivity (II.6) of the left and right dimensions implies that the lattice quantum dimension satisfies

$$\begin{aligned} & \text{qdim}_{\text{lat}}\left(\sum_{i=1}^n \mathsf{D}_{X_i}\right)^2 - \left(\sum_{i=1}^n \text{qdim}_{\text{lat}}(\mathsf{D}_{X_i})\right)^2 \\ &= \frac{1}{2} \sum_{i,j} (\text{ldim}(\mathsf{D}_{X_i}) \text{rdim}(\mathsf{D}_{X_j}) + \text{rdim}(\mathsf{D}_{X_i}) \text{ldim}(\mathsf{D}_{X_j}) - 2 \text{qdim}_{\text{lat}}(\mathsf{D}_{X_i}) \text{qdim}_{\text{lat}}(\mathsf{D}_{X_j})) \\ &= \frac{1}{2} \sum_{i,j} \left(\sqrt{\text{ldim}(\mathsf{D}_{X_i}) \text{rdim}(\mathsf{D}_{X_j})} - \sqrt{\text{rdim}(\mathsf{D}_{X_i}) \text{ldim}(\mathsf{D}_{X_j})} \right)^2. \end{aligned} \quad (\text{III.6})$$

Therefore, $\text{qdim}_{\text{lat}}(\sum_{i=1}^n \mathsf{D}_{X_i})$ agrees with $\sum_{i=1}^n \text{qdim}_{\text{lat}}(\mathsf{D}_{X_i})$ if and only if

$$\sqrt{\text{ldim}(\mathsf{D}_{X_i}) \text{rdim}(\mathsf{D}_{X_j})} = \sqrt{\text{rdim}(\mathsf{D}_{X_i}) \text{ldim}(\mathsf{D}_{X_j})}, \quad \forall i, j = 1, 2, \dots, n. \quad (\text{III.7})$$

By dividing both sides by $\text{rdim}(\mathsf{D}_{X_i}) \text{rdim}(\mathsf{D}_{X_j})$, we obtain

$$\text{ind}(\mathsf{D}_{X_i}) = \text{ind}(\mathsf{D}_{X_j}), \quad \forall i, j = 1, 2, \dots, n, \quad (\text{III.8})$$

which shows (III.4).

⁷ The GNVW index has been generalized in several different ways in the literature. In [48], the GNVW index was generalized to QCAs on abstract spin chains that do not admit a tensor product decomposition. In [49], the GNVW index was generalized to QCAs on algebras of G -symmetric local operators, where G is a finite abelian group. These generalizations have some overlap with ours. For example, the index of the Kramers-Wannier duality operator is defined in all cases and given by $\sqrt{2}$; cf. equation (VI.81).

We can also show (III.5) by using the additivity (II.6) of the left and right dimensions. More specifically, the additivity (II.6) implies that the index satisfies

$$\begin{aligned} \text{ind}(\mathsf{D}_X + \mathsf{D}_Y)^2 - \text{ind}(\mathsf{D}_X)^2 &= \frac{\text{ldim}(\mathsf{D}_X) + \text{ldim}(\mathsf{D}_Y)}{\text{rdim}(\mathsf{D}_X) + \text{rdim}(\mathsf{D}_Y)} - \frac{\text{ldim}(\mathsf{D}_X)}{\text{rdim}(\mathsf{D}_X)} \\ &= \frac{\text{rdim}(\mathsf{D}_X)\text{ldim}(\mathsf{D}_Y) - \text{ldim}(\mathsf{D}_X)\text{rdim}(\mathsf{D}_Y)}{(\text{rdim}(\mathsf{D}_X) + \text{rdim}(\mathsf{D}_Y))\text{rdim}(\mathsf{D}_X)}. \end{aligned} \quad (\text{III.9})$$

Therefore, $\text{ind}(\mathsf{D}_X + \mathsf{D}_Y)$ agrees with $\text{ind}(\mathsf{D}_X)$ if and only if

$$\text{rdim}(\mathsf{D}_X)\text{ldim}(\mathsf{D}_Y) = \text{ldim}(\mathsf{D}_X)\text{rdim}(\mathsf{D}_Y). \quad (\text{III.10})$$

By dividing both sides by $\text{rdim}(\mathsf{D}_X)^2\text{rdim}(\mathsf{D}_Y)^2$ and taking the square root, we obtain

$$\text{ind}(\mathsf{D}_X) = \text{ind}(\mathsf{D}_Y), \quad (\text{III.11})$$

which shows (III.5).

B. Homogeneity of the index

In this subsection, we define the notion of homogeneity of the index, which plays a crucial role in constraining possible fusion rules of symmetry operators on a tensor product Hilbert space.

Definition III.2. *Let D_X and D_Y be indecomposable symmetry operators whose fusion rule is given by*

$$\mathsf{D}_X \mathsf{D}_Y = \sum_{Z \in S_{XY}} \mathsf{D}_Z, \quad (\text{III.12})$$

where D_Z is an indecomposable symmetry operator for every $Z \in S_{XY}$.⁸ We say that the index is homogeneous for the product of D_X and D_Y if all fusion channels have the same index, i.e.,

$$\text{ind}(\mathsf{D}_Z) = \text{ind}(\mathsf{D}_W), \quad \forall Z, W \in S_{XY}. \quad (\text{III.13})$$

We note that equation (III.13) is equivalent to

$$\text{ind}(\mathsf{D}_Z) = \text{ind}(\mathsf{D}_X)\text{ind}(\mathsf{D}_Y), \quad \forall Z \in S_{XY}. \quad (\text{III.14})$$

Indeed, if the index satisfies (III.13), it follows that

$$\text{ind}(\mathsf{D}_Z) \stackrel{(\text{III.5})}{=} \text{ind} \left(\sum_{W \in S_{XY}} \mathsf{D}_W \right) \stackrel{(\text{III.12})}{=} \text{ind}(\mathsf{D}_X \mathsf{D}_Y) \stackrel{(\text{III.3})}{=} \text{ind}(\mathsf{D}_X)\text{ind}(\mathsf{D}_Y). \quad (\text{III.15})$$

Conversely, if the index satisfies (III.14), it is clear that $\text{ind}(\mathsf{D}_Z) = \text{ind}(\mathsf{D}_W)$ for all $Z, W \in S_{XY}$.

⁸ A symmetry operator is said to be indecomposable if it cannot be written as a sum of two symmetry operators.

For later use, let us give another equivalent characterization of the homogeneity of the index. Specifically, we show that the index is homogeneous if and only if the lattice quantum dimension gives a one-dimensional representation of the fusion rule (III.12), that is,

$$\text{qdim}_{\text{lat}}(\mathsf{D}_X)\text{qdim}_{\text{lat}}(\mathsf{D}_Y) = \sum_{Z \in S_{XY}} \text{qdim}_{\text{lat}}(\mathsf{D}_Z) \Leftrightarrow \text{ind}(\mathsf{D}_Z) = \text{ind}(\mathsf{D}_W), \quad \forall Z, W \in S_{XY}. \quad (\text{III.16})$$

To show this, we compute the lattice quantum dimension of $\mathsf{D}_X \mathsf{D}_Y$ in two different ways. On the one hand, $\text{qdim}_{\text{lat}}(\mathsf{D}_X \mathsf{D}_Y)$ is equal to $\text{qdim}_{\text{lat}}(\mathsf{D}_X)\text{qdim}_{\text{lat}}(\mathsf{D}_Y)$ due to the multiplicativity (III.2). On the other hand, due to (III.4), $\text{qdim}_{\text{lat}}(\mathsf{D}_X \mathsf{D}_Y)$ is equal to $\sum_{Z \in S_{XY}} \text{qdim}_{\text{lat}}(\mathsf{D}_Z)$ if and only if all the fusion channels have the same index. Therefore, we find that $\text{qdim}_{\text{lat}}(\mathsf{D}_X)\text{qdim}_{\text{lat}}(\mathsf{D}_Y)$ is equal to $\sum_{Z \in S_{XY}} \text{qdim}_{\text{lat}}(\mathsf{D}_Z)$ if and only if the index is homogeneous, which shows (III.16)

C. Homogeneity of the index implies weak integrality

The homogeneity of the index imposes a strong constraint on possible fusion rules of symmetry operators on a tensor product Hilbert space. To see this, we suppose that there exists a finite set of indecomposable symmetry operators $\{\mathsf{D}_X \mid X \in \text{Irr}(\mathcal{C})\}$ that obey the fusion rules of a unitary fusion category \mathcal{C} up to QCAs, that is,

$$\mathsf{D}_X \mathsf{D}_Y = \sum_{Z \in X \otimes Y} \mathsf{D}_Z U_{XY}^Z, \quad (\text{III.17})$$

where U_{XY}^Z is an arbitrary QCA. In what follows, we will show that if the index is homogeneous for the product of any two symmetry operators, i.e., if the index satisfies $\text{ind}(\mathsf{D}_Z U_{XY}^Z) = \text{ind}(\mathsf{D}_W U_{XY}^W)$ for all $X, Y \in \text{Irr}(\mathcal{C})$ and all $Z, W \in X \otimes Y$, then the unitary fusion category \mathcal{C} must be weakly integral. In other words, the conjecture in [32, 33] holds if the index is homogeneous.

To show the above statement, we first recall that the homogeneity of the index implies that the lattice quantum dimension gives a one-dimensional representation of the fusion rules (III.17), i.e.,

$$\text{qdim}_{\text{lat}}(\mathsf{D}_X)\text{qdim}_{\text{lat}}(\mathsf{D}_Y) = \sum_{Z \in X \otimes Y} \text{qdim}_{\text{lat}}(\mathsf{D}_Z U_{XY}^Z). \quad (\text{III.18})$$

Since the lattice quantum dimension is multiplicative (III.2), the summand on the right-hand side can be written as $\text{qdim}_{\text{lat}}(\mathsf{D}_Z)\text{qdim}_{\text{lat}}(U_{XY}^Z)$. Furthermore, as shown in (II.10), the lattice quantum dimension of any QCA is one under Assumption 4. Therefore, equation (III.18) reduces to

$$\text{qdim}_{\text{lat}}(\mathsf{D}_X)\text{qdim}_{\text{lat}}(\mathsf{D}_Y) = \sum_{Z \in X \otimes Y} \text{qdim}_{\text{lat}}(\mathsf{D}_Z). \quad (\text{III.19})$$

Namely, if the index is homogeneous, the lattice quantum dimension gives a one-dimensional representation of the fusion rules of \mathcal{C} . Now, we recall that the lattice quantum dimension is positive because it is the square root of a positive rational number. Since a positive one-dimensional representation of the fusion rules of \mathcal{C} is uniquely given by the quantum dimension [34, Proposition 3.3.6], we find

$$\text{qdim}_{\text{lat}}(\mathsf{D}_X) = \text{qdim}_{\mathcal{C}}(X). \quad (\text{III.20})$$

Furthermore, since $\text{qdim}_{\text{lat}}(\mathcal{D}_X)$ is the square root of a rational number, the above equation implies that the total dimension of \mathcal{C} is rational:

$$\text{Dim}(\mathcal{C}) := \sum_{X \in \text{Irr}(\mathcal{C})} \text{qdim}_{\mathcal{C}}(X)^2 = \sum_{X \in \text{Irr}(\mathcal{C})} \text{qdim}_{\text{lat}}(\mathcal{D}_X)^2 \in \mathbb{Q}. \quad (\text{III.21})$$

On the other hand, the total dimension $\text{Dim}(\mathcal{C})$ is an algebraic integer because $\text{qdim}_{\mathcal{C}}(X)$ is an algebraic integer for every $X \in \text{Irr}(\mathcal{C})$.⁹ Thus, $\text{Dim}(\mathcal{C})$ is a rational algebraic integer, and hence, it is an integer [46, Chapter 2]. This shows that \mathcal{C} is weakly integral.

Remarks. The above proof also shows that the quantum dimension of every simple object of \mathcal{C} must be a square root of an integer. This is not an additional constraint. Indeed, it is known that the quantum dimension of every simple object of any weakly integral unitary fusion category is a square root of an integer [34, Proposition 9.6.9].

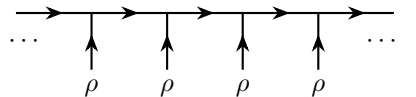
We note that \mathcal{C} must be integral if $\text{ind}(U_{XY}^Z) = 1$ for all $X, Y \in \text{Irr}(\mathcal{C})$ and $Z \in X \otimes Y$. Indeed, in this case, the proof in Section II B is valid because the condition $\text{ind}(U_{XY}^Z) = 1$ together with (II.10) implies that $\text{ldim}(U_{XY}^Z) = \text{rdim}(U_{XY}^Z) = 1$ and hence the logic of the proof is not affected.

However, \mathcal{C} is not necessarily integral if the index of U_{XY}^Z is non-trivial for some $X, Y \in \text{Irr}(\mathcal{C})$ and $Z \in X \otimes Y$. Indeed, there are examples of weakly integral fusion categories that are not integral and whose fusion rules can be realized on a tensor product Hilbert space by allowing mixing with lattice translation [28]. It is still an open problem whether the fusion rules of all weakly integral fusion categories can be realized on a tensor product Hilbert space by allowing mixing with non-trivial QCAs.

We also emphasize that the homogeneity of the index has not been proven. To study the properties of the index in depth, it is desirable to have a precise formulation of non-invertible symmetry operators on a tensor product Hilbert space. In Section IV, we will provide a tensor network description of non-invertible symmetry operators on a tensor product Hilbert space. Within this framework, we will write down sufficient conditions for the index to be homogeneous in Section V.

D. A comment on the case without tensor product decomposition

The discussions so far have relied on the assumption that the Hilbert space on the lattice can be decomposed into a tensor product of local Hilbert spaces. The conclusions are modified if we relax this assumption. To see this, let us consider the anyon chain model based on a unitary fusion category \mathcal{C} [23–25]. The anyon chain model based on \mathcal{C} is a 1+1d lattice model with a constrained Hilbert space and has an exact fusion category symmetry described by \mathcal{C} . The state space \mathcal{H} of the model without a defect is given by the vector space spanned by the fusion diagrams of the following form:

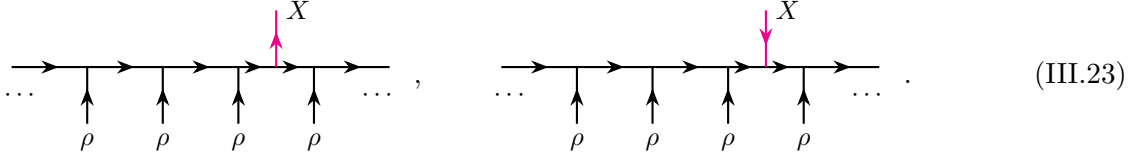


$$\dots \xrightarrow{\quad} \xrightarrow{\quad} \xrightarrow{\quad} \xrightarrow{\quad} \dots. \quad (\text{III.22})$$

Here, $\rho \in \mathcal{C}$ is a fixed object of \mathcal{C} , which we can choose arbitrarily. Similarly, the defect Hilbert spaces $\mathcal{H}_{\mathcal{D}_X}^l$ and $\mathcal{H}_{\mathcal{D}_X}^r$ associated with the symmetry operator \mathcal{D}_X for $X \in \text{Irr}(\mathcal{C})$ are spanned by

⁹ We recall that the algebraic integers form a ring. In particular, for any algebraic integers α and β , the sum $\alpha + \beta$ and the product $\alpha\beta$ are also algebraic integers.

the fusion diagrams of the following form [24, 25, 50]:



For the above definition of the defect Hilbert spaces, the left and right dimensions in (II.1) generally depend on the system size and are not multiplicative for a fixed system size. This motivates us to define the left and right dimensions of D_X in this model by taking the limit

$$\text{ldim}(D_X) := \lim_{N \rightarrow \infty} \frac{\dim(\mathcal{H}_{D_X}^l)}{\dim(\mathcal{H})}, \quad \text{rdim}(D_X) := \lim_{N \rightarrow \infty} \frac{\dim(\mathcal{H}_{D_X}^r)}{\dim(\mathcal{H})}, \quad (\text{III.24})$$

where N is the number of vertical lines labeled by ρ in (III.22) and (III.23). As long as the boundary conditions are sufficiently generic, one can show that the above quantities are given by

$$\text{ldim}(D_X) = \text{rdim}(D_X) = \text{qdim}_{\mathcal{C}}(X). \quad (\text{III.25})$$

We will give a proof of this equation shortly.

We note that the left and right dimensions defined above are multiplicative and additive, as in the case when the state space admits a tensor product decomposition. However, as opposed to the case of a tensor product Hilbert space, the left and right dimensions in (III.25) are no longer rational in general. Therefore, the discussion in the previous subsection does not apply to the anyon chain. This is in accordance with the fact that the anyon chain model can realize an arbitrary unitary fusion category symmetry \mathcal{C} without mixing with non-trivial QCAs.

A proof of (III.25). Now, we show (III.25).¹⁰ To this end, we first fix the boundary conditions so that the left and right ends of the chain in (III.22) are labeled by fixed objects

$$B_L := \bigoplus_{a \in \text{Irr}(\mathcal{C})} n_{a;L} a^*, \quad B_R := \bigoplus_{a \in \text{Irr}(\mathcal{C})} n_{a;R} a^*, \quad (\text{III.26})$$

where $n_{a;L}$ and $n_{a;R}$ are positive integers, and a^* denotes the dual of a . In what follows, we will write the column vectors with entries $n_{a;L}$ and $n_{a;R}$ as \mathbf{n}_L and \mathbf{n}_R , respectively.

For the above choice of boundary conditions, the dimension of the Hilbert space \mathcal{H} on an open chain with N vertical legs can be computed as

$$\dim(\mathcal{H}) = \dim(\text{Hom}_{\mathcal{C}}(B_L \otimes \rho^{\otimes N}, B_R)) = \mathbf{n}_L^T \mathbf{N}_{\rho}^N \mathbf{n}_R, \quad (\text{III.27})$$

where \mathbf{n}_L^T is the transpose of \mathbf{n}_L , and \mathbf{N}_{ρ} is the fusion matrix whose (a, b) -component is given by the fusion coefficient $N_{\rho b}^a$. When N is large, the right-hand side of the above equation is dominated by the contribution from the largest eigenvalue of \mathbf{N}_{ρ} . Since the largest eigenvalue of \mathbf{N}_{ρ} agrees with the quantum dimension of ρ [34], it follows that

$$\dim(\mathcal{H}) \sim (\mathbf{n}_L^T \mathbf{d})(\mathbf{d}^T \mathbf{n}_R) \text{qdim}_{\mathcal{C}}(\rho)^N, \quad \text{for } N \gg 1, \quad (\text{III.28})$$

¹⁰ The author thanks Kantaro Ohmori for explaining the proof.

where we neglected the subleading terms on the right-hand side. Here, \mathbf{d} is the normalized Perron-Frobenius eigenvector of \mathbf{N}_ρ , whose a th component is given by $\text{qdim}_\mathcal{C}(a)/\sqrt{\text{Dim}(\mathcal{C})}$, where $\text{Dim}(\mathcal{C})$ is the total dimension of \mathcal{C} .¹¹ We note that \mathbf{d} is independent of ρ , and in particular it satisfies $\mathbf{N}_a \mathbf{d} = \text{qdim}_\mathcal{C}(a) \mathbf{d}$ for all $a \in \text{Irr}(\mathcal{C})$. We also note that the non-universal factors $\mathbf{n}_L^T \mathbf{d}$ and $\mathbf{d}^T \mathbf{n}_R$ in (III.28) are non-zero as long as the boundary conditions in (III.26) are sufficiently generic.

Similarly, the dimensions of the defect Hilbert spaces $\mathcal{H}_{D_X}^l$ and $\mathcal{H}_{D_X}^r$ on an open chain with boundary condition (III.26) can be computed as

$$\dim(\mathcal{H}_{D_X}^l) = \dim(\text{Hom}_\mathcal{C}(B_L \otimes \rho^{\otimes N}, X \otimes B_R)) = \mathbf{n}_L^T C \mathbf{N}_X C \mathbf{N}_\rho^N \mathbf{n}_R, \quad (\text{III.29})$$

$$\dim(\mathcal{H}_{D_X}^r) = \dim(\text{Hom}_\mathcal{C}(B_L \otimes \rho^{\otimes N}, X^* \otimes B_R)) = \mathbf{n}_L^T C \mathbf{N}_{X^*} C \mathbf{N}_\rho^N \mathbf{n}_R, \quad (\text{III.30})$$

where C is the charge conjugation matrix whose (a, b) -component is given by δ_{a, b^*} . If we take N to be large, the above quantities are dominated by the contributions from the largest eigenvalue of \mathbf{N}_ρ . Since the corresponding eigenvector \mathbf{d} satisfies $\mathbf{N}_X \mathbf{d} = \text{qdim}_\mathcal{C}(X) \mathbf{d}$ and $C \mathbf{d} = \mathbf{d}$, it follows that

$$\dim(\mathcal{H}_{D_X}^l) \sim (\mathbf{n}_L^T \mathbf{d})(\mathbf{d}^T \mathbf{n}_R) \text{qdim}_\mathcal{C}(X) \text{qdim}_\mathcal{C}(\rho)^N, \quad (\text{III.31})$$

$$\dim(\mathcal{H}_{D_X}^r) \sim (\mathbf{n}_L^T \mathbf{d})(\mathbf{d}^T \mathbf{n}_R) \text{qdim}_\mathcal{C}(X^*) \text{qdim}_\mathcal{C}(\rho)^N, \quad (\text{III.32})$$

where $N \gg 1$.

By plugging the formulae (III.28), (III.31), and (III.32) into the definition (III.24), we find that the left and right dimensions of D_X are given by

$$\text{ldim}(D_X) = \text{qdim}_\mathcal{C}(X), \quad \text{rdim}(D_X) = \text{qdim}_\mathcal{C}(X^*) = \text{qdim}_\mathcal{C}(X). \quad (\text{III.33})$$

Here, we used the fact that $\mathbf{n}_L^T \mathbf{d}$ and $\mathbf{d}^T \mathbf{n}_R$ in (III.28), (III.31), and (III.32) are non-zero for a generic choice of boundary conditions. This concludes the proof of (III.25).

IV. TENSOR NETWORK FORMULATION OF NON-INVERTIBLE SYMMETRIES

In this section, we discuss a possible approach to establishing the index theory for non-invertible symmetry operators in 1+1d within the framework of tensor networks. More specifically, we first propose a general class of tensor network operators that describe non-invertible symmetries on a tensor product Hilbert space in 1+1 dimensions. We then study the corresponding defect Hilbert spaces and the associated quantities, such as the lattice quantum dimension and the index. The properties of these quantities are not yet fully understood: for example, the homogeneity of the index has not been proven.

Before going into details, we mention that most of the computations in this section can be found in [51–53] in the context of matrix product unitaries. Our contribution is to point out that many computations in [51–53] are valid for a more general class of tensor network operators that are generally non-invertible. This observation enables us to define the index of non-invertible symmetry operators without relying on the physical assumptions in Section I A. Throughout this section, the state space on the lattice is given by the tensor product of finite dimensional on-site Hilbert spaces.

¹¹ One can show that \mathbf{d} defined in this way is an eigenvector of \mathbf{N}_ρ with eigenvalue $\text{qdim}_\mathcal{C}(\rho)$ as follows: $(\mathbf{N}_\rho \mathbf{d})_a = \sum_b N_{\rho b}^a \text{qdim}_\mathcal{C}(b) / \sqrt{\text{Dim}(\mathcal{C})} = \sum_b N_{a^* \rho}^b \text{qdim}_\mathcal{C}(b) / \sqrt{\text{Dim}(\mathcal{C})} = \text{qdim}_\mathcal{C}(\rho) \text{qdim}_\mathcal{C}(a) / \sqrt{\text{Dim}(\mathcal{C})}$. Here, we used $\text{qdim}_\mathcal{C}(a) = \text{qdim}_\mathcal{C}(a^*)$ for all $a \in \text{Irr}(\mathcal{C})$. We note that this eigenvector is unique due to the Perron-Frobenius theorem.

A. Preliminaries

We first briefly review the basic notions of tensor networks that we will use later. We refer the reader to [54] and references therein for more details of tensor networks.

Injective MPOs. A matrix product operator (MPO) is a tensor network operator constructed from a four-leg tensor \mathcal{O} as follows:

$$D[\mathcal{O}] := // \xrightarrow{\mathcal{O}} \circlearrowleft \xrightarrow{\mathcal{O}} \circlearrowleft \xrightarrow{\mathcal{O}} \circlearrowleft \cdots \xrightarrow{\mathcal{O}} \circlearrowleft \xrightarrow{\mathcal{O}} // . \quad (\text{IV.1})$$

Here, the double slashes on both ends indicate the periodic boundary condition, and the arrows specify the source and target vector spaces of each tensor. In what follows, we consider only translationally invariant MPOs on a periodic chain. The physical Hilbert space on each site is denoted by \mathcal{H}_o , while the bond Hilbert space is denoted by V .

The MPO tensor \mathcal{O} is said to be injective if it is injective as a linear map from the virtual bonds to the physical legs. Due to the fundamental theorem of MPS/MPO [55, 56], two injective MPO tensors \mathcal{O} and \mathcal{O}' generate the same MPO $D[\mathcal{O}] = D[\mathcal{O}']$ on a periodic chain of any length if and only if they are related by a gauge transformation

$$\mathcal{O}' = \xrightarrow{M} \bullet \xrightarrow{\mathcal{O}} \circlearrowleft \xrightarrow{M^{-1}} , \quad (\text{IV.2})$$

where M is an arbitrary invertible linear map.

Blocking. The MPO tensors supported on n physical sites can be viewed as a single MPO tensor with physical Hilbert space $\mathcal{H}_o^{\otimes n}$. This operation is called blocking. The MPO tensor obtained by blocking n physical sites is denoted by $\mathcal{O}^{[n]}$. For example, when $n = 2$, we have

$$\mathcal{O}^{[2]} := \xrightarrow{\mathcal{O}} \circlearrowleft \xrightarrow{\mathcal{O}} . \quad (\text{IV.3})$$

We note that $\mathcal{O}^{[n]}$ is injective if \mathcal{O} is injective.

Transfer matrix and fixed points. The transfer matrix of an MPO tensor \mathcal{O} is the linear map defined by the following diagram:

$$T[\mathcal{O}] := \begin{array}{c} \mathcal{O}^\dagger \\ \uparrow \\ \circlearrowleft \xrightarrow{\mathcal{O}} \circlearrowleft \end{array} . \quad (\text{IV.4})$$

The loop on the right-hand side represents the trace over the physical Hilbert space. The MPO tensor \mathcal{O}^\dagger in the above equation is the Hermitian conjugate of \mathcal{O} , whose components are explicitly given by

$$a \xleftarrow{\mathcal{O}^\dagger} \begin{array}{c} i \\ \circlearrowleft \\ j \end{array} = \left(a \xrightarrow{\mathcal{O}} \begin{array}{c} j \\ \circlearrowleft \\ i \end{array} b \right)^*, \quad (\text{IV.5})$$

where $*$ denotes the complex conjugation, and the labels of the physical leg and the virtual bond take values in orthonormal bases of \mathcal{H}_o and V , respectively.

When \mathcal{O} is injective, the transfer matrix $T[\mathcal{O}]$ has a unique left eigenvector Λ^l such that the corresponding eigenvalue agrees with the spectral radius of $T[\mathcal{O}]$. We denote the spectral radius of $T[\mathcal{O}]$ by λ . Similarly, $T[\mathcal{O}]$ has a unique right eigenvector Λ^r with eigenvalue λ . The eigenvectors Λ^l and Λ^r are referred to as the left and right fixed points of $T[\mathcal{O}]$.¹² Diagrammatically, the eigenvalue equations for the fixed points can be written as

$$\begin{array}{c} \text{Diagram of } \Lambda^l \text{ and } \mathcal{O}^\dagger \text{ in a box} \\ \text{Diagram of } \Lambda^l \text{ and } \mathcal{O} \text{ in a box} \end{array} = \lambda \Lambda^l \quad , \quad \begin{array}{c} \text{Diagram of } \mathcal{O}^\dagger \text{ and } \Lambda^r \text{ in a box} \\ \text{Diagram of } \mathcal{O} \text{ and } \Lambda^r \text{ in a box} \end{array} = \lambda \Lambda^r \quad . \quad (\text{IV.6})$$

We note that Λ^l and Λ^r are also the fixed points of the transfer matrix $T[\mathcal{O}^\dagger]$, i.e.,

$$\begin{array}{c} \text{Diagram of } \Lambda^l \text{ and } \mathcal{O}^\dagger \text{ in a box} \\ \text{Diagram of } \Lambda^l \text{ and } \mathcal{O} \text{ in a box} \end{array} = \lambda \Lambda^l \quad , \quad \begin{array}{c} \text{Diagram of } \mathcal{O}^\dagger \text{ and } \Lambda^r \text{ in a box} \\ \text{Diagram of } \mathcal{O} \text{ and } \Lambda^r \text{ in a box} \end{array} = \lambda \Lambda^r \quad , \quad (\text{IV.7})$$

where λ in (IV.7) is the same as that in (IV.6). In later subsections, we will often use the fact that the fixed points Λ^l and Λ^r are positive definite [55, 57] and, in particular, they have full rank and are Hermitian.

Left and right ranks. We define the left rank of an MPO tensor \mathcal{O} as the rank of \mathcal{O} viewed as a linear map from the bottom left to the top right in its diagrammatic representation. Similarly, the right rank of \mathcal{O} is defined as the rank of \mathcal{O} viewed as a linear map from the bottom right to the top left. Diagrammatically, these quantities are written as

$$\text{rank}_l(\mathcal{O}) := \text{rank} \left(\begin{array}{c} \text{Diagram of } \mathcal{O} \text{ in a box} \\ \text{Diagram of } \mathcal{O}^\dagger \text{ in a box} \end{array} \right) , \quad \text{rank}_r(\mathcal{O}) := \text{rank} \left(\begin{array}{c} \text{Diagram of } \mathcal{O}^\dagger \text{ in a box} \\ \text{Diagram of } \mathcal{O} \text{ in a box} \end{array} \right) . \quad (\text{IV.8})$$

We note that the left and right ranks of \mathcal{O}^\dagger are given by the right and left ranks of \mathcal{O} , that is,

$$\text{rank}_l(\mathcal{O}^\dagger) = \text{rank}_r(\mathcal{O}), \quad \text{rank}_r(\mathcal{O}^\dagger) = \text{rank}_l(\mathcal{O}). \quad (\text{IV.9})$$

These quantities were used in [51, 52] to define the index of matrix product unitaries. In the next subsection, we will use these quantities to define the left and right dimensions, the lattice quantum dimension, and the index of more general MPOs that are not necessarily unitary.

B. Definitions

In Sections II and III, we defined various quantities associated with non-invertible symmetry operators in 1+1d, assuming the existence of defect Hilbert spaces. In this subsection, we define these quantities directly using tensor network representations of the symmetry operators.

¹² In the literature, Λ^l and Λ^r are often referred to as the fixed points only when \mathcal{O} is normalized so that $\lambda = 1$. In this paper, however, we do not assume this normalization.

1. General case

We first specify the class of MPOs that we consider to be indecomposable symmetry operators, which are generally non-invertible.

Definition IV.1 (Topological injective MPO). *An injective MPO tensor \mathcal{O} is said to be topological if it satisfies*

$$\Lambda^l \circlearrowleft \begin{array}{c} \mathcal{O}^\dagger \\ \mathcal{O} \end{array} \circlearrowright \Lambda^l = \left| \begin{array}{c} \mathcal{O}^\dagger \\ \mathcal{O} \end{array} \right|, \quad \begin{array}{c} \mathcal{O}^\dagger \\ \mathcal{O} \end{array} \circlearrowleft \Lambda^r = \left| \begin{array}{c} \mathcal{O}^\dagger \\ \mathcal{O} \end{array} \right|, \quad (\text{IV.10})$$

$$\Lambda^l \circlearrowleft \begin{array}{c} \mathcal{O} \\ \mathcal{O}^\dagger \end{array} \circlearrowright \Lambda^l = \left| \begin{array}{c} \mathcal{O} \\ \mathcal{O}^\dagger \end{array} \right|, \quad \begin{array}{c} \mathcal{O} \\ \mathcal{O}^\dagger \end{array} \circlearrowleft \Lambda^r = \left| \begin{array}{c} \mathcal{O} \\ \mathcal{O}^\dagger \end{array} \right|, \quad (\text{IV.11})$$

where Λ^l and Λ^r are the left and right fixed points of the transfer matrix $\mathsf{T}[\mathcal{O}]$. The MPO $\mathsf{D}[\mathcal{O}]$ generated by such a tensor \mathcal{O} is called a topological injective MPO.

As we will see in Section IV B 2, topological injective MPOs include all matrix product unitaries, which represent invertible symmetries. More precisely, any matrix product unitary can be made into a topological injective MPO by blocking a sufficient number of physical sites.

We note that topological injective MPOs do not include the product of local projectors. In particular, the projector onto the state space of the anyon chain model is not a topological injective MPO. Hence, the symmetry operators of the anyon chain model are excluded from the discussion.¹³

A topological injective MPO also has the following equivalent definition.

Definition IV.2 (Equivalent definition of topological injective MPO). *An injective MPO tensor \mathcal{O} is said to be topological if it satisfies (IV.10) and there exist non-zero complex numbers $\delta_l(\mathcal{O})$ and $\delta_r(\mathcal{O})$ such that*

$$\Lambda^l \circlearrowleft \begin{array}{c} \mathcal{O} \\ \mathcal{O}^\dagger \\ \mathcal{O} \end{array} \circlearrowright \Lambda^l = \delta_l(\mathcal{O}) \left| \begin{array}{c} \mathcal{O} \end{array} \right|, \quad \begin{array}{c} \mathcal{O} \\ \mathcal{O}^\dagger \\ \mathcal{O} \end{array} \circlearrowleft \Lambda^r = \delta_r(\mathcal{O}) \left| \begin{array}{c} \mathcal{O} \end{array} \right|. \quad (\text{IV.12})$$

We refer to the above equation as the zigzag relations.

The equivalence of the above two definitions will be shown in Appendix B. Furthermore, as we will show in Appendix C, the coefficients $\delta_l(\mathcal{O})$ and $\delta_r(\mathcal{O})$ in (IV.12) are uniquely given by the real numbers (IV.31), which depend on the normalizations of Λ^l and Λ^r .

¹³ See [42, 43] for MPO representations of general fusion category symmetries of the anyon chain models.

When \mathcal{O} is a topological injective MPO tensor, any other MPO tensor \mathcal{O}' related to \mathcal{O} by the gauge transformation (IV.2) is also topological. Thus, due to the fundamental theorem of injective MPS/MPO [55, 56], any injective MPO tensor generating a topological injective MPO is topological. Furthermore, it is clear from Definition IV.1 that the Hermitian conjugate of a topological injective MPO is also topological.

We emphasize that we generally need at least two physical legs in the defining equations (IV.10) and (IV.11); in particular, we do not require that the virtual bond can be detached from all the physical legs simultaneously. Indeed, in the case of invertible symmetries, the only symmetry operator that can be detached from all the physical legs simultaneously is the tensor product of on-site operators; see Section IVB 2 for more details.

As we will show in Section IVD, topological injective MPOs have the corresponding defect Hilbert spaces that satisfy Assumption 1. These defect Hilbert spaces are defined so that the left and right dimensions defined by (II.1) agree with those defined as follows:

Definition IV.3 (Left and right dimensions). *The left dimension $\text{ldim}(\mathcal{O})$ and the right dimension $\text{rdim}(\mathcal{O})$ of a topological injective MPO tensor \mathcal{O} are defined by*

$$\text{ldim}(\mathcal{O}) := \frac{\text{rank}_l(\mathcal{O})}{\dim(\mathcal{H}_o)}, \quad \text{rdim}(\mathcal{O}) := \frac{\text{rank}_r(\mathcal{O})}{\dim(\mathcal{H}_o)}, \quad (\text{IV.13})$$

where $\text{rank}_l(\mathcal{O})$ and $\text{rank}_r(\mathcal{O})$ are the left and right ranks defined by (IV.8).

By definition, the left and right dimensions of \mathcal{O} are less than or equal to the bond dimension of \mathcal{O} . We note that topological injective MPO tensors generating the same MPO have the same dimensions. Namely, if two topological injective MPO tensors \mathcal{O} and \mathcal{O}' satisfy $D[\mathcal{O}] = D[\mathcal{O}']$ on a periodic chain of any length, we have $\text{ldim}(\mathcal{O}) = \text{ldim}(\mathcal{O}')$ and $\text{rdim}(\mathcal{O}) = \text{rdim}(\mathcal{O}')$. This is an immediate consequence of the fundamental theorem of injective MPS/MPO [55, 56]. Furthermore, due to (IV.9), the left and right dimensions of \mathcal{O} and \mathcal{O}^\dagger are related by

$$\text{ldim}(\mathcal{O}^\dagger) = \text{rdim}(\mathcal{O}), \quad \text{rdim}(\mathcal{O}^\dagger) = \text{ldim}(\mathcal{O}). \quad (\text{IV.14})$$

By using the left and right dimensions, we can define the lattice quantum dimension and the index as in (III.1). For completeness, we repeat the definition here.

Definition IV.4 (Lattice quantum dimension and index). *The lattice quantum dimension $\text{qdim}_{\text{lat}}(\mathcal{O})$ and the index $\text{ind}(\mathcal{O})$ of a topological injective MPO tensor \mathcal{O} are defined by*

$$\text{qdim}_{\text{lat}}(\mathcal{O}) := \sqrt{\text{ldim}(\mathcal{O})\text{rdim}(\mathcal{O})}, \quad \text{ind}(\mathcal{O}) := \sqrt{\frac{\text{ldim}(\mathcal{O})}{\text{rdim}(\mathcal{O})}}. \quad (\text{IV.15})$$

Since $\text{ldim}(\mathcal{O})$ and $\text{rdim}(\mathcal{O})$ depend only on $D[\mathcal{O}]$, so do $\text{qdim}_{\text{lat}}(\mathcal{O})$ and $\text{ind}(\mathcal{O})$. Furthermore, due to (IV.14), the lattice quantum dimension and index of \mathcal{O} and \mathcal{O}^\dagger are related by

$$\text{qdim}_{\text{lat}}(\mathcal{O}^\dagger) = \text{qdim}_{\text{lat}}(\mathcal{O}), \quad \text{ind}(\mathcal{O}^\dagger) = \text{ind}(\mathcal{O})^{-1}. \quad (\text{IV.16})$$

2. Example: invertible symmetries

Topological injective MPOs include all invertible symmetry operators defined by translationally invariant QCAs. To see this, let us recall the tensor network description of QCAs. As shown in [51, 52], any translationally invariant QCA in 1+1 dimensions can be represented by a matrix product unitary (MPU), and conversely, any translationally invariant MPU with periodic boundary conditions is a QCA. Here, an MPU is an MPO that is unitary. Without loss of generality, we can take the local tensor \mathcal{U} of an MPU to be injective [51, 52].¹⁴ Furthermore, by blocking finitely many physical sites, one can always make \mathcal{U} into a simple tensor that satisfies [51, 52]

$$\begin{array}{c} \text{Diagram 1: } \text{A square loop with vertices } \Lambda^l \text{ and } \Lambda^r. \text{ The top edge is } \mathcal{U}^\dagger, \text{ the bottom edge is } \mathcal{U}, \text{ the left edge is } \mathcal{U}^\dagger, \text{ and the right edge is } \mathcal{U}. \text{ A dot at the center is labeled } \Lambda^r. \\ \text{Diagram 2: } \text{A square loop with vertices } \Lambda^l \text{ and } \Lambda^r. \text{ The top edge is } \mathcal{U}^\dagger, \text{ the bottom edge is } \mathcal{U}, \text{ the left edge is } \mathcal{U}^\dagger, \text{ and the right edge is } \mathcal{U}. \text{ A dot at the center is labeled } \Lambda^r. \\ \text{Diagram 3: } \text{A square loop with vertices } \Lambda^l \text{ and } \Lambda^r. \text{ The top edge is } \mathcal{U}^\dagger, \text{ the bottom edge is } \mathcal{U}, \text{ the left edge is } \mathcal{U}^\dagger, \text{ and the right edge is } \mathcal{U}. \text{ A dot at the center is labeled } \Lambda^l. \end{array} = \uparrow, \quad \text{Diagram 2} = \text{Diagram 3}. \quad (\text{IV.17})$$

Here, the fixed points Λ^l and Λ^r are supposed to be properly normalized. The above equation readily implies that the MPU tensor \mathcal{U} satisfies (IV.10). Furthermore, since \mathcal{U}^\dagger also generates an MPU, it satisfies¹⁵

$$\begin{array}{c} \text{Diagram 1: } \text{A square loop with vertices } \Lambda^l \text{ and } \Lambda^r. \text{ The top edge is } \mathcal{U}, \text{ the bottom edge is } \mathcal{U}^\dagger, \text{ the left edge is } \mathcal{U}, \text{ and the right edge is } \mathcal{U}^\dagger. \text{ A dot at the center is labeled } \Lambda^r. \\ \text{Diagram 2: } \text{A square loop with vertices } \Lambda^l \text{ and } \Lambda^r. \text{ The top edge is } \mathcal{U}, \text{ the bottom edge is } \mathcal{U}^\dagger, \text{ the left edge is } \mathcal{U}, \text{ and the right edge is } \mathcal{U}^\dagger. \text{ A dot at the center is labeled } \Lambda^r. \\ \text{Diagram 3: } \text{A square loop with vertices } \Lambda^l \text{ and } \Lambda^r. \text{ The top edge is } \mathcal{U}, \text{ the bottom edge is } \mathcal{U}^\dagger, \text{ the left edge is } \mathcal{U}, \text{ and the right edge is } \mathcal{U}^\dagger. \text{ A dot at the center is labeled } \Lambda^l. \end{array} = \uparrow, \quad \text{Diagram 2} = \text{Diagram 3}, \quad (\text{IV.18})$$

which implies (IV.11). Thus, any invertible symmetry operator can be represented by a topological injective MPO.

In [51, Theorem III.8], it was shown that the left and right ranks of the MPU tensor satisfying (IV.17) obey

$$\text{rank}_l(\mathcal{U})\text{rank}_r(\mathcal{U}) = \dim(\mathcal{H}_o)^2. \quad (\text{IV.19})$$

This implies that the lattice quantum dimension of any MPU is equal to one because

$$\text{qdim}_{\text{lat}}(\mathcal{U}) = \sqrt{\frac{\text{rank}_l(\mathcal{U})\text{rank}_r(\mathcal{U})}{\dim(\mathcal{H}_o)^2}} = 1. \quad (\text{IV.20})$$

On the other hand, it was shown in [51, 52] that the index of an MPU defined by (IV.15) agrees with the GNVW index defined in [40], i.e.,

$$\text{ind}(\mathcal{U}) = \text{GNVW}(\mathcal{D}[\mathcal{U}]), \quad (\text{IV.21})$$

where the right-hand side is the GNVW index of the MPU $\mathcal{D}[\mathcal{U}]$. Due to (IV.20) and (IV.21), the left and right dimensions of \mathcal{U} can be written in terms of the GNVW index as

$$\text{lind}(\mathcal{U}) = \text{GNVW}(\mathcal{D}[\mathcal{U}]), \quad \text{rdim}(\mathcal{U}) = \text{GNVW}(\mathcal{D}[\mathcal{U}])^{-1}. \quad (\text{IV.22})$$

¹⁴ More precisely, the local tensor of any MPU has a single block in its canonical form [51, 52], and thus we can make it injective by blocking a finite number of physical sites.

¹⁵ We can always block sufficiently many physical sites so that both (IV.17) and (IV.18) are satisfied at the same time.

As we will discuss in Section IV D, the left and right dimensions defined by (IV.13) agree with (II.1) defined in terms of defect Hilbert spaces. Thus, equation (IV.22) implies that the dimension of the defect Hilbert space associated with a QCA is given by the GNVW index multiplied by the dimension of the original Hilbert space. This fact was observed in [28, 45] in the case of the lattice translation operator.

Detachable MPU is a tensor product operator. Before proceeding, we demonstrate the importance of having at least two physical legs in the defining equations (IV.10) and (IV.11) of topological injective MPOs. To this end, we consider an MPU tensor \mathcal{U} that satisfies an analogue of (IV.10) for a single physical leg, that is,

$$\begin{array}{c} \text{Diagram: } \Lambda^l \text{ (left leg)} \xrightarrow{\mathcal{U}} \text{ (right leg)} \xrightarrow{\mathcal{U}^\dagger} \Lambda^r \\ \text{Diagram: } \Lambda^l \text{ (left leg)} \xrightarrow{\mathcal{U}} \text{ (right leg)} \xrightarrow{\mathcal{U}^\dagger} \Lambda^r \end{array} = \begin{array}{c} \text{Diagram: } \Lambda^l \text{ (left leg)} \xrightarrow{\mathcal{U}} \text{ (right leg)} \\ \text{Diagram: } \Lambda^r \text{ (left leg)} \xrightarrow{\mathcal{U}^\dagger} \text{ (right leg)} \end{array} \quad (\text{IV.23})$$

Namely, we consider an MPU that is detachable from the physical legs. In this case, we can show that the MPU $D[\mathcal{U}]$ is the tensor product of on-site operators; in other words, the bond Hilbert space V of the MPU tensor \mathcal{U} is one-dimensional. To see this, we compute the left and right ranks of \mathcal{U} as

$$\text{rank}_l(\mathcal{U}) = \text{rank} \left(\begin{array}{c} \text{Diagram: } \Lambda^l \text{ (left leg)} \xrightarrow{\mathcal{U}} \text{ (right leg)} \xrightarrow{\mathcal{U}^\dagger} \Lambda^r \\ \text{Diagram: } \Lambda^l \text{ (left leg)} \xrightarrow{\mathcal{U}} \text{ (right leg)} \xrightarrow{\mathcal{U}^\dagger} \Lambda^r \end{array} \right) = \text{rank} \left(\begin{array}{c} \text{Diagram: } \Lambda^l \text{ (left leg)} \xrightarrow{\mathcal{U}} \text{ (right leg)} \xrightarrow{\mathcal{U}^\dagger} \Lambda^r \\ \text{Diagram: } \Lambda^r \text{ (left leg)} \xrightarrow{\mathcal{U}^\dagger} \text{ (right leg)} \end{array} \right) \stackrel{(\text{IV.23})}{=} \dim(V) \dim(\mathcal{H}_o), \quad (\text{IV.24})$$

$$\text{rank}_r(\mathcal{U}) = \text{rank} \left(\begin{array}{c} \text{Diagram: } \Lambda^l \text{ (left leg)} \xrightarrow{\mathcal{U}} \text{ (right leg)} \xrightarrow{\mathcal{U}^\dagger} \Lambda^r \\ \text{Diagram: } \Lambda^r \text{ (left leg)} \xrightarrow{\mathcal{U}^\dagger} \text{ (right leg)} \xrightarrow{\mathcal{U}} \Lambda^l \end{array} \right) \stackrel{(\text{IV.23})}{=} \dim(V) \dim(\mathcal{H}_o), \quad (\text{IV.25})$$

where we used the fact that Λ^l and Λ^r are positive definite and $\text{rank}(f) = \text{rank}(f^\dagger f)$ for any linear map f . The above equation implies that $\text{rank}_l(\mathcal{U})\text{rank}_r(\mathcal{U}) = \dim(V)^2 \dim(\mathcal{H}_o)^2$. On the other hand, as shown in [51, Theorem III.8], the product of the left and right ranks of a general MPU tensor satisfying (IV.17) is given by (IV.19). Therefore, it follows that $\dim(V) = 1$, i.e., the MPU satisfying the stronger condition (IV.23) must be the tensor product of on-site operators.

C. Topological injective MPOs

In this subsection, we derive several properties of topological injective MPO tensors.

Normalization of \mathcal{O} . We first point out that the normalization of a topological injective MPO tensor \mathcal{O} is fixed by the condition (IV.10). Indeed, the condition (IV.10) implies that \mathcal{O} is normalized

so that the largest eigenvalue of the transfer matrix $T[\mathcal{O}]$ is given by $\dim(\mathcal{H}_o)$, that is,

$$\Lambda^l \otimes \mathcal{O}^\dagger \otimes \mathcal{O} = \dim(\mathcal{H}_o) \Lambda^l, \quad \mathcal{O}^\dagger \otimes \mathcal{O} \otimes \Lambda^r = \dim(\mathcal{H}_o) \Lambda^r. \quad (\text{IV.26})$$

The first equality can be verified by taking a partial trace in the first equality of (IV.10). More specifically, by taking the trace only over the left physical leg in the first equality of (IV.10), we obtain

$$\dim(\mathcal{H}_o) \Lambda^l \otimes \mathcal{O}^\dagger \otimes \mathcal{O} \stackrel{(\text{IV.10})}{=} \Lambda^l \otimes \mathcal{O}^\dagger \otimes \mathcal{O}^\dagger \otimes \mathcal{O} \stackrel{(\text{IV.6})}{=} \lambda \Lambda^l \otimes \mathcal{O}^\dagger \otimes \mathcal{O}. \quad (\text{IV.27})$$

The above equation implies that $\lambda = \dim(\mathcal{H}_o)$, which shows the first equality of (IV.26). The second equality of (IV.26) can also be verified similarly. Due to the normalization (IV.26), a scalar multiple of a topological injective MPO tensor is no longer topological in general. We note that the same normalization of an MPO tensor is employed in [36].

Bubble removal. The condition (IV.10) also implies that a small loop of a topological injective MPO acting on a single physical leg can be removed at the cost of a scalar multiplication. More specifically, one can show that

$$\Lambda^l \otimes \mathcal{O}^\dagger \otimes \mathcal{O} \otimes \Lambda^r = \gamma \uparrow, \quad (\text{IV.28})$$

where the proportionality constant γ is given by

$$\gamma := \Lambda^l \otimes \Lambda^r = \text{tr}(\Lambda^l \Lambda^r). \quad (\text{IV.29})$$

We note that γ is a positive real number because Λ^l and Λ^r are positive definite.¹⁶ By definition, γ depends on the normalization of Λ^l and Λ^r . To show (IV.28), we again consider a partial trace in the first equation of (IV.10). By taking the trace only for the right physical leg in the first equality and capping the virtual leg with Λ^r , we obtain

$$\Lambda^l \otimes \mathcal{O}^\dagger \otimes \mathcal{O} \otimes \Lambda^r \stackrel{(\text{IV.26})}{=} \frac{1}{\dim(\mathcal{H}_o)} \Lambda^l \otimes \mathcal{O}^\dagger \otimes \mathcal{O}^\dagger \otimes \Lambda^r \stackrel{(\text{IV.10})}{=} \frac{1}{\dim(\mathcal{H}_o)} \left| \Lambda^l \otimes \mathcal{O}^\dagger \otimes \mathcal{O} \otimes \Lambda^r \right| \stackrel{(\text{IV.26})}{=} \gamma \uparrow,$$

¹⁶ Since $\sqrt{\Lambda^l} \Lambda^r \sqrt{\Lambda^l}$ is positive definite, we have $\text{tr}(\Lambda^l \Lambda^r) = \text{tr}(\sqrt{\Lambda^l} \Lambda^r \sqrt{\Lambda^l}) > 0$.

which shows (IV.28). We note that a loop of a topological injective MPO acting on multiple physical legs can also be removed similarly. This is because the condition (IV.10) allows us to shrink the loop into the one acting only on a single physical leg, which can be removed by (IV.28).

Zigzag relations. Using the conditions (IV.10) and (IV.11) together with the injectivity, one can show that a topological injective MPO tensor \mathcal{O} satisfies the following zigzag relations:¹⁷

$$\text{Left Diagram: } \Lambda^l \circ \mathcal{O} \circ \mathcal{O}^\dagger \circ \Lambda^r = \delta_l(\mathcal{O}) \circ \mathcal{O} \circ \Lambda^r, \quad \text{Right Diagram: } \Lambda^l \circ \mathcal{O}^\dagger \circ \mathcal{O} \circ \Lambda^r = \delta_r(\mathcal{O}) \circ \mathcal{O} \circ \Lambda^r. \quad (\text{IV.30})$$

Here, $\delta_l(\mathcal{O})$ and $\delta_r(\mathcal{O})$ are the positive real numbers defined by

$$\delta_l(\mathcal{O}) := \frac{\gamma}{\text{ldim}(\mathcal{O})}, \quad \delta_r(\mathcal{O}) := \frac{\gamma}{\text{rdim}(\mathcal{O})}, \quad (\text{IV.31})$$

where γ is given by (IV.29). We note that $\delta_l(\mathcal{O})$ and $\delta_r(\mathcal{O})$ depend on the normalization of Λ^l and Λ^r just as γ does. We also emphasize that when $\text{ind}(\mathcal{O}) \neq 1$, we cannot set $\delta_l(\mathcal{O})$ and $\delta_r(\mathcal{O})$ to one simultaneously because $\delta_l(\mathcal{O})/\delta_r(\mathcal{O}) = \text{ind}(\mathcal{O})^{-2}$. Equation (IV.30) can be verified by following the proof of [53, Proposition 1]. For completeness, we give a proof below.

To show the first equality of (IV.30), we notice that the linear map defined by the left-hand side, which we denoted by s , commutes with \mathcal{O} in the following sense:

$$\text{Left Diagram: } s \circ \mathcal{O} = \text{Middle Diagram: } \Lambda^l \circ \mathcal{O} \circ \mathcal{O}^\dagger \circ \Lambda^r = \text{Right Diagram: } \mathcal{O} \circ s = s \circ \mathcal{O}. \quad (\text{IV.32})$$

Here, the second equality follows from (IV.10) and (IV.11). By applying the above equation repeatedly, we obtain

$$\text{Left Diagram: } s \circ \mathcal{O} = \text{Right Diagram: } s \circ \mathcal{O} \circ s \circ \mathcal{O} \circ s \circ \mathcal{O} \circ s. \quad (\text{IV.33})$$

Now, since \mathcal{O} is injective, it has a left inverse $\tilde{\mathcal{O}}$ that satisfies

$$\text{Left Diagram: } \tilde{\mathcal{O}} \circ \mathcal{O} = \text{Right Diagram: } \tilde{\mathcal{O}} \circ \mathcal{O} \circ \tilde{\mathcal{O}} = \tilde{\mathcal{O}} \circ \tilde{\mathcal{O}}. \quad (\text{IV.34})$$

By applying $\tilde{\mathcal{O}}$ to the middle physical leg of (IV.33) and taking the trace over this physical leg, we obtain

$$\text{Left Diagram: } s \circ \mathcal{O} = \text{Right Diagram: } \mathcal{O} \circ s. \quad (\text{IV.35})$$

¹⁷ In other words, a topological injective MPO in the sense of Definition IV.1 is a topological injective MPO in the sense of Definition IV.2. The converse is also true; we refer the reader to Appendix B for a proof.

Therefore, there exists a constant $\delta_l(\mathcal{O})$ such that

$$\begin{array}{c} \text{---} \nearrow s \\ \text{---} \end{array} = \delta_l(\mathcal{O}) \begin{array}{c} \text{---} \nearrow \mathcal{O} \\ \text{---} \end{array}. \quad (\text{IV.36})$$

This shows the first equality of (IV.30). A similar computation shows that there also exists another constant $\delta_r(\mathcal{O})$ that satisfies the second equation of (IV.30). In Appendix C, we will show that $\delta_l(\mathcal{O})$ and $\delta_r(\mathcal{O})$ are given by (IV.31).

D. Defect Hilbert spaces and movement operators

In this subsection, we define the defect Hilbert spaces associated with a topological injective MPO $D[\mathcal{O}]$ and describe the unitary operator that moves the defect.

Defect Hilbert spaces. The defect Hilbert spaces $\mathcal{H}_{D[\mathcal{O}]}^l$ and $\mathcal{H}_{D[\mathcal{O}]}^r$ are defined by replacing the on-site Hilbert space \mathcal{H}_o on a single site with another finite dimensional Hilbert space L or R . More specifically, we define

$$\mathcal{H}_{D[\mathcal{O}]}^l := L \otimes \mathcal{H}_o^{\otimes N-1}, \quad \mathcal{H}_{D[\mathcal{O}]}^r := R \otimes \mathcal{H}_o^{\otimes N-1}, \quad (\text{IV.37})$$

where N is the total number of sites. Here, the vector spaces L and R are given by

$$L := \text{Im}(P_l), \quad R := \text{Im}(P_r), \quad (\text{IV.38})$$

where P_l and P_r are the projectors defined by

$$P_l := \frac{1}{\delta_l(\mathcal{O})} \begin{array}{c} \text{---} \nearrow \sqrt{\Lambda^l} \otimes \mathcal{O}^\dagger \\ \text{---} \nearrow \mathcal{O} \\ \text{---} \end{array}, \quad P_r := \frac{1}{\delta_r(\mathcal{O})} \begin{array}{c} \text{---} \nearrow \mathcal{O}^\dagger \\ \text{---} \nearrow \Lambda^r \\ \text{---} \end{array}. \quad (\text{IV.39})$$

In particular, L and R are subspaces of $V \otimes \mathcal{H}_o$ and $\mathcal{H}_o \otimes V^*$, where V is the bond Hilbert space of \mathcal{O} and V^* is its dual vector space. We note that P_l is an orthogonal projector, i.e., it satisfies $P_l^2 = P_l$ and $P_l^\dagger = P_l$. The first equality follows from the zigzag equation (IV.30) and the second equality follows from the Hermiticity of $\sqrt{\Lambda^l}$ and Λ^r . Similarly, P_r is also an orthogonal projector.

For the above definition of the defect Hilbert spaces, the left and right dimensions defined by (IV.13) agree with those in (II.1), that is,

$$\text{ldim}(\mathcal{O}) := \frac{\text{rank}_l(\mathcal{O})}{\dim(\mathcal{H}_o)} = \frac{\dim(\mathcal{H}_{D[\mathcal{O}]}^l)}{\dim(\mathcal{H})}, \quad \text{rdim}(\mathcal{O}) := \frac{\text{rank}_r(\mathcal{O})}{\dim(\mathcal{H}_o)} = \frac{\dim(\mathcal{H}_{D[\mathcal{O}]}^r)}{\dim(\mathcal{H})}. \quad (\text{IV.40})$$

This can be verified by a direct computation as follows:

$$\frac{\dim(\mathcal{H}_{D[\mathcal{O}]}^l)}{\dim(\mathcal{H})} = \frac{\text{tr}(P_l)}{\dim(\mathcal{H}_o)} = \frac{\gamma}{\delta_l(\mathcal{O})} = \text{ldim}(\mathcal{O}), \quad \frac{\dim(\mathcal{H}_{D[\mathcal{O}]}^r)}{\dim(\mathcal{H})} = \frac{\text{tr}(P_r)}{\dim(\mathcal{H}_o)} = \frac{\gamma}{\delta_r(\mathcal{O})} = \text{rdim}(\mathcal{O}).$$

Here, we used (IV.28) and (IV.31).

Movement operators. On the defect Hilbert spaces $\mathcal{H}_{D[\mathcal{O}]}^l$ and $\mathcal{H}_{D[\mathcal{O}]}^r$, one can define unitary operators that move the defect by one site. We refer to such unitary operators as movement operators following [28, 45, 58]. Concretely, the movement operators on $\mathcal{H}_{D[\mathcal{O}]}^l$ and $\mathcal{H}_{D[\mathcal{O}]}^r$ are given by

$$u_l := \frac{1}{\delta_l(\mathcal{O})} \begin{array}{c} \text{Diagram of } u_l \text{ (left)} \\ \text{Diagram of } u_r \text{ (right)} \end{array}, \quad u_r := \frac{1}{\delta_r(\mathcal{O})} \begin{array}{c} \text{Diagram of } u_r \text{ (left)} \\ \text{Diagram of } u_l \text{ (right)} \end{array}. \quad (\text{IV.41})$$

Here, the wiggly and thick lines represent the new physical legs L and R at the defect locus, and $\pi_l : V \otimes \mathcal{H}_o \rightarrow L$ and $\pi_r : \mathcal{H}_o \otimes V^* \rightarrow R$ are the linear maps obtained by restricting the target vector spaces of P_l and P_r to their images L and R , respectively. The unlabeled dots in the first and second equations of (IV.41) represent $\sqrt{\Lambda^l}$ and $\sqrt{\Lambda^r}$. For later use, we mention that π_l and π_r satisfy

$$\pi_l^\dagger \pi_l = P_l, \quad \pi_l \pi_l^\dagger = \text{id}_L, \quad \pi_r^\dagger \pi_r = P_r, \quad \pi_r \pi_r^\dagger = \text{id}_R. \quad (\text{IV.42})$$

The operators u_l and u_r defined above move the defect to the right by one site. On the other hand, the operators that move the defect to the left by one site are given by

$$u_l^\dagger = \frac{1}{\delta_l(\mathcal{O})} \begin{array}{c} \text{Diagram of } u_l^\dagger \text{ (left)} \\ \text{Diagram of } u_r^\dagger \text{ (right)} \end{array}, \quad u_r^\dagger = \frac{1}{\delta_r(\mathcal{O})} \begin{array}{c} \text{Diagram of } u_r^\dagger \text{ (left)} \\ \text{Diagram of } u_l^\dagger \text{ (right)} \end{array}. \quad (\text{IV.43})$$

The operators in (IV.43) are the inverses of those in (IV.41). In particular, the movement operators u_l and u_r are unitary. The unitarity of u_l can be verified by a direct computation as follows:

$$u_l^\dagger u_l = \frac{1}{\delta_l(\mathcal{O})^3} \begin{array}{c} \text{Diagram of } u_l^\dagger u_l \text{ (left)} \\ = \end{array} \frac{1}{\delta_l(\mathcal{O})} \begin{array}{c} \text{Diagram of } u_l^\dagger \text{ (left)} \\ = \end{array} \frac{1}{\delta_l(\mathcal{O})} \begin{array}{c} \text{Diagram of } u_l \text{ (left)} \\ = \end{array} \text{id}_{L \otimes \mathcal{H}_o}.$$

Here, the first equality follows from $\pi_l^\dagger \pi_l = P_l$, the second equality follows from the zigzag relation (IV.30), the third equality follows from the condition (IV.10), and the last equality follows

from $\pi_l P_l = \pi_l$ and $\pi_l \pi_l^\dagger = \text{id}_L$. A similar computation also shows $u_l u_l^\dagger = \text{id}_{\mathcal{H}_o \otimes L}$, and hence u_l is unitary. One can also show the unitarity of u_r in the same way.

Compatibility with the unitary structure. As an immediate consequence of (IV.40) and (IV.14), the dimensions of the defect Hilbert spaces associated with topological injective MPOs $D[\mathcal{O}]$ and $D[\mathcal{O}]^\dagger = D[\mathcal{O}^\dagger]$ are related by

$$\dim(\mathcal{H}_{D[\mathcal{O}]^\dagger}^l) = \dim(\mathcal{H}_{D[\mathcal{O}]}^r), \quad \dim(\mathcal{H}_{D[\mathcal{O}]^\dagger}^r) = \dim(\mathcal{H}_{D[\mathcal{O}]}^l). \quad (\text{IV.44})$$

This implies that there exist isomorphisms between these defect Hilbert spaces, i.e.,

$$\mathcal{H}_{D[\mathcal{O}]^\dagger}^l \cong \mathcal{H}_{D[\mathcal{O}]}^r, \quad \mathcal{H}_{D[\mathcal{O}]^\dagger}^r \cong \mathcal{H}_{D[\mathcal{O}]}^l. \quad (\text{IV.45})$$

In other words, the defect Hilbert spaces defined above satisfy Assumption 4.

Let us now construct these isomorphisms in a canonical way. To this end, we notice that the projectors P_l and P_r defined for \mathcal{O} and \mathcal{O}^\dagger are related by¹⁸

$$P_l[\mathcal{O}^\dagger] = f_{lr} P_r[\mathcal{O}] f_{lr}^\dagger, \quad P_r[\mathcal{O}^\dagger] = f_{rl} P_l[\mathcal{O}] f_{rl}^\dagger, \quad (\text{IV.46})$$

where f_{lr} and f_{rl} are defined by

$$f_{lr} := \frac{1}{\sqrt{\delta_r(\mathcal{O})}} \begin{array}{c} \sqrt{\Lambda^l} \otimes \\ \nearrow \\ \text{---} \end{array} \text{---} \begin{array}{c} \mathcal{O} \\ \nearrow \\ \text{---} \end{array} \begin{array}{c} \text{---} \\ \nearrow \\ \bullet \sqrt{\Lambda^r} \end{array}, \quad f_{rl} := \frac{1}{\sqrt{\delta_l(\mathcal{O})}} \begin{array}{c} \text{---} \\ \nearrow \\ \bullet \sqrt{\Lambda^r} \end{array} \begin{array}{c} \mathcal{O} \\ \nearrow \\ \text{---} \end{array} \begin{array}{c} \text{---} \\ \nearrow \\ \bullet \sqrt{\Lambda^l} \otimes \end{array}. \quad (\text{IV.47})$$

Equation (IV.46) readily follows from the zigzag relations (IV.30). Similarly, one can also show that

$$P_l[\mathcal{O}] = f_{rl}^\dagger P_r[\mathcal{O}^\dagger] f_{rl}, \quad P_r[\mathcal{O}] = f_{lr}^\dagger P_l[\mathcal{O}^\dagger] f_{lr}. \quad (\text{IV.48})$$

Using the linear maps f_{lr} and f_{rl} , we can construct canonical isomorphisms (IV.45) between the defect Hilbert spaces. More specifically, we can define unitary maps between the local Hilbert spaces at the defect locus as follows:

$$g_{lr} := \pi_l[\mathcal{O}^\dagger] f_{lr} \pi_r[\mathcal{O}]^\dagger : R[\mathcal{O}] \xrightarrow{\cong} L[\mathcal{O}^\dagger], \quad g_{rl} := \pi_r[\mathcal{O}^\dagger] f_{rl} \pi_l[\mathcal{O}]^\dagger : L[\mathcal{O}] \xrightarrow{\cong} R[\mathcal{O}^\dagger]. \quad (\text{IV.49})$$

The unitarity of g_{lr} can be verified by a direct computation as

$$\begin{aligned} g_{lr}^\dagger g_{lr} &= \pi_r[\mathcal{O}] f_{lr}^\dagger P_l[\mathcal{O}^\dagger] f_{lr} \pi_r[\mathcal{O}]^\dagger = \pi_r[\mathcal{O}] P_r[\mathcal{O}] \pi_r[\mathcal{O}]^\dagger = \text{id}_{R[\mathcal{O}]}, \\ g_{lr} g_{lr}^\dagger &= \pi_l[\mathcal{O}^\dagger] f_{lr} P_r[\mathcal{O}] f_{lr}^\dagger \pi_l[\mathcal{O}^\dagger]^\dagger = \pi_l[\mathcal{O}^\dagger] P_l[\mathcal{O}]^\dagger \pi_l[\mathcal{O}^\dagger] = \text{id}_{L[\mathcal{O}^\dagger]}. \end{aligned} \quad (\text{IV.50})$$

Here, we used equations (IV.46), (IV.48), and (IV.42). A similar computation shows that g_{rl} is also unitary. The unitary maps (IV.49) give isomorphisms (IV.45) between the defect Hilbert spaces.

¹⁸ To avoid confusion, the projectors P_l and P_r defined by (IV.39) are denoted by $P_l[\mathcal{O}]$ and $P_r[\mathcal{O}]$ for now. The same convention applies to π_l and π_r , as well as the vector spaces L and R defined by (IV.38).

E. Relation to sequential quantum circuits

It was recently argued in [36] that non-invertible symmetry operators on the lattice can be generally implemented by using sequential quantum circuits [59]. In this subsection, we discuss the relation between sequential quantum circuits and topological injective MPOs. In particular, we will derive the sequential circuit representations of topological injective MPOs and show that each local unitary gate comprising the circuit can be identified with the movement operator defined in the previous subsection. We will also write down the defect creation and annihilation operators, which complement the unitary circuit part of the symmetry operator and make the full symmetry action non-invertible.

Decompositions of topological injective MPO tensors. To derive the sequential circuit representation, we first decompose a topological injective MPO tensor \mathcal{O} into two three-leg tensors as was done in the case of MPUs in [51]. To this end, we begin with the singular value decomposition of \mathcal{O} , which can be depicted as follows:

$$\begin{array}{c} \text{Diagram of } \mathcal{O} \\ \text{Diagram of } V_l^\dagger D_l U_l \\ \text{Diagram of } D_r V_r^\dagger U_r \end{array} = \quad \text{.} \quad \text{(IV.51)}$$

Here, the bond dimensions of the red wiggly and blue thick lines are given by $\text{rank}_l(\mathcal{O})$ and $\text{rank}_r(\mathcal{O})$, respectively. The two-leg tensors D_i for $i = l, r$ are diagonal matrices with positive diagonal entries, and (the Hermitian conjugates of) the three-leg tensors V_i and U_i are isometries, which satisfy

$$\begin{array}{c} \text{Diagram of } V_l \\ \text{Diagram of } U_l \\ \text{Diagram of } V_r^\dagger \\ \text{Diagram of } U_r^\dagger \end{array} = \quad \text{.} \quad \text{(IV.52)}$$

Using the above decomposition, we can also write the four-leg tensor \mathcal{O} as

$$\begin{array}{c} \text{Diagram of } \mathcal{O} \\ \text{Diagram of } A_l \\ \text{Diagram of } B_l \\ \text{Diagram of } A_r \\ \text{Diagram of } B_r \end{array} = \quad \text{.} \quad \text{(IV.53)}$$

where A_l , B_l , A_r , and B_r are defined by

$$A_l := V_l^\dagger \left(V_l (\text{id} \otimes \Lambda^r) V_l^\dagger \right)^{-\frac{1}{2}}, \quad B_l := U_l \left(V_l (\text{id} \otimes \Lambda^r) V_l^\dagger \right)^{\frac{1}{2}} D_l, \quad \text{(IV.54)}$$

$$A_r := U_r \left(V_r (\Lambda^l \otimes \text{id}) V_r^\dagger \right)^{-\frac{1}{2}}, \quad B_r := U_r \left(V_r (\Lambda^l \otimes \text{id}) V_r^\dagger \right)^{\frac{1}{2}} D_r. \quad \text{(IV.55)}$$

We note that the two-leg tensors $\left(V_l(\text{id} \otimes \Lambda^r)V_l^\dagger\right)^{\pm 1/2}$ and $\left(V_r(\Lambda^l \otimes \text{id})V_r^\dagger\right)^{\pm 1/2}$ make sense because Λ^l and Λ^r are positive definite. By construction, A_l and A_r satisfy

$$A_l^\dagger \begin{array}{c} \text{---} \\ \text{---} \end{array} \bullet \Lambda^r = \text{---}, \quad \Lambda^l \begin{array}{c} \text{---} \\ \text{---} \end{array} A_r^\dagger = \text{---}. \quad (\text{IV.56})$$

We remark that the same decomposition was used in [51] to derive the standard form of MPUs. We also note that the above decomposition is always possible for any MPO tensor \mathcal{O} and any positive definite linear maps Λ^l and Λ^r . In what follows, we will be interested in the case where \mathcal{O} is a topological injective MPO tensor and Λ^l and Λ^r are the fixed points of the transfer matrix $\mathsf{T}[\mathcal{O}]$.

Sequential circuit representation. Using the decomposition (IV.53), we can express the topological injective MPO $D[\mathcal{O}]$ on a periodic chain as

$$D[\mathcal{O}] = \begin{array}{c} \text{Diagram of } \mathcal{O} \text{ with } w_l, B_l, A_l \text{ and } \dots \end{array} = \begin{array}{c} \text{Diagram of } \mathcal{O} \text{ with } w_r, A_r, B_r \text{ and } \dots \end{array}, \quad (\text{IV.57})$$

where the local operators w_l and w_r are defined by

$$w_l := A_l \xrightarrow{\text{red spring}} B_l \quad , \quad w_r := B_r \xrightarrow{\text{blue spring}} A_r \quad . \quad (\text{IV.58})$$

Let us show that w_l and w_r are unitary when \mathcal{O} is topological. To show the unitarity of w_l , we express the second equation in (IV.10) using A_l and B_l as follows:

$$\begin{array}{c} \text{Diagram showing two coupled oscillators:} \\ \text{Left: Two coupled oscillators. The top oscillator has a mass } w_l^\dagger \text{ and spring } B_l^\dagger. \text{ The bottom oscillator has a mass } w_l \text{ and spring } B_l. \text{ They are coupled by a spring } A_l \text{ and a mass } \Lambda^r. \\ \text{Right: The coupled system is equivalent to a single oscillator with mass } \Lambda^r \text{ and spring } B_l. \end{array} = \text{ (IV.59)}$$

The small loops involving Λ^r on both sides can be removed by using (IV.56). Furthermore, we can remove B_l from both sides by multiplying its right inverse

$$\tilde{B}_l := U_l^\dagger D_l^{-1} \left(V_l (\text{id} \otimes \Lambda^r) V_l^\dagger \right)^{-\frac{1}{2}}, \quad (\text{IV.60})$$

which satisfies $B_l \tilde{B}_l = \text{id}$. Similarly, we can also remove B_l^\dagger from both sides of (IV.59) by multiplying its left inverse \tilde{B}_l^\dagger . Thus, after multiplying \tilde{B}_l from the bottom and \tilde{B}_l^\dagger from the top, equation (IV.59) reduces to

$$w_l^\dagger w_l = \text{id.} \quad (\text{IV.61})$$

Since w_l is a square matrix of finite size, the above equation also implies

$$w_l w_l^\dagger = \text{id}, \quad (\text{IV.62})$$

which shows that w_l is unitary. The unitarity of w_r can also be shown similarly. The sequence of local unitary operators w_l or w_r in (IV.57) is referred to as a sequential quantum circuit [59]. The entire MPO of the form (IV.57) is called a sequential MPO in [36].

We note that the derivation of the sequential circuit representation (IV.57) does not directly use the injectivity of \mathcal{O} . More specifically, even if the MPO tensor \mathcal{O} is not injective, the MPO $D[\mathcal{O}]$ has a sequential circuit representation as long as there exist positive definite matrices Λ^l and Λ^r that satisfy (IV.10). When \mathcal{O} is injective, such Λ^l and Λ^r , if they exist, can always be chosen to be the fixed points of the transfer matrix as shown in Appendix A.

Movement operators revisited. The sequential circuit representation (IV.57) suggests that w_l and w_r can be regarded as movement operators. Indeed, due to the decomposition (IV.53), the movement operators u_l and u_r defined by (IV.41) can be expressed in terms of w_l and w_r as follows:

$$u_l = \begin{array}{c} \text{wiggly line} \\ \text{horizontal bar} \\ \text{wiggly line} \end{array} \quad , \quad u_r = \begin{array}{c} \text{horizontal bar} \\ \text{wiggly line} \\ \text{horizontal bar} \end{array} \quad . \quad (\text{IV.63})$$

Here, the linear maps f_l and f_r are defined by

$$f_l := \frac{1}{\sqrt{\delta_l(\mathcal{O})}} \sqrt{\Lambda^l} \otimes \begin{array}{c} \text{wiggly line} \\ \text{horizontal bar} \\ \text{wiggly line} \end{array} \quad , \quad f_r := \frac{1}{\sqrt{\delta_r(\mathcal{O})}} \begin{array}{c} \text{horizontal bar} \\ \text{wiggly line} \\ \text{horizontal bar} \end{array} \otimes \sqrt{\Lambda^r} . \quad (\text{IV.64})$$

We note that f_l and f_r are unitary because

$$f_l^\dagger f_l = \begin{array}{c} \text{wiggly line} \\ \text{horizontal bar} \\ \text{wiggly line} \end{array} \otimes \begin{array}{c} \text{wiggly line} \\ \text{horizontal bar} \\ \text{wiggly line} \end{array} = \pi_l P_l \pi_l^\dagger = \text{id}_L, \quad f_r^\dagger f_r = \begin{array}{c} \text{horizontal bar} \\ \text{wiggly line} \\ \text{horizontal bar} \end{array} \otimes \begin{array}{c} \text{horizontal bar} \\ \text{wiggly line} \\ \text{horizontal bar} \end{array} = \pi_r P_r \pi_r^\dagger = \text{id}_R, \quad (\text{IV.65})$$

where we used (IV.56) and (IV.42). Since f_l and f_r are linear maps between finite dimensional vector spaces of the same dimension, the above equation guarantees that $f_l f_l^\dagger$ and $f_r f_r^\dagger$ are also the identity maps, which implies that f_l and f_r are unitary. Thus, equation (IV.63) shows that w_l and w_r agree with the movement operators u_l and u_r up to on-site unitary acting on the physical Hilbert space at the defect locus. In other words, w_l and w_r can be regarded as movement operators on the defect Hilbert spaces isomorphic to (IV.37). More specifically, w_l and w_r are the movement operators on

$$\tilde{\mathcal{H}}_{D[\mathcal{O}]}^l := \tilde{L} \otimes \mathcal{H}_o^{\otimes N-1}, \quad \tilde{\mathcal{H}}_{D[\mathcal{O}]}^r := \tilde{R} \otimes \mathcal{H}_o^{\otimes N-1}, \quad (\text{IV.66})$$

where \tilde{L} and \tilde{R} are the $\text{rank}_l(\mathcal{O})$ -dimensional and $\text{rank}_r(\mathcal{O})$ -dimensional vector spaces associated with the red wiggly line and the blue thick line, respectively. Equation (IV.63) then shows that the

movement operators on the isomorphic defect Hilbert spaces (IV.37) and (IV.66) are intertwined by unitary operators f_l and f_r . We mention that the movement operators w_l and w_r for invertible symmetries are studied in [53].

Defect creation and annihilation operators. The sequential circuit representation (IV.57) was obtained by using the same decomposition of \mathcal{O} on all physical sites. We can obtain other variants of the sequential circuit representation by using different decompositions of \mathcal{O} depending on the sites. For example, if we use a different decomposition of \mathcal{O} only on the first site, we obtain

$$\mathcal{D}[\mathcal{O}] = \text{Diagram with } w_l \text{ on the first site} = \text{Diagram with } w_r \text{ on the first site} \quad . \quad (\text{IV.67})$$

Here, the local operators c and a are defined by

$$c := B_r \xrightarrow{\text{red spring}} B_l \quad , \quad a := A_l \xrightarrow{\text{red spring}} A_r \quad . \quad (\text{IV.68})$$

Physically, c and a are regarded as operators that create and annihilate a pair of defects. We refer to these operators as defect creation and annihilation operators. These operators were originally introduced in [51] for MPUs. We note that the defect creation and annihilation operators are not unitary when the topological injective MPO $\mathcal{D}[\mathcal{O}]$ is non-invertible. Indeed, as is clear from (IV.67), these operators can be unitary only when $\mathcal{D}[\mathcal{O}]$ is unitary. Conversely, when $\mathcal{D}[\mathcal{O}]$ is unitary, these operators are indeed unitary as long as Λ^l and Λ^r are normalized properly [51]. In general, c and a^\dagger are isometries up to scalar, i.e., they satisfy

$$c^\dagger c = \Lambda^l \circ \mathcal{O}^\dagger \circ \mathcal{O} \circ \Lambda^r = \Lambda^l \circ \mathcal{O}^\dagger \circ \mathcal{O} \circ \Lambda^r \mid = \gamma \text{id}_{\mathcal{H}_o \otimes \mathcal{H}_o}, \quad (\text{IV.69})$$

$$aa^\dagger = \frac{1}{\delta_l(\mathcal{O})\delta_r(\mathcal{O})} \Lambda^l \circ \mathcal{O}^\dagger \circ \mathcal{O} \circ \Lambda^r = \frac{\text{ldim}(\mathcal{O})\text{rdim}(\mathcal{O})}{\gamma} \text{id}_{\mathcal{H}_o \otimes \mathcal{H}_o}. \quad (\text{IV.70})$$

Here, the first equality of (IV.69) follows from (IV.53) and (IV.56). Similarly, the first equality of (IV.70) follows from (IV.53) and (B.2). Using the defect creation and annihilation operators, we can also write $\mathcal{D}[\mathcal{O}]$ as

$$\mathcal{D}[\mathcal{O}] = \text{Diagram with } a \text{ and } c \quad . \quad (\text{IV.71})$$

F. Properties of dimensions

In this subsection, we show several basic properties of the left and right dimensions (IV.13) and the lattice quantum dimension (IV.15) of a topological injective MPO tensor \mathcal{O} .

Invariance under blocking. We first show that the left and right dimensions are invariant under blocking a finite number of physical sites. To this end, we consider the local tensor $\mathcal{O}^{[2]}$ obtained by blocking two physical sites as follows:

$$\mathcal{O}^{[2]} = \text{Diagram showing two sites with local tensors } \mathcal{O} \text{ and a central block } \Lambda^r.$$
 (IV.72)

Since \mathcal{O} is topological and injective, $\mathcal{O}^{[2]}$ is also topological and injective. By definition, the left dimension of $\mathcal{O}^{[2]}$ is given by

$$\text{ldim}(\mathcal{O}^{[2]}) = \frac{\text{rank}_l(\mathcal{O}^{[2]})}{\dim(\mathcal{H}_o)^2}. \quad (\text{IV.73})$$

Following the proof of [52, Theorem 3], one can compute the left rank of $\mathcal{O}^{[2]}$ as

$$\text{rank}_l(\mathcal{O}^{[2]}) = \text{rank} \left(\text{Diagram showing two sites with local tensors } \mathcal{O}^\dagger \text{ and a central block } \Lambda^r \right) = \text{rank} \left(\text{Diagram showing two sites with local tensors } \mathcal{O}^\dagger \text{ and a central block } \Lambda^r \right) = \text{rank}_l(\mathcal{O}) \dim(\mathcal{H}_o). \quad (\text{IV.74})$$

In the first and third equalities, we used the fact that Λ^r is positive definite and $\text{rank}(f) = \text{rank}(f^\dagger f)$ for an arbitrary linear map f . The second equality follows from (IV.10). Plugging the above equation into (IV.73), we find

$$\text{ldim}(\mathcal{O}^{[2]}) = \frac{\text{rank}_l(\mathcal{O})}{\dim(\mathcal{H}_o)} = \text{ldim}(\mathcal{O}). \quad (\text{IV.75})$$

The same computation shows that $\text{ldim}(\mathcal{O}^{[n+1]}) = \text{ldim}(\mathcal{O}^{[n]})$ for any positive integer n , where $\mathcal{O}^{[n]}$ is the local tensor obtained by blocking n physical sites. Thus, combining this with (IV.75), we find

$$\text{ldim}(\mathcal{O}^{[n]}) = \text{ldim}(\mathcal{O}). \quad (\text{IV.76})$$

This shows that the left dimension is invariant under blocking any number of physical sites. A similar computation shows that the right dimension is also invariant under blocking. We note that the lattice quantum dimension and the index defined by (IV.15) are also invariant under blocking because they consist only of the left and right dimensions.

Upper and lower bounds of the lattice quantum dimension. Next, we show that the lattice quantum dimension defined in (IV.15) satisfies

$$1 \leq \text{qdim}_{\text{lat}}(\mathcal{O}) \leq \dim(V), \quad (\text{IV.77})$$

where V is the bond Hilbert space of \mathcal{O} . We note that the upper bound in (IV.77) is invariant under the gauge transformation of the MPO tensor \mathcal{O} . Thus, it depends only on the operator $D[\mathcal{O}]$ due to

the fundamental theorem of injective MPS/MPO [55, 56]. The upper bound in (IV.77) immediately follows from the fact that the left and right dimensions of \mathcal{O} are less than or equal to $\dim(V)$ by definition (IV.13). On the other hand, the lower bound in (IV.77) can be obtained by following the proof of [51, Lemma III.7]. More specifically, to derive the lower bound of $\text{qdim}_{\text{lat}}(\mathcal{O})$, we recall that the defect creation operator c satisfies (IV.69), i.e.,

$$c^\dagger c = \gamma \text{id}_{\mathcal{H}_o \otimes \mathcal{H}_o}. \quad (\text{IV.78})$$

Since γ is non-zero, the above equation implies that $\text{rank}(c) = \text{rank}(c^\dagger c) = \dim(\mathcal{H}_o)^2$. On the other hand, since the codomain of c has dimension $\text{rank}_l(\mathcal{O})\text{rank}_r(\mathcal{O})$, the rank of c must be less than or equal to $\text{rank}_l(\mathcal{O})\text{rank}_r(\mathcal{O})$. Therefore, it follows that

$$\text{qdim}_{\text{lat}}(\mathcal{O}) = \frac{\text{rank}_l(\mathcal{O})\text{rank}_r(\mathcal{O})}{\dim(\mathcal{H}_o)^2} \geq 1. \quad (\text{IV.79})$$

We note that $\text{qdim}_{\text{lat}}(\mathcal{O}) = 1$ if and only if the MPO $D[\mathcal{O}]$ is unitary [51, Theorem III.8].

Multiplicativity. The left and right dimensions are multiplicative under the composition of topological injective MPO tensors. More specifically, after blocking a sufficient number of physical sites, we have

$$\text{ldim}(\mathcal{O}_X \mathcal{O}_Y) = \text{ldim}(\mathcal{O}_X) \text{ldim}(\mathcal{O}_Y), \quad \text{rdim}(\mathcal{O}_X \mathcal{O}_Y) = \text{rdim}(\mathcal{O}_X) \text{rdim}(\mathcal{O}_Y), \quad (\text{IV.80})$$

where \mathcal{O}_X and \mathcal{O}_Y are topological injective MPO tensors, and $\mathcal{O}_X \mathcal{O}_Y$ is the composite tensor defined by

$$\mathcal{O}_X \mathcal{O}_Y := \begin{array}{c} \text{Diagram showing the tensor product of } \mathcal{O}_X \text{ and } \mathcal{O}_Y \text{ tensors. The vertical stack of sites is } \mathcal{O}_X \text{ on top, followed by } \mathcal{O}_Y \text{ on the bottom.} \\ \text{Arrows indicate the flow of indices: pink arrows for } \mathcal{O}_X \text{ and blue arrows for } \mathcal{O}_Y. \end{array} \quad (\text{IV.81})$$

In (IV.80), the left and right dimensions of a generally non-injective MPO tensor $\mathcal{O}_X \mathcal{O}_Y$ are defined in the same way as (IV.13), that is, $\text{ldim}(\mathcal{O}_X \mathcal{O}_Y) := \text{rank}_l(\mathcal{O}_X \mathcal{O}_Y) / \dim(\mathcal{H}_o)$ and $\text{rdim}(\mathcal{O}_X \mathcal{O}_Y) := \text{rank}_r(\mathcal{O}_X \mathcal{O}_Y) / \dim(\mathcal{H}_o)$. Following the proof of [52, Theorem 3], we can show the multiplicativity of the left dimension by computing the left rank of $\mathcal{O}_X^{[2]} \mathcal{O}_Y^{[2]}$ as follows:

$$\begin{aligned} \text{rank}_l(\mathcal{O}_X^{[2]} \mathcal{O}_Y^{[2]}) &= \text{rank} \left(\begin{array}{c} \text{Diagram showing the tensor product of } \mathcal{O}_X^{[2]} \text{ and } \mathcal{O}_Y^{[2]}. \\ \text{The vertical stack of sites is } \mathcal{O}_X^{[2]} \text{ on top, followed by } \mathcal{O}_Y^{[2]} \text{ on the bottom.} \\ \text{Arrows indicate the flow of indices: pink arrows for } \mathcal{O}_X^{[2]} \text{ and blue arrows for } \mathcal{O}_Y^{[2]}. \\ \text{A dashed box highlights the central region where the two tensors interact.} \end{array} \right) \\ &= \text{rank} \left(\begin{array}{c} \text{Diagram showing the tensor product of } \mathcal{O}_X^{[2]} \text{ and } \mathcal{O}_Y^{[2]}. \\ \text{The vertical stack of sites is } \mathcal{O}_X^{[2]} \text{ on top, followed by } \mathcal{O}_Y^{[2]} \text{ on the bottom.} \\ \text{Arrows indicate the flow of indices: pink arrows for } \mathcal{O}_X^{[2]} \text{ and blue arrows for } \mathcal{O}_Y^{[2]}. \\ \text{A dashed box highlights the central region where the two tensors interact.} \end{array} \right) \\ &= \text{rank} \left(\begin{array}{c} \text{Diagram showing the tensor product of } \mathcal{O}_X^{[2]} \text{ and } \mathcal{O}_Y^{[2]}. \\ \text{The vertical stack of sites is } \mathcal{O}_X^{[2]} \text{ on top, followed by } \mathcal{O}_Y^{[2]} \text{ on the bottom.} \\ \text{Arrows indicate the flow of indices: pink arrows for } \mathcal{O}_X^{[2]} \text{ and blue arrows for } \mathcal{O}_Y^{[2]}. \\ \text{A dashed box highlights the central region where the two tensors interact.} \end{array} \right) \\ &= \text{rank} \left(\begin{array}{c} \text{Diagram showing the tensor product of } \mathcal{O}_X^{[2]} \text{ and } \mathcal{O}_Y^{[2]}. \\ \text{The vertical stack of sites is } \mathcal{O}_X^{[2]} \text{ on top, followed by } \mathcal{O}_Y^{[2]} \text{ on the bottom.} \\ \text{Arrows indicate the flow of indices: pink arrows for } \mathcal{O}_X^{[2]} \text{ and blue arrows for } \mathcal{O}_Y^{[2]}. \\ \text{A dashed box highlights the central region where the two tensors interact.} \end{array} \right) \\ &= \text{rank}_l(\mathcal{O}_X) \text{rank}_l(\mathcal{O}_Y). \end{aligned}$$

By dividing both sides by $\dim(\mathcal{H}_o)^2$, we find

$$\text{ldim}(\mathcal{O}_X^{[2]} \mathcal{O}_Y^{[2]}) = \text{ldim}(\mathcal{O}_X) \text{ldim}(\mathcal{O}_Y) = \text{ldim}(\mathcal{O}_X^{[2]}) \text{ldim}(\mathcal{O}_Y^{[2]}), \quad (\text{IV.82})$$

where the last equality follows from the fact that $\text{ldim}(\mathcal{O}_X)$ and $\text{ldim}(\mathcal{O}_Y)$ are invariant under blocking. Thus, by blocking two physical sites in the above equation, we obtain the first equality of (IV.80).¹⁹ By a similar computation, we can also show the multiplicativity of the right dimension. The multiplicativity (IV.80) implies that the lattice quantum dimension and the index are also multiplicative in the sense that

$$\text{qdim}_{\text{lat}}(\mathcal{O}_X \mathcal{O}_Y) = \text{qdim}_{\text{lat}}(\mathcal{O}_X) \text{qdim}_{\text{lat}}(\mathcal{O}_Y), \quad \text{ind}(\mathcal{O}_X \mathcal{O}_Y) = \text{ind}(\mathcal{O}_X) \text{ind}(\mathcal{O}_Y). \quad (\text{IV.83})$$

Additivity. It immediately follows from the definition (IV.13) that the left and right dimensions are additive under the direct sum of MPO tensors, i.e.,

$$\text{ldim}(\mathcal{O}_X \oplus \mathcal{O}_Y) = \text{ldim}(\mathcal{O}_X) + \text{ldim}(\mathcal{O}_Y), \quad \text{rdim}(\mathcal{O}_X \oplus \mathcal{O}_Y) = \text{rdim}(\mathcal{O}_X) + \text{rdim}(\mathcal{O}_Y). \quad (\text{IV.84})$$

Here, $\mathcal{O}_X \oplus \mathcal{O}_Y$ is the block injective MPO tensor whose injective blocks are given by \mathcal{O}_X and \mathcal{O}_Y . In other words, $\mathcal{O}_X \oplus \mathcal{O}_Y$ is the direct sum of the linear maps $\mathcal{O}_X : V_X \otimes \mathcal{H}_o \rightarrow \mathcal{H}_o \otimes V_X$ and $\mathcal{O}_Y : V_Y \otimes \mathcal{H}_o \rightarrow \mathcal{H}_o \otimes V_Y$, where V_X and V_Y are the bond Hilbert spaces of \mathcal{O}_X and \mathcal{O}_Y . In (IV.84), the left and right dimensions of a non-injective MPO tensor $\mathcal{O}_X \oplus \mathcal{O}_Y$ are defined in the same way as (IV.13), that is, $\text{ldim}(\mathcal{O}_X \oplus \mathcal{O}_Y) := \text{rank}_l(\mathcal{O}_X \oplus \mathcal{O}_Y) / \dim(\mathcal{H}_o)$ and $\text{rdim}(\mathcal{O}_X \oplus \mathcal{O}_Y) := \text{rank}_r(\mathcal{O}_X \oplus \mathcal{O}_Y) / \dim(\mathcal{H}_o)$. The additivity (IV.84) does not imply that the lattice quantum dimension and the index are additive.

Remark. The multiplicativity (IV.80) and the additivity (IV.84) do not necessarily imply that the left and right dimensions are one-dimensional representations of the fusion rules. This is because the rank of the non-injective MPO tensor $\mathcal{O}_X \mathcal{O}_Y$ may not be equal to the sum of the ranks of its injective blocks due to the off-diagonal components of the tensor. Nevertheless, under the conditions spelled out in Section V, the left and right dimensions of topological injective MPO tensors become one-dimensional representations of the fusion rules; see Section VC2 for more details.

V. SUFFICIENT CONDITIONS FOR THE HOMOGENEITY OF THE INDEX

In this section, we discuss sufficient conditions for the homogeneity of the index of topological injective MPOs. To this end, we first define fusion and splitting tensors for the fusion channels of topological injective MPOs and introduce two conditions on them, which we refer to as the broken zipper condition and the two-sided zipper condition. Assuming that these conditions are satisfied, we will show that the fusion channels of topological injective MPOs are topological, the left and right dimensions are one-dimensional representations of the fusion rules, and the index is homogeneous. As a result, as long as these conditions hold, the fusion category symmetry \mathcal{C} realized by topological injective MPOs must be weakly integral even if we allow mixing with non-trivial QCAs. The broken zipper condition and the two-sided zipper condition for general topological injective MPOs are not proven.²⁰

¹⁹ More precisely, in (IV.80), we have redefined \mathcal{O}_X and \mathcal{O}_Y by $\mathcal{O}_X^{[2]}$ and $\mathcal{O}_Y^{[2]}$, respectively.

²⁰ Nevertheless, all examples of topological injective MPOs discussed in Section VI have fusion and splitting tensors that satisfy both the broken zipper condition and the two-sided zipper condition.

A. Fusion and splitting tensors

Let us first define fusion tensors and splitting tensors for the fusion channels of topological injective MPOs.

Definition V.1 (Fusion and splitting tensors). *Let \mathcal{O}_X and \mathcal{O}_Y be topological injective MPO tensors. We suppose that MPOs $D[\mathcal{O}_X]$ and $D[\mathcal{O}_Y]$ on a periodic chain obey the fusion rule*

$$D[\mathcal{O}_X]D[\mathcal{O}_Y] = \sum_{Z \in S_{XY}} D[\mathcal{O}_Z], \quad (\text{V.1})$$

where \mathcal{O}_Z is an injective MPO tensor for every $Z \in S_{XY}$. We denote the bond Hilbert spaces of \mathcal{O}_X , \mathcal{O}_Y , and \mathcal{O}_Z by V_X , V_Y , and V_Z , respectively. The fusion tensor $\phi_Z : V_X \otimes V_Y \rightarrow V_Z$ and the splitting tensor $\bar{\phi}_Z : V_Z \rightarrow V_X \otimes V_Y$ for fusion channel Z are three-leg tensors that satisfy

$$\begin{array}{c} \text{Diagram showing } \bar{\phi}_Z \text{ and } \phi_Z \text{ tensors} \\ \text{Diagram showing } \bar{\phi}_Z \text{ and } \phi_Z \text{ tensors} \end{array} = \sum_{Z \in S_{XY}} \text{Diagram showing } \bar{\phi}_Z \text{ and } \phi_Z \text{ tensors} \quad (\text{V.2})$$

$$\begin{array}{c} \text{Diagram showing } \bar{\phi}_Z \text{ and } \phi_Z \text{ tensors} \\ \text{Diagram showing } \bar{\phi}_Z \text{ and } \phi_Z \text{ tensors} \end{array} = \sum_{Z \in S_{XY}} \text{Diagram showing } \bar{\phi}_Z \text{ and } \phi_Z \text{ tensors} \quad (\text{V.3})$$

where the first equality is required to be satisfied for any number of physical legs.

As we will see in Section VIA, the fusion and splitting tensors exist when both $D[\mathcal{O}_X]$ and $D[\mathcal{O}_Y]$ are MPUs. For more general topological injective MPOs, the existence of the fusion and splitting tensors has not been proven except for the concrete examples discussed in Section VI. In what follows, we assume that these tensors exist for general topological injective MPOs.

Remark. As long as we block a sufficient number of physical legs, there always exist three-leg tensors satisfying (V.2) according to the general theory of MPS/MPO [55, 60]. For example, the pair of the projection and inclusion map for each injective block satisfies (V.2). However, it is non-trivial whether such tensors also satisfy (V.3). We note that the condition (V.3) was not imposed in the original definition of fusion tensors in [60]. We also mention that the fusion and splitting tensors defined above are more general than those discussed in, e.g., [61–63]. More specifically, the fusion and splitting tensors in [61–63] are supposed to satisfy the zipper condition in Definition V.4, which does not hold in general as we will see later.

B. Broken zipper condition and two-sided zipper condition

Let us introduce the broken zipper condition and the two-sided zipper condition for the fusion and splitting tensors.

Definition V.2 (Broken zipper condition). *Let \mathcal{O}_X and \mathcal{O}_Y be topological injective MPO tensors whose fusion rule is given by (V.1). We say that the fusion tensor ϕ_Z and the splitting tensor $\bar{\phi}_Z$ for fusion channel $Z \in S_{XY}$ satisfy the broken zipper condition if the following equations hold:*

$$\begin{array}{c} \text{Diagram showing } \bar{\phi}_Z \text{ and } \phi_Z \text{ tensors} \\ \text{Diagram showing } \bar{\phi}_Z \text{ and } \phi_Z \text{ tensors} \end{array} = \begin{array}{c} \text{Diagram showing } \bar{\phi}_Z \text{ and } \phi_Z \text{ tensors} \\ \text{Diagram showing } \bar{\phi}_Z \text{ and } \phi_Z \text{ tensors} \end{array}, \quad \begin{array}{c} \text{Diagram showing } \bar{\phi}_Z \text{ and } \phi_Z \text{ tensors} \\ \text{Diagram showing } \bar{\phi}_Z \text{ and } \phi_Z \text{ tensors} \end{array} = \begin{array}{c} \text{Diagram showing } \bar{\phi}_Z \text{ and } \phi_Z \text{ tensors} \\ \text{Diagram showing } \bar{\phi}_Z \text{ and } \phi_Z \text{ tensors} \end{array}. \quad (\text{V.4})$$

We note that the above condition is called a weaker zipping condition in [64]. The term “broken zipper condition” was introduced in [65] in the case where the fusion channel is unique.

Definition V.3 (Two-sided zipper condition). *Let \mathcal{O}_X and \mathcal{O}_Y be topological injective MPO tensors whose fusion rule is given by (V.1). We say that the fusion tensor ϕ_Z and the splitting tensor $\bar{\phi}_Z$ for fusion channel $Z \in S_{XY}$ satisfy the two-sided zipper condition if there exist non-zero complex numbers a_Z^l , a_Z^r , b_Z^l , and b_Z^r such that*

$$\begin{array}{c} \text{Diagram 1: } \Lambda_Y^l \otimes \Lambda_X^l \xrightarrow{\mathcal{O}_Y^\dagger, \phi_Z^\dagger, \mathcal{O}_X^\dagger, \mathcal{O}_X, \phi_Z, \mathcal{O}_Y} a_Z^l \otimes \Lambda_Z^l \otimes \mathcal{O}_Z^\dagger, \\ \text{Diagram 2: } \Lambda_X^r \otimes \Lambda_Y^r \xrightarrow{\phi_Z^\dagger, \mathcal{O}_X^\dagger, \mathcal{O}_Y^\dagger, \mathcal{O}_X, \phi_Z, \mathcal{O}_Y} a_Z^r \otimes \Lambda_Z^r \otimes \mathcal{O}_Z^\dagger, \end{array} \quad (\text{V.5})$$

$$\begin{array}{c} \text{Diagram 3: } \Lambda_X^l \otimes \Lambda_Y^l \xrightarrow{\mathcal{O}_X, \phi_Z, \mathcal{O}_Y^\dagger, \mathcal{O}_Y^\dagger, \mathcal{O}_X^\dagger, \phi_Z^\dagger} b_Z^l \otimes \Lambda_Z^l \otimes \mathcal{O}_Z^\dagger, \\ \text{Diagram 4: } \Lambda_X^r \otimes \Lambda_Y^r \xrightarrow{\phi_Z^\dagger, \mathcal{O}_Y^\dagger, \mathcal{O}_X^\dagger, \mathcal{O}_Y, \phi_Z, \mathcal{O}_X} b_Z^r \otimes \Lambda_Z^r \otimes \mathcal{O}_Z^\dagger, \end{array} \quad (\text{V.6})$$

where $\Lambda_X^{l/r}$, $\Lambda_Y^{l/r}$, and $\Lambda_Z^{l/r}$ are the left/right fixed points of the transfer matrices $\mathsf{T}[\mathcal{O}_X]$, $\mathsf{T}[\mathcal{O}_Y]$, and $\mathsf{T}[\mathcal{O}_Z]$.

As we will see in Section VIA, the fusion and splitting tensors satisfy both the broken zipper condition and the two-sided zipper condition when $\mathsf{D}[\mathcal{O}_X]$ and $\mathsf{D}[\mathcal{O}_Y]$ are MPUs. For more general topological injective MPOs, these conditions have not been proven except for the concrete examples discussed in Section VI.

Before proceeding, we mention that the broken zipper condition defined above is weaker than the following zipper condition [60]:

Definition V.4 (Zipper condition). *Let \mathcal{O}_X and \mathcal{O}_Y be topological injective MPO tensors whose fusion rule is given by (V.1). We say that the fusion tensor ϕ_Z and the splitting tensor $\bar{\phi}_Z$ satisfy the zipper condition if the following equations hold:*

$$\begin{array}{c} \text{Diagram 1: } \mathcal{O}_X \otimes \mathcal{O}_Y \xrightarrow{\phi_Z} \mathcal{O}_Z, \\ \text{Diagram 2: } \mathcal{O}_Z \otimes \mathcal{O}_Y \xrightarrow{\bar{\phi}_Z} \mathcal{O}_X, \end{array} \quad (\text{V.7})$$

The zipper condition (V.7) does not hold in general. To see this, let us consider the case when $\mathsf{D}[\mathcal{O}_X]$ and $\mathsf{D}[\mathcal{O}_Y]$ are MPUs. If we choose $\mathcal{O}_X = \mathcal{O}_Y^\dagger$, the fusion and splitting tensors for the unique fusion channel (i.e., the identity channel) are given by the normalized right and left fixed points of the transfer matrix $\mathsf{T}[\mathcal{O}_Y]$.²¹ Thus, the zipper condition for this fusion channel reduces to (IV.23). However, as discussed in Section IV B 2, an MPU tensor satisfying (IV.23) must be an on-site operator. Therefore, the zipper condition does not hold in general.

²¹ Indeed, the normalized fixed points of the transfer matrix satisfy the defining equations (V.2) and (V.3) of fusion and splitting tensors due to (IV.17).

C. Consequences

We now discuss some consequences of the broken zipper condition and the two-sided zipper condition. In what follows, unless otherwise specified, the black and white dots in tensor network diagrams represent the right and left fixed points of the transfer matrices, respectively.

1. Fusion channels are topological

We first show that the fusion channel $Z \in S_{XY}$ is topological if the fusion tensor ϕ_Z and the splitting tensor $\bar{\phi}_Z$ satisfy both the broken zipper condition and the two-sided zipper condition. More specifically, the broken zipper condition and the two-sided zipper condition imply

$$\Lambda_Z^l \otimes \begin{array}{c} \mathcal{O}_Z^\dagger \\ \mathcal{O}_Z \\ \mathcal{O}_Z \end{array} = \begin{array}{c} \Lambda_Z^l \otimes \mathcal{O}_Z^\dagger \\ \mathcal{O}_Z \\ \mathcal{O}_Z \end{array}, \quad \begin{array}{c} \mathcal{O}_Z^\dagger \\ \mathcal{O}_Z \\ \mathcal{O}_Z \end{array} \otimes \Lambda_Z^r = \begin{array}{c} \mathcal{O}_Z^\dagger \\ \mathcal{O}_Z \\ \mathcal{O}_Z \end{array} \otimes \Lambda_Z^r, \quad (V.8)$$

$$\Lambda_Z^l \otimes \begin{array}{c} \mathcal{O}_Z \\ \mathcal{O}_Z^\dagger \\ \mathcal{O}_Z^\dagger \end{array} = \begin{array}{c} \Lambda_Z^l \otimes \mathcal{O}_Z \\ \mathcal{O}_Z^\dagger \\ \mathcal{O}_Z^\dagger \end{array}, \quad \begin{array}{c} \mathcal{O}_Z \\ \mathcal{O}_Z^\dagger \\ \mathcal{O}_Z^\dagger \end{array} \otimes \Lambda_Z^r = \begin{array}{c} \mathcal{O}_Z \\ \mathcal{O}_Z^\dagger \\ \mathcal{O}_Z^\dagger \end{array} \otimes \Lambda_Z^r, \quad (V.9)$$

as long as the physical legs are blocked sufficiently,

To show the first equality of (V.8), we note that the broken zipper condition and the two-sided zipper condition lead to the following equality:

$$\begin{array}{c} \mathcal{O}_Y^\dagger \\ \mathcal{O}_X^\dagger \\ \mathcal{O}_Y \end{array} \otimes \begin{array}{c} \mathcal{O}_Z^\dagger \\ \mathcal{O}_Z \\ \mathcal{O}_Z \end{array} = a_Z^l \otimes \begin{array}{c} \mathcal{O}_Z^\dagger \\ \mathcal{O}_Z \\ \mathcal{O}_Z \end{array}. \quad (V.10)$$

The left-hand side of the above equation can also be computed as

$$\begin{array}{c} \mathcal{O}_Y^\dagger \\ \mathcal{O}_X^\dagger \\ \mathcal{O}_Y \end{array} \otimes \begin{array}{c} \mathcal{O}_Z^\dagger \\ \mathcal{O}_Z \\ \mathcal{O}_Z \end{array} = \begin{array}{c} \mathcal{O}_Y^\dagger \\ \mathcal{O}_X^\dagger \\ \mathcal{O}_Y \end{array} \otimes a_Z^l = a_Z^l \otimes \begin{array}{c} \mathcal{O}_Z^\dagger \\ \mathcal{O}_Z \\ \mathcal{O}_Z \end{array}, \quad (V.11)$$

where the first equality follows from the topological property (IV.10) of \mathcal{O}_X and \mathcal{O}_Y . By comparing the above two equations, we find

$$\begin{array}{c} \mathcal{O}_Y^\dagger \\ \mathcal{O}_X^\dagger \\ \mathcal{O}_Y \end{array} \otimes \begin{array}{c} \mathcal{O}_Z^\dagger \\ \mathcal{O}_Z \\ \mathcal{O}_Z \end{array} = \begin{array}{c} \mathcal{O}_Y^\dagger \\ \mathcal{O}_X^\dagger \\ \mathcal{O}_Y \end{array} = \begin{array}{c} \mathcal{O}_Z^\dagger \\ \mathcal{O}_Z \\ \mathcal{O}_Z \end{array}. \quad (V.12)$$

By blocking two physical legs in the above equation, we obtain the first equality of (V.8). The other equalities in (V.8) and (V.9) can also be obtained similarly.

2. The left and right dimensions obey the fusion rules

We next show that the left and right dimensions are one-dimensional representations of the fusion rules (V.1) if the fusion and splitting tensors for all fusion channels satisfy both the broken zipper condition and the two-sided zipper condition. More specifically, if (V.4), (V.5), and (V.6) hold for all $Z \in S_{XY}$, it follows that

$$\text{ldim}(\mathcal{O}_X)\text{ldim}(\mathcal{O}_Y) = \sum_{Z \in S_{XY}} \text{ldim}(\mathcal{O}_Z), \quad (\text{V.13})$$

$$\text{rdim}(\mathcal{O}_X)\text{rdim}(\mathcal{O}_Y) = \sum_{Z \in S_{XY}} \text{rdim}(\mathcal{O}_Z), \quad (\text{V.14})$$

as long as the physical sites are blocked sufficiently.

To show (V.13), we first recall that the left dimension is multiplicative (IV.80), i.e., it satisfies $\text{ldim}(\mathcal{O}_X)\text{ldim}(\mathcal{O}_Y) = \text{ldim}(\mathcal{O}_X\mathcal{O}_Y)$, where $\mathcal{O}_X\mathcal{O}_Y$ is the composite tensor defined by (IV.81). Thus, equation (V.13) reduces to $\text{ldim}(\mathcal{O}_X\mathcal{O}_Y) = \sum_{Z \in S_{XY}} \text{ldim}(\mathcal{O}_Z)$, or equivalently,

$$\text{rank}_l(\mathcal{O}_X\mathcal{O}_Y) = \sum_{Z \in S_{XY}} \text{rank}_l(\mathcal{O}_Z). \quad (\text{V.15})$$

To show the above equality, we note that the MPO matrices of the composite tensor $\mathcal{O}_X\mathcal{O}_Y$ can be made into a block upper triangular form, where the non-zero block diagonal components are given by the injective blocks $\{\mathcal{O}_Z \mid Z \in S_{XY}\}$ [55, 56]. Since the rank of an upper triangular matrix is greater than or equal to the sum of the ranks of its block diagonal components, it follows that

$$\sum_{Z \in S_{XY}} \text{rank}_l(\mathcal{O}_Z) \leq \text{rank}_l(\mathcal{O}_X\mathcal{O}_Y). \quad (\text{V.16})$$

On the other hand, due to the defining equation (V.3) of the fusion and splitting tensors, the rank of $\mathcal{O}_X\mathcal{O}_Y$ also satisfies

$$\text{rank}_l(\mathcal{O}_X\mathcal{O}_Y) = \frac{\text{rank}_l(\mathcal{O}_X^{[2]}\mathcal{O}_Y^{[2]})}{\dim(\mathcal{H}_o)} \leq \frac{1}{\dim(\mathcal{H}_o)} \sum_{Z \in S_{XY}} \text{rank}_l \left(\begin{array}{c} \mathcal{O}_X \\ \text{---} \\ \mathcal{O}_Y \end{array} \right) \left(\begin{array}{c} \text{---} \\ \phi_Z \\ \text{---} \end{array} \right) \left(\begin{array}{c} \text{---} \\ \bar{\phi}_Z \\ \text{---} \end{array} \right) \left(\begin{array}{c} \mathcal{O}_X \\ \text{---} \\ \mathcal{O}_Y \end{array} \right), \quad (\text{V.17})$$

where the inequality follows from $\text{rank}(f_1 + f_2) \leq \text{rank}(f_1) + \text{rank}(f_2)$ for any linear maps f_1 and f_2 . The first equality in (V.17) holds as long as we block a sufficient number of physical sites.²² Using the broken zipper condition and the two-sided zipper condition, we can compute the summand on

²² More precisely, for any pair of topological injective MPO tensors \mathcal{O}_X and \mathcal{O}_Y , it follows that $\text{rank}_l(\mathcal{O}_X^{[4]}\mathcal{O}_Y^{[4]}) = \text{rank}_l(\mathcal{O}_X^{[2]}\mathcal{O}_Y^{[2]})\dim(\mathcal{H}_o)^2$ due to (IV.10). Thus, by blocking two physical sites, we obtain the first equality of (V.17).

the right-hand side of (V.17) as follows:

$$\begin{aligned}
 \text{rank}_l \left(\begin{array}{c} \text{circuit diagram} \\ \phi_Z \quad \bar{\phi}_Z \end{array} \right) &= \text{rank} \left(\begin{array}{c} \text{circuit diagram} \\ \phi_Z^\dagger \quad \bar{\phi}_Z^\dagger \end{array} \right) = \text{rank} \left(\begin{array}{c} \text{circuit diagram} \\ \phi_Z^\dagger \quad \mathcal{O}_Z^\dagger \end{array} \right) \\
 &= \text{rank}_l \left(\begin{array}{c} \text{circuit diagram} \\ \phi_Z \end{array} \right) = \text{rank} \left(\begin{array}{c} \text{circuit diagram} \\ \phi_Z^\dagger \end{array} \right) = \text{rank}_l \left(\begin{array}{c} \text{circuit diagram} \\ \mathcal{O}_Z \end{array} \right) \\
 &= \dim(\mathcal{H}_o) \text{rank}_l(\mathcal{O}_Z).
 \end{aligned} \tag{V.18}$$

Thus, equation (V.17) reduces to

$$\text{rank}_l(\mathcal{O}_X \mathcal{O}_Y) \leq \sum_{Z \in S_{XY}} \text{rank}_l(\mathcal{O}_Z). \tag{V.19}$$

Equations (V.16) and (V.19) imply (V.15), which in turn implies (V.13). Equation (V.14) can also be obtained in the same way.

3. The index is homogeneous

Finally, we show that the index is homogeneous if the broken zipper condition and the two-sided zipper condition hold for all fusion channels. More specifically, if (V.4), (V.5), and (V.6) hold for fusion channel $Z \in S_{XY}$, we have

$$\text{ind}(\mathcal{O}_Z) = \text{ind}(\mathcal{O}_X) \text{ind}(\mathcal{O}_Y). \tag{V.20}$$

In particular, if this holds for all fusion channels, it follows that $\text{ind}(\mathcal{O}_Z) = \text{ind}(\mathcal{O}_W)$ for any pair of $Z, W \in S_{XY}$, and hence the index is homogeneous.

To show (V.20), we consider the following equalities:

$$\begin{array}{c} \text{circuit diagram} \\ \mathcal{O}_X \quad \phi_Z \quad \mathcal{O}_Z \\ \mathcal{O}_Y \quad \mathcal{O}_Y^\dagger \\ \mathcal{O}_Z^\dagger \quad \mathcal{O}_X \\ \mathcal{O}_Z \quad \bar{\phi}_Z \quad \mathcal{O}_Y \end{array} = \begin{array}{c} \text{circuit diagram} \\ \mathcal{O}_X \quad \phi_Z \\ \mathcal{O}_Y \quad \mathcal{O}_Y^\dagger \\ \mathcal{O}_Z^\dagger \quad \mathcal{O}_X \\ \bar{\phi}_Z \quad \mathcal{O}_Y \end{array} = c_Z^l, \tag{V.21}$$

$$\begin{array}{c} \text{circuit diagram} \\ \mathcal{O}_Z \quad \mathcal{O}_X \\ \mathcal{O}_Y^\dagger \quad \bar{\phi}_Z \quad \mathcal{O}_Y \\ \mathcal{O}_X^\dagger \quad \mathcal{O}_X \\ \mathcal{O}_Y \quad \phi_Z \end{array} = \begin{array}{c} \text{circuit diagram} \\ \bar{\phi}_Z \quad \mathcal{O}_Y \quad \mathcal{O}_Y^\dagger \\ \mathcal{O}_X \quad \mathcal{O}_X^\dagger \\ \mathcal{O}_Y \quad \phi_Z \end{array} = c_Z^r. \tag{V.22}$$

The left equalities of (V.21) and (V.22) follow from the broken zipper condition (V.4), and the right equalities of (V.21) and (V.22) follow from the fact that \mathcal{O}_X , \mathcal{O}_Y , and \mathcal{O}_Z are topological. Due to the zigzag relations (IV.30), the complex numbers c_Z^l and c_Z^r can be written as

$$c_Z^l = \frac{\gamma_X \gamma_Y}{\gamma_Z} \frac{\text{ldim}(\mathcal{O}_Z)}{\text{ldim}(\mathcal{O}_X) \text{ldim}(\mathcal{O}_Y)}, \quad c_Z^r = \frac{\gamma_X \gamma_Y}{\gamma_Z} \frac{\text{rdim}(\mathcal{O}_Z)}{\text{rdim}(\mathcal{O}_X) \text{rdim}(\mathcal{O}_Y)}, \quad (\text{V.23})$$

where we defined $\gamma_i := \text{tr}(\Lambda_i^l \Lambda_i^r)$ for $i = X, Y, Z$. The above equation implies that equation (V.20) is equivalent to $c_Z^l = c_Z^r$. In what follows, we will show that $c_Z^l = c_Z^r$.

To show that $c_Z^l = c_Z^r$, we first show the following equality:

$$\text{tr} \left(\begin{array}{c} \text{Diagram 1: A 3D-like structure with vertical lines and horizontal connections involving } \mathcal{O}_Z, \mathcal{O}_X, \mathcal{O}_Y, \phi_Z, \bar{\phi}_Z, \mathcal{O}_Y^\dagger, \mathcal{O}_X^\dagger, \mathcal{O}_Z^\dagger. \end{array} \right) = \text{tr} \left(\begin{array}{c} \text{Diagram 2: A 3D-like structure similar to Diagram 1, but with different internal connections and labels.} \end{array} \right). \quad (\text{V.24})$$

Using the cyclicity of the trace and the zigzag relations for \mathcal{O}_Z , one can compute the left-hand side and the right-hand side of the above equation as

$$\text{LHS} = \delta_l(\mathcal{O}_Z) \delta_r(\mathcal{O}_Z) \dim(\mathcal{H}_o)^3 \text{tr} \left(\begin{array}{c} \text{Diagram 3: A 2D-like structure with a central diamond and various boundary conditions involving } \mathcal{O}_Y, \mathcal{O}_X, \phi_Z, \bar{\phi}_Z, \mathcal{O}_Y^\dagger, \mathcal{O}_X^\dagger. \end{array} \right) = \text{RHS}, \quad (\text{V.25})$$

where δ_l and δ_r are defined by (IV.31). The above equation shows (V.24). On the other hand, due to (V.21) and (V.22), the left-hand side and the right-hand side of (V.24) can also be written as

$$\text{LHS} = c_Z^l \delta_l(\mathcal{O}_Z) \delta_r(\mathcal{O}_Z) \gamma_Z \dim(\mathcal{H}_o)^6, \quad \text{RHS} = c_Z^r \delta_l(\mathcal{O}_Z) \delta_r(\mathcal{O}_Z) \gamma_Z \dim(\mathcal{H}_o)^6. \quad (\text{V.26})$$

Therefore, equation (V.24) implies that $c_Z^l = c_Z^r$, which in turn implies (V.20).

VI. EXAMPLES

In this section, we discuss various examples of topological injective MPOs and show that the fusion and splitting tensors for their fusion channels satisfy both the broken zipper condition and the two-sided zipper condition. We also compute the lattice quantum dimension and the index of these topological injective MPOs.

A. Invertible symmetries

Invertible symmetry operators defined by QCAs in 1+1d can be represented by injective MPUs [51, 52]. As shown in Section IV B 2, injective MPUs are examples of topological injective MPOs. In this subsection, we show the existence of the fusion and splitting tensors for the unique fusion

channel of any pair of injective MPUs. We will also show that the fusion and splitting tensors satisfy both the broken zipper condition and the two-sided zipper condition.

Fusion and splitting tensors. Let \mathcal{O}_X and \mathcal{O}_Y be injective MPU tensors with bond Hilbert spaces V_X and V_Y . Since the product of two MPUs is an MPU, there exists an MPU tensor \mathcal{O}_Z such that

$$\mathsf{D}[\mathcal{O}_X]\mathsf{D}[\mathcal{O}_Y] = \mathsf{D}[\mathcal{O}_Z] \quad (\text{VI.1})$$

on a periodic chain of any length. We can take \mathcal{O}_Z to be injective by blocking a sufficient number of physical sites. We denote the bond Hilbert space of \mathcal{O}_Z by V_Z . The above equation implies that the composite tensor $\mathcal{O}_X\mathcal{O}_Y$ defined by (IV.81) generates the same MPO as an injective MPO tensor \mathcal{O}_Z . Therefore, due to [66, Proposition 20], there exists a pair of three leg tensors $\phi_Z : V_X \otimes V_Y \rightarrow V_Z$ and $\bar{\phi}_Z : V_Z \rightarrow V_X \otimes V_Y$ that satisfies (V.2) for any number of physical legs. In [66, Definition 7], the pair $(\phi_Z, \bar{\phi}_Z)$ satisfying (V.2) is called a reduction from $\mathcal{O}_X\mathcal{O}_Y$ to \mathcal{O}_Z . In what follows, we will show that the reduction $(\phi_Z, \bar{\phi}_Z)$ also satisfies (V.3), that is, ϕ_Z and $\bar{\phi}_Z$ are the fusion and splitting tensors for the unique fusion channel Z .

To show (V.3), we first show the following equality:

$$\quad (\text{VI.2})$$

Using (IV.17), one can compute the left-hand side and the right-hand side of the above equation as

$$\quad (\text{VI.3})$$

where the black and white dots represent the normalized fixed points of the transfer matrices $\mathsf{T}[\mathcal{O}_X]$ and $\mathsf{T}[\mathcal{O}_Y]$. The middle diagram on the right-hand side of the second equation can further be computed as

$$= \text{D}[\mathcal{O}_X]^\dagger \text{D}[\mathcal{O}_Z] \text{D}[\mathcal{O}_Y]^\dagger = 1, \quad (\text{VI.4})$$

where the double slashes indicate the periodic boundary conditions. The first equality follows from (IV.17),²³ the second equality follows from (V.2), and the third equality follows from (VI.1). Equations (VI.3) and (VI.4) show that (VI.2) holds.

²³ More specifically, we used the second equality of (IV.17). The left and right physical legs in (IV.17) correspond to the right and left physical legs in (VI.4), respectively.

Equation (VI.2) implies

$$\begin{array}{c} \text{Diagram 1: } \text{Two vertical columns of nodes. The left column has } \mathcal{O}_Y \text{ on top and } \mathcal{O}_X \text{ on bottom. The right column has } \mathcal{O}_X \text{ on top and } \mathcal{O}_Y \text{ on bottom. Horizontal arrows connect nodes in the same column.} \\ \text{Diagram 2: } \text{The same structure as Diagram 1, but with a red diamond at the bottom of the left column and a blue diamond at the top of the right column.} \end{array} = \begin{array}{c} \text{Diagram 3: } \text{The same structure as Diagram 1, but with a red diamond at the bottom of the left column and a blue diamond at the top of the right column. A red arrow labeled } \phi_Z \text{ and a blue arrow labeled } \bar{\phi}_Z \text{ connect the red and blue diamonds.} \end{array} . \quad (\text{VI.5})$$

Furthermore, due to the zigzag relations (IV.30) for \mathcal{O}_X and \mathcal{O}_Y , the above equation implies

$$\begin{array}{c} \text{Diagram 1: } \text{Two vertical columns of nodes. The left column has } \mathcal{O}_Y \text{ on top and } \mathcal{O}_X \text{ on bottom. The right column has } \mathcal{O}_X \text{ on top and } \mathcal{O}_Y \text{ on bottom. Horizontal arrows connect nodes in the same column.} \\ \text{Diagram 2: } \text{The same structure as Diagram 1, but with red and blue dots at the top and bottom of each column.} \\ \text{Diagram 3: } \text{The same structure as Diagram 1, but with red and blue dots at the top and bottom of each column. Red and blue arrows labeled } \phi_Z \text{ and } \bar{\phi}_Z \text{ connect the dots.} \end{array} = \alpha_{XY} \begin{array}{c} \text{Diagram 4: } \text{The same structure as Diagram 1, but with red and blue dots at the top and bottom of each column. Red and blue arrows labeled } \phi_Z \text{ and } \bar{\phi}_Z \text{ connect the dots.} \end{array} = \alpha_{XY} \begin{array}{c} \text{Diagram 5: } \text{The same structure as Diagram 1, but with red and blue dots at the top and bottom of each column. Red and blue arrows labeled } \phi_Z \text{ and } \bar{\phi}_Z \text{ connect the dots.} \end{array} = \begin{array}{c} \text{Diagram 6: } \text{The same structure as Diagram 1, but with red and blue dots at the top and bottom of each column. Red and blue arrows labeled } \phi_Z \text{ and } \bar{\phi}_Z \text{ connect the dots.} \end{array} , \quad (\text{VI.6})$$

where $\alpha_{XY} = (\delta_l(\mathcal{O}_X)\delta_r(\mathcal{O}_X)\delta_l(\mathcal{O}_Y)\delta_r(\mathcal{O}_Y))^{-1}$. Equation (VI.6) shows that the reduction $(\phi_Z, \bar{\phi}_Z)$ satisfies (V.3).

Broken zipper condition. It was shown in [65, Proposition 5] that the reduction $(\phi_Z, \bar{\phi}_Z)$ satisfies

$$\begin{array}{c} \text{Diagram 1: } \text{Two vertical columns of nodes. The left column has } \mathcal{O}_Y \dots \mathcal{O}_Y \text{ on top and } \mathcal{O}_X \dots \mathcal{O}_X \text{ on bottom. The right column has } \mathcal{O}_Z \text{ on top and } \phi_Z \text{ on bottom. Horizontal arrows connect nodes in the same column.} \\ \text{Diagram 2: } \text{The same structure as Diagram 1, but with a red diamond at the bottom of the left column and a blue diamond at the top of the right column.} \end{array} = \begin{array}{c} \text{Diagram 3: } \text{The same structure as Diagram 1, but with a red diamond at the bottom of the left column and a blue diamond at the top of the right column.} \end{array} , \quad (\text{VI.7})$$

where the number of physical legs is supposed to be greater than or equal to a positive integer called the nilpotency length of the reduction [66, Definition 8]. We note that the nilpotency length of the reduction is independent of the system size [66]. Therefore, after blocking a finite number of physical legs, the reduction $(\phi_Z, \bar{\phi}_Z)$ satisfies the first equality of the broken zipper condition (V.4). The second equality of (V.4) also follows similarly.

Two-sided zipper condition. To show the two-sided zipper condition (V.5), we first show the following equality:

$$\begin{array}{c} \text{Diagram 1: } \text{Two vertical columns of nodes. The left column has } \bar{\phi}_Z \text{ on top and } \mathcal{O}_Y \dots \mathcal{O}_Y \text{ on bottom. The right column has } \phi_Z \text{ on top and } \mathcal{O}_X \dots \mathcal{O}_X \text{ on bottom. Horizontal arrows connect nodes in the same column.} \\ \text{Diagram 2: } \text{The same structure as Diagram 1, but with red and blue dots at the top and bottom of each column. Red and blue arrows labeled } \phi_Z \text{ and } \bar{\phi}_Z \text{ connect the dots.} \end{array} = \begin{array}{c} \text{Diagram 3: } \text{Two vertical columns of nodes. The left column has } \mathcal{O}_Z \text{ on top and } \bar{\phi}_Z \text{ on bottom. The right column has } \mathcal{O}_Z \text{ on top and } \phi_Z \text{ on bottom. Horizontal arrows connect nodes in the same column.} \end{array} . \quad (\text{VI.8})$$

One can show the above equation by a direct computation as

$$\text{LHS} = \begin{array}{c} \text{Diagram 1: } \text{Two vertical columns of nodes. The left column has } \bar{\phi}_Z \text{ on top and } \mathcal{O}_Y \dots \mathcal{O}_Y \text{ on bottom. The right column has } \phi_Z \text{ on top and } \mathcal{O}_X \dots \mathcal{O}_X \text{ on bottom. Horizontal arrows connect nodes in the same column.} \\ \text{Diagram 2: } \text{The same structure as Diagram 1, but with red and blue dots at the top and bottom of each column. Red and blue arrows labeled } \phi_Z \text{ and } \bar{\phi}_Z \text{ connect the dots.} \end{array} = \begin{array}{c} \text{Diagram 3: } \text{Two vertical columns of nodes. The left column has } \mathcal{O}_Z \text{ on top and } \bar{\phi}_Z \text{ on bottom. The right column has } \mathcal{O}_Z \text{ on top and } \phi_Z \text{ on bottom. Horizontal arrows connect nodes in the same column.} \end{array} = \text{RHS}, \quad (\text{VI.9})$$

where the first equality follows from (IV.17) and (IV.10), and the second equality follows from (V.2). Equation (VI.8) implies that there exist complex numbers a_Z^l and a_Z^r such that

$$\text{Diagram (VI.10): } \text{Left: } \text{Complex network with } \phi_Z^\dagger \text{ at center} = a_Z^l \text{ (simplified diagram with } O_Z \text{ only)} , \text{ Right: } \text{Complex network with } \bar{\phi}_Z^\dagger \text{ at center} = a_Z^r \text{ (simplified diagram with } O_Z \text{ only)} . \quad (\text{VI.10})$$

We note that a_Z^l and a_Z^r are non-zero because the diagrams on the left-hand side of the above two equations are non-zero, which also follows from (VI.8). Equation (VI.10) shows that the reduction $(\phi_Z, \bar{\phi}_Z)$ satisfies the two-sided zipper condition (V.5) after blocking two physical sites. One can also show the other half (V.6) of the two-sided zipper condition similarly.

Lattice quantum dimension and index. As discussed in Section IV B 2, the lattice quantum dimension and the index of an injective MPU tensor \mathcal{O} are given by

$$\text{qdim}_{\text{lat}}(\mathcal{O}) = 1, \quad \text{ind}(\mathcal{O}) = \text{GNVW}(\mathbf{D}[\mathcal{O}]), \quad (\text{VI.11})$$

where $\text{GNVW}(\mathbf{D}[\mathcal{O}])$ is the GNVW index of the MPU $\mathbf{D}[\mathcal{O}]$. Equivalently, the left and right dimensions of \mathcal{O} are given by

$$\text{ldim}(\mathcal{O}) = \text{GNVW}(\mathbf{D}[\mathcal{O}]), \quad \text{rdim}(\mathcal{O}) = \text{GNVW}(\mathbf{D}[\mathcal{O}])^{-1}. \quad (\text{VI.12})$$

Example: lattice translation. As an example of an injective MPU, let us consider the lattice translation operator T . The MPO tensor of T and its Hermitian conjugate can be written as

$$\mathcal{O}_T = \text{Diagram with two horizontal arrows pointing right}, \quad \mathcal{O}_T^\dagger = \text{Diagram with two horizontal arrows pointing left}. \quad (\text{VI.13})$$

We note that the bond Hilbert space and the physical Hilbert space are both given by \mathcal{H}_o . The left and right fixed points of the transfer matrix $\mathbf{T}[\mathcal{O}_T]$ are given by

$$\Lambda_T^l = \frac{1}{\sqrt{\dim(\mathcal{H}_o)}} \text{Diagram with two horizontal arrows pointing right}, \quad \Lambda_T^r = \frac{1}{\sqrt{\dim(\mathcal{H}_o)}} \text{Diagram with two horizontal arrows pointing left}. \quad (\text{VI.14})$$

Here, we normalized Λ_T^l and Λ_T^r so that they satisfy (IV.17). Since $T^\dagger T = 1$, the product $\mathcal{O}_T^\dagger \mathcal{O}_T$ has a unique fusion channel, which is the identity channel denoted by $\mathbb{1}$. The corresponding fusion tensor $\phi_{\mathbb{1}}$ and the splitting tensor $\bar{\phi}_{\mathbb{1}}$ satisfying (V.2) and (V.3) are given by

$$\phi_{\mathbb{1}} = \Lambda_T^r, \quad \bar{\phi}_{\mathbb{1}} = \Lambda_T^l. \quad (\text{VI.15})$$

A direct computation shows that the above fusion and splitting tensors satisfy the broken zipper condition and the two-sided zipper condition. The complex numbers in the defining equations (V.5) and (V.6) of the two-sided zipper condition are given by

$$a_{\mathbb{1}}^l = \dim(\mathcal{H}_o)^{-1}, \quad a_{\mathbb{1}}^r = \dim(\mathcal{H}_o), \quad b_{\mathbb{1}}^l = \dim(\mathcal{H}_o), \quad b_{\mathbb{1}}^r = \dim(\mathcal{H}_o)^{-1}. \quad (\text{VI.16})$$

B. Non-anomalous fusion category symmetries

As an example of non-invertible topological injective MPOs, we consider the symmetry operators of a non-anomalous fusion category symmetry $\text{Rep}(A)$, where A is a finite dimensional semisimple Hopf $*$ -algebra. We will write down the fusion and splitting tensors for any fusion channel of these symmetry operators and show that they satisfy both the broken zipper condition and the two-sided zipper condition.

Hopf $*$ -algebras and their representations. Let us begin with the definitions of a Hopf $*$ -algebra and its $*$ -representations. We refer the reader to [67] for a review of this subject.

Definition VI.1 (Hopf algebra). *A Hopf algebra is a vector space A equipped with multiplication $m : A \otimes A \rightarrow A$, unit $\eta : \mathbb{C} \rightarrow A$, comultiplication $\Delta : A \rightarrow A \otimes A$, counit $\epsilon : A \rightarrow \mathbb{C}$, and antipode $S : A \rightarrow A$, which satisfy the following axioms:*

1. *the triple (A, m, η) is a unital algebra, i.e.,*

$$m \circ (m \otimes \text{id}_A) = m \circ (\text{id}_A \otimes m), \quad m \circ (\eta \otimes \text{id}_A) = m \circ (\text{id}_A \otimes \eta) = \text{id}_A; \quad (\text{VI.17})$$

2. *the triple (A, Δ, ϵ) is a counital coalgebra, i.e.,*

$$(\Delta \otimes \text{id}_A) \circ \Delta = (\text{id}_A \otimes \Delta) \circ \Delta, \quad (\epsilon \otimes \text{id}_A) \circ \Delta = (\text{id}_A \otimes \epsilon) \circ \Delta = \text{id}_A; \quad (\text{VI.18})$$

3. *the comultiplication Δ and the counit ϵ are unital algebra homomorphisms;*

4. *the antipode S satisfies*

$$m \circ (S \otimes \text{id}_A) \circ \Delta = m \circ (\text{id}_A \otimes S) \circ \Delta = \eta \circ \epsilon. \quad (\text{VI.19})$$

We note that the antipode S is both a unital algebra antihomomorphism and a counital coalgebra antihomomorphism [67, Proposition 1.3.12]. When A is finite dimensional, S is also invertible [68, 69]. Furthermore, when A is semisimple, we have $S^2 = \text{id}_A$ [70].

Definition VI.2 (Hopf $*$ -algebra). *A Hopf $*$ -algebra is a Hopf algebra A equipped with a conjugate-linear involution $* : A \rightarrow A$ that satisfies*

$$m(a \otimes b)^* = m(b^* \otimes a^*), \quad \Delta(a)^* = \Delta(a^*), \quad \forall a, b \in A, \quad (\text{VI.20})$$

where $\Delta(a)^*$ is defined by $\Delta(a)^* := ((* \otimes *) \circ \Delta)(a)$.

We note that the antipode of a Hopf $*$ -algebra satisfies $S \circ * \circ S \circ * = \text{id}_A$ [67, Proposition 1.3.28]. In particular, when A is finite dimensional and semisimple, we have $S \circ * = * \circ S$ due to $S^2 = \text{id}_A$.

In what follows, we will restrict our attention to finite dimensional semisimple Hopf $*$ -algebras.²⁴ For later use, we mention that a finite dimensional semisimple Hopf $*$ -algebra A can be equipped with the structure of a Hilbert space with the inner product defined by [67, Example 3.1.6]

$$(a, b) := \Lambda(a^* b), \quad \forall a, b \in A, \quad (\text{VI.21})$$

where $\Lambda : A \rightarrow \mathbb{C}$ is the Haar measure of A . The above inner product will be used to define the Hermitian conjugate of MPO representations of the symmetry operators.

²⁴ We note that every finite dimensional semisimple (Hopf) $*$ -algebra is a finite dimensional (Hopf) C^* -algebra, and vice versa.

Definition VI.3 (*-representation). A finite dimensional *-representation of a finite dimensional semisimple Hopf *-algebra A is a pair (V, ρ) , where V is a finite dimensional Hilbert space and $\rho : A \rightarrow \text{End}(V)$ is a unital *-algebra homomorphism. Here, $\text{End}(V)$ denotes the *-algebra of endomorphisms of V with the *-operation given by the Hermitian conjugation.

It is known that finite dimensional *-representations of a finite dimensional semisimple Hopf *-algebra A form a unitary fusion category denoted by $\text{Rep}(A)$ [34, 71]. More concretely, the tensor product of *-representations (V_X, ρ_X) and (V_Y, ρ_Y) is given by $(V_X \otimes V_Y, \rho_{XY})$, where the representation map $\rho_{XY} : A \rightarrow \text{End}(V_X \otimes V_Y)$ is given by

$$\rho_{XY} := (\rho_X \otimes \rho_Y) \circ \Delta. \quad (\text{VI.22})$$

We note that $(V_X \otimes V_Y, \rho_{XY})$ is a *-representation. The unit of the above tensor product is given by the trivial *-representation $(\mathbb{C}, \rho_\epsilon)$, where \mathbb{C} is equipped with the canonical Hilbert space structure and the representation map $\rho_\epsilon : A \rightarrow \text{End}(\mathbb{C}) \cong \mathbb{C}$ is given by

$$\rho_\epsilon(a) := \epsilon(a), \quad \forall a \in A. \quad (\text{VI.23})$$

Furthermore, for any finite dimensional *-representation (V, ρ) , one can define the dual *-representation $(V^*, \bar{\rho})$, where V^* is the dual vector space equipped with the inner product induced by that of V , and the representation map $\bar{\rho} : A \rightarrow \text{End}(V^*)$ is given by

$$\bar{\rho}(a) := \rho(S(a))^T, \quad \forall a \in A. \quad (\text{VI.24})$$

Here, the superscript T denotes the transpose.

An isomorphism between *-representations (V, ρ) and (W, σ) is a unitary $u : V \rightarrow W$ that intertwines the representation maps ρ and σ in the sense that $u \circ \rho(a) = \sigma(a) \circ u$ for all $a \in A$. Two *-representations are said to be isomorphic if there exists an isomorphism between them.

MPO representation of $\text{Rep}(A)$ symmetry. Let us now introduce MPO representations of the symmetry operators of $\text{Rep}(A)$ symmetry following [22, 41, 47]. For concreteness, we take the physical Hilbert space on each site to be the Hopf algebra A equipped with the inner product defined by (VI.21). We then define the MPO tensor of the symmetry operator labeled by a *-representation $(V, \rho) \in \text{Rep}(A)$ as follows:

$$\mathcal{O}_{(V, \rho)} := \begin{array}{c} \uparrow \\ \Delta \\ \nearrow \rho \\ \text{---} \end{array} \quad (\text{VI.25})$$

Here, the Hilbert space on the virtual bond is the representation space V . The above MPO representation is called an “on-site” representation of $\text{Rep}(A)$ symmetry according to the terminology introduced in [72].

By definition, it follows that the periodic MPOs generated by the above MPO tensors obey

$$\mathsf{D}[\mathcal{O}_{(V_X, \rho_X)}] \mathsf{D}[\mathcal{O}_{(V_Y, \rho_Y)}] = \mathsf{D}[\mathcal{O}_{(V_X \otimes V_Y, \rho_{XY})}], \quad (\text{VI.26})$$

where $(V_X \otimes V_Y, \rho_{XY})$ is the tensor product representation defined above. In addition, one can easily see that isomorphic *-representations give rise to the same MPO on a periodic chain because

the corresponding MPO tensors differ only by a gauge transformation. As a result, the MPOs on a periodic chain obey the same fusion rules as those of $\text{Rep}(A)$, i.e.,

$$(V_X, \rho_X) \otimes (V_Y, \rho_Y) \cong \bigoplus_{Z \in S_{XY}} (V_Z, \rho_Z) \Rightarrow \mathbb{D}[\mathcal{O}_{(V_X, \rho_X)}] \mathbb{D}[\mathcal{O}_{(V_Y, \rho_Y)}] = \sum_{Z \in S_{XY}} \mathbb{D}[\mathcal{O}_{(V_Z, \rho_Z)}], \quad (\text{VI.27})$$

where S_{XY} is the set of fusion channels of (V_X, ρ_X) and (V_Y, ρ_Y) , including fusion multiplicities.

The set of MPO tensors of the form (VI.25) is closed under Hermitian conjugation. Indeed, as shown in Appendix D, the Hermitian conjugate of $\mathcal{O}_{(V, \rho)}$ agrees with the MPO tensor $\mathcal{O}_{(V^*, \bar{\rho})}$ labeled by the dual $*$ -representation $(V^*, \bar{\rho})$. More specifically, we have

$$\mathcal{O}_{(V, \rho)}^\dagger = \begin{array}{c} \text{---} \\ \text{---} \\ \text{---} \\ \text{---} \end{array} \xrightarrow{\rho^\dagger} \Delta^\dagger = \begin{array}{c} \text{---} \\ \text{---} \\ \text{---} \\ \text{---} \end{array} \xrightarrow{\rho} \Delta \xrightarrow{S} \mathcal{O}_{(V^*, \bar{\rho})}, \quad (\text{VI.28})$$

where the last equality follows from the definition of the dual representation map (VI.24).

The MPO tensor $\mathcal{O}_{(V, \rho)}$ is injective when (V, ρ) is an irreducible $*$ -representation of A . Indeed, when (V, ρ) is irreducible, Schur's lemma implies that an operator acting on the virtual bond commutes with $\mathcal{O}_{(V, \rho)}$ if and only if it is proportional to the identity, and hence $\mathcal{O}_{(V, \rho)}$ is injective. When $\mathcal{O}_{(V, \rho)}$ is injective, the left and right fixed points of the transfer matrix $\mathbb{T}[\mathcal{O}_{(V, \rho)}]$ are both given by the identity, i.e.,

$$\Lambda_{(V, \rho)}^l = \begin{array}{c} \text{---} \\ \text{---} \\ \text{---} \\ \text{---} \end{array}, \quad \Lambda_{(V, \rho)}^r = \begin{array}{c} \text{---} \\ \text{---} \\ \text{---} \\ \text{---} \end{array}. \quad (\text{VI.29})$$

A direct computation shows that $\Lambda_{(V, \rho)}^l$ and $\Lambda_{(V, \rho)}^r$ defined above satisfy²⁵

$$\Lambda_{(V, \rho)}^l \mathbb{T}[\mathcal{O}_{(V, \rho)}] = \dim(A) \Lambda_{(V, \rho)}^l, \quad \mathbb{T}[\mathcal{O}_{(V, \rho)}] \Lambda_{(V, \rho)}^r = \dim(A) \Lambda_{(V, \rho)}^r. \quad (\text{VI.30})$$

Since $\Lambda_{(V, \rho)}^l$ and $\Lambda_{(V, \rho)}^r$ are positive definite, the above equation implies that they are the fixed points of $\mathbb{T}[\mathcal{O}_{(V, \rho)}]$.²⁶

The $\text{Rep}(A)$ MPOs are topological. The MPO tensor $\mathcal{O}_{(V, \rho)}$ labeled by an irreducible $*$ -representation $(V, \rho) \in \text{Rep}(A)$ is a topological injective MPO tensor, i.e., it satisfies (IV.10) and (IV.11). More specifically, $\mathcal{O}_{(V, \rho)}$ satisfies the following stronger conditions:

$$\begin{array}{c} \text{---} \\ \text{---} \\ \text{---} \\ \text{---} \end{array} \xrightarrow{\mathcal{O}_{(V, \rho)}^\dagger} \begin{array}{c} \text{---} \\ \text{---} \\ \text{---} \\ \text{---} \end{array} = \begin{array}{c} \text{---} \\ \text{---} \\ \text{---} \\ \text{---} \end{array}, \quad \begin{array}{c} \text{---} \\ \text{---} \\ \text{---} \\ \text{---} \end{array} \xrightarrow{\mathcal{O}_{(V, \rho)}^\dagger} \begin{array}{c} \text{---} \\ \text{---} \\ \text{---} \\ \text{---} \end{array} = \begin{array}{c} \text{---} \\ \text{---} \\ \text{---} \\ \text{---} \end{array}, \quad (\text{VI.31})$$

$$\begin{array}{c} \text{---} \\ \text{---} \\ \text{---} \\ \text{---} \end{array} \xrightarrow{\mathcal{O}_{(V, \rho)}} \begin{array}{c} \text{---} \\ \text{---} \\ \text{---} \\ \text{---} \end{array} = \begin{array}{c} \text{---} \\ \text{---} \\ \text{---} \\ \text{---} \end{array}, \quad \begin{array}{c} \text{---} \\ \text{---} \\ \text{---} \\ \text{---} \end{array} \xrightarrow{\mathcal{O}_{(V, \rho)}^\dagger} \begin{array}{c} \text{---} \\ \text{---} \\ \text{---} \\ \text{---} \end{array} = \begin{array}{c} \text{---} \\ \text{---} \\ \text{---} \\ \text{---} \end{array}. \quad (\text{VI.32})$$

²⁵ Equation (VI.30) immediately follows from (VI.31) that we will show shortly.

²⁶ We recall that a positive definite eigenvector of the transfer matrix of an injective MPO tensor is uniquely given by the fixed point due to [73, Theorem 2.4].

One can show the above equations by a direct computation. For example, the left equation in (VI.31) can be obtained as

$$\text{LHS} = \begin{array}{c} \text{Diagram with } S \text{ and } \rho \text{ on the left} \end{array} = \begin{array}{c} \text{Diagram with } S \text{ and } m \text{ on the left} \end{array} = \begin{array}{c} \text{Diagram with } S, \epsilon, \eta \text{ on the left} \end{array} = \text{RHS}, \quad (\text{VI.33})$$

where the first equality follows from (VI.28) and the third equality follows from the antipode axiom (VI.19) together with the fact that S is a coalgebra antihomomorphism. The other equations in (VI.31) and (VI.32) can also be obtained similarly.

Fusion and splitting tensors. As shown in (VI.27), the MPOs $\{\mathcal{D}[\mathcal{O}_{(V,\rho)}] \mid (V,\rho) \in \text{Rep}(A)\}$ on a periodic chain obey the same fusion rules as $\text{Rep}(A)$. For each fusion channel $Z \in S_{XY}$, the fusion tensor $\phi_Z : V_X \otimes V_Y \rightarrow V_Z$ and the splitting tensor $\bar{\phi}_Z : V_Z \rightarrow V_X \otimes V_Y$ are given by

$$\phi_Z = \pi_Z \circ u_{XY}, \quad \bar{\phi}_Z = u_{XY}^\dagger \circ \iota_Z, \quad (\text{VI.34})$$

where $u_{XY} : V_X \otimes V_Y \rightarrow \bigoplus_{Z \in S_{XY}} V_Z$ is an isomorphism of $*$ -representations, $\pi_Z : \bigoplus_{Z' \in S_{XY}} V_{Z'} \rightarrow V_Z$ is the projection, and $\iota_Z : V_Z \rightarrow \bigoplus_{Z' \in S_{XY}} V_{Z'}$ is the inclusion. By definition, the above fusion and splitting tensors satisfy

$$\begin{array}{c} \text{Diagram showing the defining equations for } \phi_Z \text{ and } \bar{\phi}_Z \end{array} = \delta_{Z,Z'} \begin{array}{c} \text{Diagram with } \mathcal{O}_{(V_Z,\rho_Z)} \end{array}, \quad \sum_{Z \in S_{XY}} \begin{array}{c} \text{Diagram showing the compatibility of } \phi_Z \text{ and } \bar{\phi}_Z \end{array} = \begin{array}{c} \text{Diagram with } \mathcal{O}_{(V_X,\rho_X)} \end{array}. \quad (\text{VI.35})$$

This readily implies the defining equations (V.2) and (V.3) of the fusion and splitting tensors.

Broken zipper condition. The fusion and splitting tensors defined by (VI.34) satisfy the broken zipper condition. More specifically, these tensors satisfy the zipper condition

$$\begin{array}{c} \text{Diagram showing the zipper condition for } \phi_Z \end{array} = \begin{array}{c} \text{Diagram with } \mathcal{O}_{(V_Z,\rho_Z)} \end{array}, \quad \begin{array}{c} \text{Diagram showing the zipper condition for } \bar{\phi}_Z \end{array} = \begin{array}{c} \text{Diagram with } \mathcal{O}_{(V_Z,\rho_Z)} \end{array}, \quad (\text{VI.36})$$

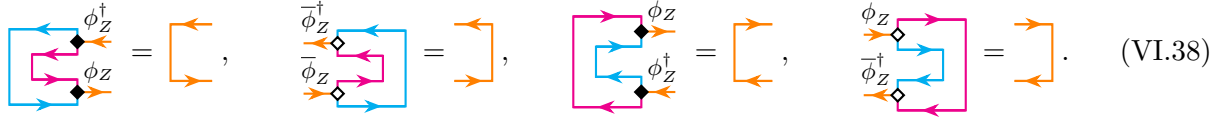
which is stronger than the broken zipper condition. The above equation immediately follows from (VI.35). For example, the first equality of (VI.36) can be obtained as

$$\begin{array}{c} \text{Diagram showing the proof of the zipper condition for } \phi_Z \end{array} = \sum_{Z' \in S_{XY}} \begin{array}{c} \text{Diagram showing the compatibility of } \phi_Z \text{ and } \bar{\phi}_Z \end{array} = \begin{array}{c} \text{Diagram with } \mathcal{O}_{(V_Z,\rho_Z)} \end{array}. \quad (\text{VI.37})$$

The second equality can also be obtained in the same way.

Two-sided zipper condition. The fusion and splitting tensors in (VI.34) also satisfy the two-sided zipper conditions (V.5) and (V.6), where $a_Z^l = a_Z^r = b_Z^l = b_Z^r = 1$ for all fusion channels

$Z \in S_{XY}$. This immediately follows from the zipper condition (VI.36) together with the following equalities:



$$\begin{array}{c} \text{Diagram 1: } \phi_Z^\dagger \text{ and } \phi_Z \text{ in adjacent boxes} \\ \text{Diagram 2: } \phi_Z^\dagger \text{ and } \phi_Z \text{ in overlapping boxes} \\ \text{Diagram 3: } \phi_Z^\dagger \text{ and } \phi_Z \text{ in offset boxes} \\ \text{Diagram 4: } \phi_Z^\dagger \text{ and } \phi_Z \text{ in offset boxes with different colors} \end{array} \quad (\text{VI.38})$$

Lattice quantum dimension and index. Finally, let us compute the lattice quantum dimension and the index of $\mathcal{O}_{(V,\rho)}$. Equation (VI.31) implies that the left and right dimensions of $\mathcal{O}_{(V,\rho)}$ are given by

$$\text{ldim}(\mathcal{O}_{(V,\rho)}) = \dim(V), \quad \text{rdim}(\mathcal{O}_{(V,\rho)}) = \dim(V). \quad (\text{VI.39})$$

Therefore, the lattice quantum dimension and the index of $\mathcal{O}_{(V,\rho)}$ can be computed as

$$\text{qdim}_{\text{lat}}(\mathcal{O}_{(V,\rho)}) = \dim(V), \quad \text{ind}(\mathcal{O}_{(V,\rho)}) = 1. \quad (\text{VI.40})$$

This result is consistent with the fact that the $\text{Rep}(A)$ symmetry is realized exactly on a tensor product Hilbert space without mixing with QCAs.

C. Kramers-Wannier symmetry for \mathbb{Z}_2 gauging

As an example of a non-invertible symmetry that mixes with a non-trivial QCA, we consider the Kramers-Wannier duality symmetry [74], i.e., the self-duality under gauging a \mathbb{Z}_2 symmetry. We will write down the fusion and splitting tensors for the fusion channels of two copies of the Kramers-Wannier duality operator and show that they satisfy both the broken zipper condition and the two-sided zipper condition. We refer the reader to [64, Appendix A] for a similar analysis. A generalization to the case of \mathbb{Z}_N gauging will be discussed in the next subsection.

The Kramers-Wannier duality operator. Let us first recall the definition of the Kramers-Wannier duality operator. We consider a one-dimensional chain of qubits on a periodic lattice of L sites. The Pauli operators on each site are denoted by $\{X_i, Y_i, Z_i\}$ for $i = 1, 2, \dots, L$. We take a basis of the Hilbert space on the entire lattice as $\{|a_1, a_2, \dots, a_L\rangle := \bigotimes_{i=1,2,\dots,L} |a_i\rangle_i \mid a_i = 0, 1\}$, where $|a_i\rangle_i$ is the eigenstate of Z_i with eigenvalue $(-1)^{a_i}$. The action of the Kramers-Wannier duality operator D_{KW} is then given by [75–77]

$$D_{\text{KW}} |a_1, a_2, \dots, a_L\rangle = \left(\bigotimes_{i=1,2,\dots,L} H_i \right) |a_1 - a_L, a_2 - a_1, \dots, a_L - a_{L-1}\rangle, \quad (\text{VI.41})$$

where $H_i = \frac{1}{\sqrt{2}}(X_i + Z_i)$ is the Hadamard gate on site i , and $a_i - a_{i-1}$ is defined modulo 2. The above operator D_{KW} obeys the fusion rule [27, 28]

$$D_{\text{KW}} D_{\text{KW}} = T(1 + U), \quad (\text{VI.42})$$

where T is the lattice translation operator defined by $T|a_1, a_2, \dots, a_L\rangle = |a_L, a_1, \dots, a_{L-1}\rangle$, and $U = \bigotimes_{i=1, \dots, L} X_i$ is the \mathbb{Z}_2 symmetry operator.

MPO representation. The Kramers-Wannier duality operator (VI.41) can be written as an MPO as follows [76, 78]:²⁷

$$D_{\text{KW}} = \text{...} \begin{array}{c} H \\ \diagup \quad \diagdown \\ \text{---} \end{array} \begin{array}{c} H \\ \diagup \quad \diagdown \\ \text{---} \end{array} \begin{array}{c} H \\ \diagup \quad \diagdown \\ \text{---} \end{array} \text{...} \quad (\text{VI.43})$$

Here, the bond Hilbert space is \mathbb{C}^2 whose basis is again labeled by 0 and 1, the yellow square represents the Hadamard gate, and the three-leg tensors represented by the black and white dots are defined by

$$\begin{array}{c} b \rightarrow \bullet \rightarrow c \\ \uparrow a \end{array} = \delta_{a,b} \delta_{a,c}, \quad \begin{array}{c} a \\ \uparrow \\ b \rightarrow \circ \rightarrow c \end{array} = \delta_{a+c,b}. \quad (\text{VI.44})$$

The above tensors are referred to as the copy tensor and the multiplication tensor, respectively. We note that these tensors are intertwined by the Hadamard gate up to a scalar, that is,

$$\begin{array}{c} \rightarrow \bullet \rightarrow \\ \uparrow \quad \uparrow \\ \text{---} \end{array} = \frac{1}{\sqrt{2}} \begin{array}{c} \rightarrow \text{---} \rightarrow \circ \rightarrow \text{---} \rightarrow \\ \uparrow \quad \uparrow \quad \uparrow \\ \text{---} \end{array}, \quad \begin{array}{c} \uparrow \\ \text{---} \end{array} = \sqrt{2} \begin{array}{c} \rightarrow \text{---} \rightarrow \bullet \rightarrow \text{---} \rightarrow \\ \uparrow \quad \uparrow \quad \uparrow \\ \text{---} \end{array}. \quad (\text{VI.45})$$

The MPO representation (VI.43) shows that the local MPO tensor of the Kramers-Wannier duality operator is given by

$$O_{\text{KW}} = \begin{array}{c} \rightarrow \text{---} \rightarrow \circ \rightarrow \bullet \rightarrow \text{---} \rightarrow \\ \uparrow \quad \uparrow \quad \uparrow \quad \uparrow \\ \text{---} \end{array}. \quad (\text{VI.46})$$

This MPO tensor is injective. Indeed, as a linear map from the virtual bonds to the physical legs, the above MPO tensor can be viewed as the controlled- X operator followed by the Hadamard gate, which is invertible and hence injective.

For later use, let us write down the left and right fixed points of the transfer matrix $T[O_{\text{KW}}]$. To this end, we first write down the Hermitian conjugate of the MPO tensor (VI.46) as follows:²⁸

$$O_{\text{KW}}^\dagger = \begin{array}{c} \leftarrow \circ \leftarrow \bullet \leftarrow \text{---} \leftarrow \\ \uparrow \quad \uparrow \quad \uparrow \\ \text{---} \end{array}. \quad (\text{VI.47})$$

Using (VI.46) and (VI.47), the transfer matrix $T[O_{\text{KW}}]$ can be written as

$$T[O_{\text{KW}}] = \begin{array}{c} \leftarrow \circ \leftarrow \bullet \leftarrow \text{---} \leftarrow \\ \uparrow \quad \uparrow \quad \uparrow \\ \text{---} \end{array}. \quad (\text{VI.48})$$

²⁷ The orientations of the physical legs and the virtual bonds do not matter in this example. Nevertheless, we keep the orientations in view of the generalization to the \mathbb{Z}_N case, which we will discuss in the next subsection.

²⁸ The MPO tensor O_{KW}^\dagger generates the Hermitian conjugate of D_{KW} . Using (VI.45), one can show that D_{KW}^\dagger and D_{KW} differ by the lattice translation, i.e., $D_{\text{KW}}^\dagger = T^{-1}D_{\text{KW}}$ [28]. The same relation holds for the Kramers-Wannier duality operator for the \mathbb{Z}_N gauging [79].

The left and right fixed points Λ_{KW}^l and Λ_{KW}^r of this transfer matrix are both given by the identity, that is,

$$\Lambda_{\text{KW}}^l = \text{[} \text{] } , \quad \Lambda_{\text{KW}}^r = \text{[} \text{] } . \quad (\text{VI.49})$$

A direct computation shows that Λ_{KW}^l and Λ_{KW}^r are eigenvectors of $\mathsf{T}[\mathcal{O}_{\text{KW}}]$ with eigenvalue 2:

$$\Lambda_{\text{KW}}^l \mathsf{T}[\mathcal{O}_{\text{KW}}] = \text{[} \text{] } = 2\Lambda_{\text{KW}}^l, \quad \mathsf{T}[\mathcal{O}_{\text{KW}}] \Lambda_{\text{KW}}^r = \text{[} \text{] } = 2\Lambda_{\text{KW}}^r. \quad (\text{VI.50})$$

Here, we used

$$\text{[} \text{] } = \text{[} \text{] } , \quad \text{[} \text{] } = 2 \text{[} \text{] } . \quad (\text{VI.51})$$

Since Λ_{KW}^l and Λ_{KW}^r in (VI.49) are positive definite, equation (VI.50) implies that they are the left and right fixed points of $\mathsf{T}[\mathcal{O}_{\text{KW}}]$; cf. footnote 26.

The Kramers-Wannier MPO is topological. Now, we show that the injective MPO tensor \mathcal{O}_{KW} is topological. Specifically, we show that \mathcal{O}_{KW} satisfies (IV.10) and (IV.11), i.e.,

$$\text{[} \text{] } \mathcal{O}_{\text{KW}}^\dagger \mathcal{O}_{\text{KW}} \mathcal{O}_{\text{KW}}^\dagger \mathcal{O}_{\text{KW}} = \text{[} \text{] } , \quad \mathcal{O}_{\text{KW}}^\dagger \mathcal{O}_{\text{KW}}^\dagger \mathcal{O}_{\text{KW}} \mathcal{O}_{\text{KW}} = \text{[} \text{] } , \quad (\text{VI.52})$$

$$\text{[} \text{] } \mathcal{O}_{\text{KW}} \mathcal{O}_{\text{KW}}^\dagger \mathcal{O}_{\text{KW}}^\dagger \mathcal{O}_{\text{KW}} = \text{[} \text{] } , \quad \mathcal{O}_{\text{KW}} \mathcal{O}_{\text{KW}}^\dagger \mathcal{O}_{\text{KW}}^\dagger \mathcal{O}_{\text{KW}} = \text{[} \text{] } . \quad (\text{VI.53})$$

To show the first equality of (VI.52), we compute the diagram on the left-hand side as follows:

$$\text{LHS} = \text{[} \text{] } = 2 \text{[} \text{] } = 2 \text{[} \text{] } = \text{RHS.} \quad (\text{VI.54})$$

In the third equality, we used

$$\text{[} \text{] } = \text{[} \text{] } , \quad \text{where } a \text{[} \text{] } := 1 \quad \text{for } a = 0, 1. \quad (\text{VI.55})$$

Equation (VI.54) shows the first equality of (VI.52). A similar computation shows the other equalities in (VI.52) and (VI.53).

Fusion and splitting tensors. As shown in (VI.42), the square of the Kramers-Wannier duality operator has two fusion channels T and TU . The fusion and splitting tensors for these fusion

channels can be written explicitly as [64]

$$\phi_T = \begin{array}{c} \text{---} \xrightarrow{\text{---}} \text{---} \\ \text{---} \xrightarrow{\text{---}} \text{---} \end{array}, \quad \bar{\phi}_T = \begin{array}{c} \text{---} \xrightarrow{\text{---}} \text{---} \\ \text{---} \xrightarrow{\text{---}} \text{---} \end{array}, \quad (\text{VI.56})$$

$$\phi_{TU} = \begin{array}{c} \text{---} \xrightarrow{\text{---}} \text{---} \\ \text{---} \xrightarrow{\text{---}} \text{---} \end{array}, \quad \bar{\phi}_{TU} = \begin{array}{c} \text{---} \xrightarrow{\text{---}} \text{---} \\ \text{---} \xrightarrow{\text{---}} \text{---} \end{array}. \quad (\text{VI.57})$$

Here, we recall that the yellow square represents the Hadamard gate and the black dot represents the copy tensor. We note that the fusion and splitting tensors in (VI.56) and (VI.57) are related by Hermitian conjugation as $\bar{\phi}_T = \phi_T^\dagger$ and $\bar{\phi}_{TU} = \phi_{TU}^\dagger$. As we will see below, the above tensors satisfy the defining equations of the fusion and splitting tensors, that is,

$$\begin{array}{c} \mathcal{O}_{\text{KW}} \cdots \\ \phi_T \quad \phi_T \end{array} = \begin{array}{c} \mathcal{O}_T \cdots \\ \phi_T \quad \phi_T \end{array}, \quad \begin{array}{c} \mathcal{O}_{\text{KW}} \cdots \\ \phi_{TU} \quad \mathcal{O}_{\text{KW}} \cdots \quad \phi_{TU} \end{array} = \begin{array}{c} \mathcal{O}_{TU} \cdots \\ \phi_{TU} \quad \mathcal{O}_{\text{KW}} \cdots \quad \phi_{TU} \end{array}, \quad (\text{VI.58})$$

$$\begin{array}{c} \mathcal{O}_{\text{KW}} \quad \mathcal{O}_{\text{KW}} \\ \mathcal{O}_{\text{KW}} \quad \mathcal{O}_{\text{KW}} \end{array} = \begin{array}{c} \mathcal{O}_{\text{KW}} \quad \mathcal{O}_{\text{KW}} \\ \mathcal{O}_{\text{KW}} \quad \phi_T \quad \bar{\phi}_T \quad \mathcal{O}_{\text{KW}} \end{array} + \begin{array}{c} \mathcal{O}_{\text{KW}} \quad \mathcal{O}_{\text{KW}} \\ \mathcal{O}_{\text{KW}} \quad \phi_{TU} \quad \bar{\phi}_{TU} \quad \mathcal{O}_{\text{KW}} \end{array}, \quad (\text{VI.59})$$

where \mathcal{O}_T and \mathcal{O}_{TU} are the local MPO tensors of T and TU defined by

$$\mathcal{O}_T = \begin{array}{c} \text{---} \xrightarrow{\text{---}} \\ \text{---} \xrightarrow{\text{---}} \end{array}, \quad \mathcal{O}_{TU} = \begin{array}{c} \text{---} \xrightarrow{\text{---}} \\ \text{---} \xrightarrow{\text{---}} \\ X \end{array}. \quad (\text{VI.60})$$

The above equations (VI.58) and (VI.59) readily follow from the following set of equalities:

$$\begin{array}{c} \mathcal{O}_{\text{KW}} \\ \phi_T \quad \phi_T \end{array} = \mathcal{O}_T, \quad \begin{array}{c} \mathcal{O}_{\text{KW}} \\ \phi_{TU} \quad \phi_{TU} \end{array} = \mathcal{O}_{TU}, \quad \begin{array}{c} \mathcal{O}_{\text{KW}} \\ \phi_T \quad \phi_T \end{array} = \begin{array}{c} \mathcal{O}_{\text{KW}} \\ \phi_{TU} \quad \phi_{TU} \end{array} = 0, \quad (\text{VI.61})$$

$$\begin{array}{c} \phi_T \quad \phi_T \\ \text{---} \xrightarrow{\text{---}} \end{array} + \begin{array}{c} \phi_{TU} \quad \phi_{TU} \\ \text{---} \xrightarrow{\text{---}} \end{array} = \begin{array}{c} \text{---} \xrightarrow{\text{---}} \\ \text{---} \xrightarrow{\text{---}} \end{array}. \quad (\text{VI.62})$$

We note that the second line is an immediate consequence of the completeness relation

$$\begin{array}{c} \text{---} \xrightarrow{\text{---}} \text{---} \\ \text{---} \xrightarrow{\text{---}} \text{---} \end{array} + \begin{array}{c} \text{---} \xrightarrow{\text{---}} \text{---} \\ X \quad \text{---} \xrightarrow{\text{---}} \text{---} \end{array} = \begin{array}{c} \text{---} \xrightarrow{\text{---}} \\ \text{---} \xrightarrow{\text{---}} \end{array}. \quad (\text{VI.63})$$

In what follows, we will show the remaining equation (VI.61).

To show (VI.61), we use the following expression of the composite tensor consisting of two copies of \mathcal{O}_{KW} :

$$\begin{array}{c} \mathcal{O}_{\text{KW}} \\ \mathcal{O}_{\text{KW}} \end{array} = \begin{array}{c} \text{---} \xrightarrow{\text{---}} \text{---} \\ \text{---} \xrightarrow{\text{---}} \text{---} \end{array} = \begin{array}{c} \text{---} \xrightarrow{\text{---}} \text{---} \\ \text{---} \xrightarrow{\text{---}} \text{---} \end{array} \quad (\text{VI.64})$$

By plugging (VI.64) and (VI.56) into the left-hand side of the first equality of (VI.61), we find

$$\text{LHS} = \text{Diagram} = \text{Diagram} = \text{RHS.} \quad (\text{VI.65})$$

Here, we used

$$\text{Diagram} = \text{Diagram}, \quad \text{where } a \rightarrow \bullet \leftarrow b := \delta_{a,b} \quad \text{for } a, b = 0, 1. \quad (\text{VI.66})$$

Similarly, by plugging (VI.64) and (VI.57) into the left-hand side of the second equality of (VI.61), we find

$$\text{LHS} = \text{Diagram} = \text{Diagram} = \text{RHS.} \quad (\text{VI.67})$$

Here, we used the following commutation relation of the Pauli- X operator with the copy and multiplication tensors:

$$\text{Diagram} = \text{Diagram}, \quad \text{Diagram} = \text{Diagram}. \quad (\text{VI.68})$$

A similar computation also shows the last two equalities in (VI.61) as follows:

$$\text{Diagram} = \text{Diagram} = \text{Diagram} = 0, \quad (\text{VI.69})$$

$$\text{Diagram} = \text{Diagram} = \text{Diagram} = 0. \quad (\text{VI.70})$$

Broken zipper condition. The fusion and splitting tensors defined by (VI.56) and (VI.57) satisfy the broken zipper condition. More specifically, these tensors satisfy the zipper condition

$$\text{Diagram} = \phi_T \text{Diagram}, \quad \text{Diagram} = \phi_T \text{Diagram}, \quad (\text{VI.71})$$

$$\text{Diagram} = \phi_{TU} \text{Diagram}, \quad \text{Diagram} = \phi_{TU} \text{Diagram}, \quad (\text{VI.72})$$

which is stronger than the broken zipper condition. The above equalities immediately follow from (VI.61) and (VI.62).

Two-sided zipper condition. The fusion and splitting tensors defined by (VI.56) and (VI.57) also satisfy the following two-sided zipper condition:

$$\begin{array}{ccc} \text{Diagram with } \mathcal{O}_{\text{KW}}^\dagger, \mathcal{O}_{\text{KW}}, \phi_T^\dagger, \phi_T & = & \text{Diagram with } \mathcal{O}_T^\dagger, \mathcal{O}_T \\ \text{Diagram with } \mathcal{O}_{\text{KW}}^\dagger, \mathcal{O}_{\text{KW}}, \phi_{\text{TU}}^\dagger, \phi_{\text{TU}} & = & \text{Diagram with } \mathcal{O}_{\text{TU}}^\dagger, \mathcal{O}_{\text{TU}} \end{array} \quad (\text{VI.73})$$

$$\begin{array}{ccc} \text{Diagram with } \mathcal{O}_{\text{KW}}^\dagger, \mathcal{O}_{\text{KW}}, \phi_T^\dagger, \phi_{\text{TU}} & = & \text{Diagram with } \mathcal{O}_{\text{TU}}^\dagger, \mathcal{O}_{\text{KW}} \\ \text{Diagram with } \mathcal{O}_{\text{KW}}^\dagger, \mathcal{O}_{\text{KW}}, \phi_{\text{TU}}^\dagger, \phi_{\text{TU}} & = & \text{Diagram with } \mathcal{O}_{\text{KW}}^\dagger, \mathcal{O}_{\text{KW}} \end{array} \quad (\text{VI.74})$$

The above equalities immediately follow from the zipper conditions (VI.71) and (VI.72) together with the following equalities:

$$\begin{array}{ccc} \text{Diagram with } \phi_T^\dagger, \phi_T & = & \text{Diagram with } \phi_{\text{TU}}^\dagger, \phi_{\text{TU}} \\ \text{Diagram with } \phi_T^\dagger, \phi_T & = & \text{Diagram with } \bar{\phi}_T^\dagger, \bar{\phi}_T \end{array} \quad (\text{VI.75})$$

Similarly, one can also show that

$$\begin{array}{ccc} \text{Diagram with } \mathcal{O}_{\text{KW}}^\dagger, \mathcal{O}_{\text{KW}}, \phi_T^\dagger, \phi_T & = & \text{Diagram with } \mathcal{O}_T^\dagger, \mathcal{O}_T \\ \text{Diagram with } \mathcal{O}_{\text{KW}}^\dagger, \mathcal{O}_{\text{KW}}, \phi_{\text{TU}}^\dagger, \phi_{\text{TU}} & = & \text{Diagram with } \mathcal{O}_{\text{TU}}^\dagger, \mathcal{O}_{\text{TU}} \end{array} \quad (\text{VI.76})$$

$$\begin{array}{ccc} \text{Diagram with } \mathcal{O}_{\text{KW}}^\dagger, \mathcal{O}_{\text{KW}}, \phi_T^\dagger, \phi_{\text{TU}} & = & \text{Diagram with } \mathcal{O}_{\text{TU}}^\dagger, \mathcal{O}_{\text{KW}} \\ \text{Diagram with } \mathcal{O}_{\text{KW}}^\dagger, \mathcal{O}_{\text{KW}}, \phi_{\text{TU}}^\dagger, \phi_{\text{TU}} & = & \text{Diagram with } \mathcal{O}_{\text{KW}}^\dagger, \mathcal{O}_{\text{KW}} \end{array} \quad (\text{VI.77})$$

These equalities immediately follow from the zipper conditions (VI.71) and (VI.72) together with the following equalities:

$$\begin{array}{ccc} \text{Diagram with } \phi_T^\dagger, \phi_T & = & \text{Diagram with } \phi_{\text{TU}}^\dagger, \phi_{\text{TU}} \\ \text{Diagram with } \phi_T^\dagger, \phi_T & = & \text{Diagram with } \bar{\phi}_T^\dagger, \bar{\phi}_T \end{array} \quad (\text{VI.78})$$

Lattice quantum dimension and index. Let us compute the lattice quantum dimension and the index of the Kramers-Wannier MPO tensor \mathcal{O}_{KW} . To this end, we first compute the left and

right dimensions of \mathcal{O}_{KW} . The left dimension of \mathcal{O}_{KW} can be computed as

$$\text{ldim}(\mathcal{O}_{\text{KW}}) = \frac{1}{\dim(\mathcal{H}_o)} \text{rank} \left(\begin{array}{c} \text{---} \\ \text{---} \end{array} \right) = 2, \quad (\text{VI.79})$$

where $\mathcal{H}_o = \mathbb{C}^2$ is the on-site Hilbert space. Here, the first equality follows from the fact that the Hadamard gate H does not affect the rank because it is invertible. The second equality follows from the fact that the diagram on the left-hand side is invertible as a linear map from the bottom left to the top right,²⁹ and hence it has full rank. Similarly, the right dimension of \mathcal{O}_{KW} can be computed as

$$\text{rdim}(\mathcal{O}_{\text{KW}}) = \frac{1}{\dim(\mathcal{H}_o)} \text{rank} \left(\begin{array}{c} \text{---} \\ \text{---} \end{array} \right) = 1. \quad (\text{VI.80})$$

Equations (VI.79) and (VI.80) imply that the lattice quantum dimension and the index of \mathcal{O}_{KW} are given by

$$\text{qdim}_{\text{lat}}(\mathcal{O}_{\text{KW}}) = \sqrt{2}, \quad \text{ind}(\mathcal{O}_{\text{KW}}) = \sqrt{2}. \quad (\text{VI.81})$$

We note that the lattice quantum dimension of \mathcal{O}_{KW} agrees with the quantum dimension of the unique non-invertible simple object of a \mathbb{Z}_2 Tambara-Yamagami category [80]. The left and right dimensions computed above agree with the dimensions of the defect Hilbert spaces associated with the Kramers-Wannier duality defect [28].³⁰ Furthermore, the index computed above agrees with the index of the Kramers-Wannier duality operator viewed as a QCA on the algebra of \mathbb{Z}_2 -symmetric local operators [49] or a QCA on a fusion spin chain [48].

D. Kramers-Wannier symmetry for \mathbb{Z}_N gauging

Let us generalize the discussion in the previous subsection to the Kramers-Wannier self-duality for gauging a \mathbb{Z}_N symmetry, where N is an arbitrary positive integer. We will see that the Kramers-Wannier duality operator for the \mathbb{Z}_N gauging is a topological injective MPO, which we refer to as the \mathbb{Z}_N Kramers-Wannier duality operator. We will then write down the fusion and splitting tensors for the fusion channels of two copies of the \mathbb{Z}_N Kramers-Wannier duality operator and show that they satisfy the broken zipper condition and the two-sided zipper condition. These results also hold for the Kramers-Wannier duality operator for a general finite abelian group because any finite abelian group is isomorphic to the direct product of finite cyclic groups.

The \mathbb{Z}_N Kramers-Wannier duality operator. We first recall the definition of the \mathbb{Z}_N Kramers-Wannier duality operator. To this end, we consider a one-dimensional chain of N -dimensional qudits on a periodic lattice of L sites. The clock and shift operators on each site are denoted by Z_i and X_i , respectively. We take a basis of the Hilbert space on the entire lattice as $\{|a_1, a_2, \dots, a_L\rangle := \bigotimes_{i=1,2,\dots,L} |a_i\rangle_i \mid a_i = 0, 1, \dots, N-1\}$, where $|a_i\rangle_i$ is the eigenstate of Z_i with eigenvalue $e^{2\pi i a_i/N}$.

²⁹ More specifically, the diagram on the left-hand side is a controlled- X operator acting on the left virtual bond and the bottom physical leg.

³⁰ See also [81–86] for earlier works on duality-twisted boundary conditions.

The action of the \mathbb{Z}_N Kramers-Wannier duality operator D_{KW_N} is then given by [79, 87, 88]

$$D_{KW_N} |a_1, a_2, \dots, a_L\rangle = \left(\bigotimes_{i=1,2,\dots,L} H_i \right) |a_1 - a_L, a_2 - a_1, \dots, a_L - a_{L-1}\rangle, \quad (VI.82)$$

where $a_i - a_{i-1}$ is defined modulo N , and H_i is the generalized Hadamard gate on site i defined by [89]

$$H |a\rangle = \frac{1}{\sqrt{N}} \sum_{b=0}^{N-1} e^{2\pi i ab/N} |b\rangle. \quad (\text{VI.83})$$

We note that $H^2 |a\rangle = |N - a\rangle$ and in particular $H^4 = 1$. A direct computation shows that the \mathbb{Z}_N Kramers-Wannier duality operator D_{KW_N} obeys the fusion rule [79, 88]

$$\mathsf{D}_{\mathsf{KW}_N} \mathsf{D}_{\mathsf{KW}_N} = T \sum_{n=0}^{N-1} U_n, \quad (\text{VI.84})$$

where T is the lattice translation operator defined by $T|a_1, a_2, \dots, a_L\rangle = |a_L, a_1, \dots, a_{L-1}\rangle$, and $U_n := \bigotimes_{i=1,2,\dots,L} X_i^n$ is the \mathbb{Z}_N symmetry operator.

MPO representation. The \mathbb{Z}_N Kramers-Wannier duality operator (VI.82) can be written as an MPO as follows [29, 87]:

$$D_{KW_N} = \text{Diagram} \quad (VI.85)$$

Here, the bond Hilbert space is \mathbb{C}^N whose basis is again labeled by $0, 1, \dots, N-1$, and we defined

$$S : |a\rangle \rightarrow |N-a\rangle. \quad (\text{VI.86})$$

We note that $S = H^2$ and in particular $SH = HS = H^{-1}$. The black and white dots in (VI.85) represent the copy and multiplication tensors (VI.44) for the \mathbb{Z}_N variables. We note that the copy tensor and the multiplication tensor are intertwined by the generalized Hadamard gate up to a scalar as follows:

$$\begin{array}{c} \text{Diagram: } \text{A horizontal line with a black dot at the top and a yellow square labeled } H \text{ at the bottom.} \\ \text{Equation: } \frac{1}{\sqrt{N}} \xrightarrow{H^{-1}} \text{ (yellow square)} \xrightarrow{H} \text{ (black dot)} \xrightarrow{H} \text{ (yellow square)} \xrightarrow{H^{-1}} \text{ (black dot)} \end{array} , \quad \begin{array}{c} \text{Diagram: } \text{A horizontal line with a yellow square labeled } H \text{ at the top and a black dot at the bottom.} \\ \text{Equation: } \sqrt{N} \xrightarrow{H} \text{ (yellow square)} \xrightarrow{\text{black dot}} \text{ (black dot)} \xrightarrow{H^{-1}} \text{ (yellow square)} \end{array} . \quad (\text{VI.87})$$

The MPO representation (VI.85) shows that the local MPO tensor of the \mathbb{Z}_N Kramers-Wannier duality operator is given by

$$\mathcal{O}_{\text{KW}_N} = \text{Diagram} \quad . \quad (\text{VI.88})$$

This MPO tensor is injective as in the case of $N = 2$.

For later use, let us write down the left and right fixed points of the transfer matrix $T[\mathcal{O}_{KW}]$. To this end, we first write the Hermitian conjugate of the MPO tensor (VI.85) as follows:

$$\mathcal{O}_{\text{KW}_N}^\dagger = \text{Diagram} \quad . \quad (\text{VI.89})$$

Based on (VI.88) and (VI.89), the transfer matrix $T[\mathcal{O}_{KW_N}]$ can be written as

$$\mathsf{T}[\mathcal{O}_{\text{KW}_N}] = \text{Diagram} \quad . \quad (\text{VI.90})$$

The left and right fixed points of this transfer matrix are both given by the identity, that is,

$$\Lambda_{\text{KW}_N}^l = \left[\begin{array}{c} \leftarrow \\ \leftarrow \end{array} \right], \quad \Lambda_{\text{KW}_N}^r = \left[\begin{array}{c} \leftarrow \\ \leftarrow \end{array} \right]. \quad (\text{VI.91})$$

It is straightforward to show that the above $\Lambda_{\text{KW}_N}^l$ and $\Lambda_{\text{KW}_N}^r$ are positive definite left and right eigenvectors of $\mathsf{T}[\mathcal{O}_{\text{KW}_N}]$ and hence the fixed points.

The \mathbb{Z}_N Kramers-Wannier MPO is topological. One can show that the injective MPO tensor $\mathcal{O}_{\text{KW}_N}$ defined by (VI.88) is topological, that is, it satisfies

$$\begin{array}{c} \text{Diagram 1: } \mathcal{O}_{\text{KW}_N}^\dagger \text{ and } \mathcal{O}_{\text{KW}_N} \text{ on top row, } \mathcal{O}_{\text{KW}_N} \text{ and } \mathcal{O}_{\text{KW}_N}^\dagger \text{ on bottom row.} \\ \text{Diagram 2: } \mathcal{O}_{\text{KW}_N}^\dagger \text{ and } \mathcal{O}_{\text{KW}_N} \text{ on top row, } \mathcal{O}_{\text{KW}_N} \text{ and } \mathcal{O}_{\text{KW}_N}^\dagger \text{ on bottom row.} \\ \text{Diagram 3: } \mathcal{O}_{\text{KW}_N}^\dagger \text{ and } \mathcal{O}_{\text{KW}_N} \text{ on top row, } \mathcal{O}_{\text{KW}_N} \text{ and } \mathcal{O}_{\text{KW}_N}^\dagger \text{ on bottom row.} \end{array} = \begin{array}{c} \text{Diagram 4: } \mathcal{O}_{\text{KW}_N}^\dagger \text{ and } \mathcal{O}_{\text{KW}_N} \text{ on top row, } \mathcal{O}_{\text{KW}_N} \text{ and } \mathcal{O}_{\text{KW}_N}^\dagger \text{ on bottom row.} \end{array}, \quad (\text{VI.92})$$

$$\begin{array}{c} \text{Diagram 1} \\ \text{Diagram 2} \\ \text{Diagram 3} \\ \text{Diagram 4} \end{array} = \begin{array}{c} \text{Diagram 5} \\ \text{Diagram 6} \end{array}, \quad \begin{array}{c} \text{Diagram 7} \\ \text{Diagram 8} \\ \text{Diagram 9} \\ \text{Diagram 10} \end{array} = \begin{array}{c} \text{Diagram 11} \\ \text{Diagram 12} \end{array}. \quad (\text{VI.93})$$

We will omit the derivation of the above equalities because it is parallel to the case of $N = 2$.

Fusion and splitting tensors. The fusion rule (VI.84) implies that the square of the \mathbb{Z}_N Kramers-Wannier duality operator has N fusion channels $\{TU_n \mid n = 0, 1, \dots, N-1\}$. The fusion and splitting tensors for each fusion channel TU_n can be written explicitly as

$$\phi_{TU_n} = \text{Diagram } (a) \text{, } \bar{\phi}_{TU_n} = \text{Diagram } (b) \text{, } \quad (\text{VI.94})$$

where the black dot represents the copy tensor and the yellow squares with and without a centered dot represent H^{-1} and H , respectively. We note that the splitting tensor is the Hermitian conjugate

of the fusion tensor, i.e., $\bar{\phi}_{TU_n} = \phi_{TU_n}^\dagger$. As we will see below, the above tensors satisfy the defining equations of the fusion and splitting tensors, that is,

$$\begin{array}{c} \text{Diagram:} \\ \text{Two horizontal rows of circles connected by horizontal lines. The top row has a diamond at the left end and circles with labels } \mathcal{O}_{\text{KW}_N}, \dots, \mathcal{O}_{\text{KW}_N}, \text{ and a diamond at the right end. The bottom row has circles with labels } \phi_{TU_n}, \dots, \phi_{TU_n}, \text{ and a diamond at the right end.} \end{array} = \begin{array}{c} \text{Diagram:} \\ \text{Two horizontal rows of circles connected by horizontal lines. The top row has a diamond at the left end and circles with labels } \mathcal{O}_{\text{TU}_n}, \mathcal{O}_{\text{TU}_n}, \dots, \mathcal{O}_{\text{TU}_n}, \text{ and a diamond at the right end.} \end{array}, \quad (\text{VI.95})$$

$$\begin{array}{c} \text{Diagram:} \\ \text{Two horizontal rows of circles connected by horizontal lines. The top row has a diamond at the left end and circles with labels } \mathcal{O}_{\text{KW}_N}, \mathcal{O}_{\text{KW}_N}, \text{ and a diamond at the right end. The bottom row has circles with labels } \mathcal{O}_{\text{KW}_N}, \mathcal{O}_{\text{KW}_N}, \text{ and a diamond at the right end.} \end{array} = \sum_{n=0}^{N-1} \begin{array}{c} \text{Diagram:} \\ \text{Two horizontal rows of circles connected by horizontal lines. The top row has a diamond at the left end and circles with labels } \mathcal{O}_{\text{KW}_N}, \dots, \phi_{TU_n}, \text{ and a diamond at the right end. The bottom row has circles with labels } \phi_{TU_n}, \bar{\phi}_{TU_n}, \text{ and a diamond at the right end.} \end{array}, \quad (\text{VI.96})$$

where $\mathcal{O}_{\text{TU}_n}$ is the MPO tensor of TU_n defined by

$$\mathcal{O}_{\text{TU}_n} = \begin{array}{c} \text{Diagram:} \\ \text{A vertical line with a blue dot at the bottom labeled } X^n, \text{ with an arrow pointing up.} \end{array}. \quad (\text{VI.97})$$

As in the case of $N = 2$, one can easily see that (VI.95) and (VI.96) follow from the following set of equalities:

$$\begin{array}{c} \text{Diagram:} \\ \text{Two horizontal rows of circles connected by horizontal lines. The top row has a diamond at the left end and circles with labels } \mathcal{O}_{\text{KW}_N}, \dots, \phi_{TU_m}, \text{ and a diamond at the right end. The bottom row has circles with labels } \mathcal{O}_{\text{KW}_N}, \text{ and a diamond at the right end.} \end{array} = \delta_{n,m} \begin{array}{c} \text{Diagram:} \\ \text{A vertical line with a blue dot at the bottom labeled } X^n, \text{ with an arrow pointing up.} \end{array}, \quad \sum_{n=0}^{N-1} \begin{array}{c} \text{Diagram:} \\ \text{Two horizontal rows of circles connected by horizontal lines. The top row has a diamond at the left end and circles with labels } \phi_{TU_n}, \text{ and a diamond at the right end. The bottom row has circles with labels } \bar{\phi}_{TU_n}, \text{ and a diamond at the right end.} \end{array} = \begin{array}{c} \text{Diagram:} \\ \text{Two horizontal rows of circles connected by horizontal lines. The top row has a diamond at the left end and circles with labels } \phi_{TU_n}, \text{ and a diamond at the right end. The bottom row has circles with labels } \phi_{TU_n}, \text{ and a diamond at the right end.} \end{array}. \quad (\text{VI.98})$$

Here, the second equality of (VI.98) is an immediate consequence of the completeness relation

$$\sum_{n=0}^{N-1} \begin{array}{c} \text{Diagram:} \\ \text{Two horizontal rows of circles connected by horizontal lines. The top row has a diamond at the left end and circles with labels } X^{-n}, \dots, X^{-n}, \text{ and a diamond at the right end. The bottom row has circles with labels } X^n, \dots, X^n, \text{ and a diamond at the right end.} \end{array} = \begin{array}{c} \text{Diagram:} \\ \text{Two horizontal rows of circles connected by horizontal lines. The top row has a diamond at the left end and circles with labels } X^n, \dots, X^n, \text{ and a diamond at the right end. The bottom row has circles with labels } X^n, \dots, X^n, \text{ and a diamond at the right end.} \end{array}. \quad (\text{VI.99})$$

In what follows, we will show the first equality of (VI.98).

To show the first equality of (VI.98), we use the following expression of the composite tensor consisting of two copies of $\mathcal{O}_{\text{KW}_N}$:

$$\begin{array}{c} \text{Diagram:} \\ \text{Two horizontal rows of circles connected by horizontal lines. The top row has a diamond at the left end and circles with labels } \mathcal{O}_{\text{KW}_N}, \text{ and a diamond at the right end. The bottom row has a diamond at the left end and circles with labels } \mathcal{O}_{\text{KW}_N}, \text{ and a diamond at the right end.} \end{array} = \begin{array}{c} \text{Diagram:} \\ \text{Two horizontal rows of circles connected by horizontal lines. The top row has a diamond at the left end and circles with labels } \mathcal{O}_{\text{KW}_N}, \text{ and a diamond at the right end. The bottom row has a diamond at the left end and circles with labels } \mathcal{O}_{\text{KW}_N}, \text{ and a diamond at the right end.} \end{array} = \begin{array}{c} \text{Diagram:} \\ \text{Two horizontal rows of circles connected by horizontal lines. The top row has a diamond at the left end and circles with labels } H, \text{ and a diamond at the right end. The bottom row has a diamond at the left end and circles with labels } H^{-1}, \text{ and a diamond at the right end.} \end{array} = \begin{array}{c} \text{Diagram:} \\ \text{Two horizontal rows of circles connected by horizontal lines. The top row has a diamond at the left end and circles with labels } H, \text{ and a diamond at the right end. The bottom row has a diamond at the left end and circles with labels } H^{-1}, \text{ and a diamond at the right end.} \end{array} = \begin{array}{c} \text{Diagram:} \\ \text{Two horizontal rows of circles connected by horizontal lines. The top row has a diamond at the left end and circles with labels } S, \text{ and a diamond at the right end. The bottom row has a diamond at the left end and circles with labels } S, \text{ and a diamond at the right end.} \end{array}. \quad (\text{VI.100})$$

Here, the last equality follows from (VI.87) and $SH = H^{-1}$. By plugging (VI.100) and (VI.94) into the left-hand side of the first equality of (VI.98), we find

$$\text{LHS} = \begin{array}{c} \text{Diagram:} \\ \text{Two horizontal rows of circles connected by horizontal lines. The top row has a diamond at the left end and circles with labels } X^{n-m}, \dots, X^{n-m}, \text{ and a diamond at the right end. The bottom row has circles with labels } S, \dots, S, \text{ and a diamond at the right end.} \end{array} = \begin{array}{c} \text{Diagram:} \\ \text{Two horizontal rows of circles connected by horizontal lines. The top row has a diamond at the left end and circles with labels } X^{n-m}, \dots, X^{n-m}, \text{ and a diamond at the right end. The bottom row has circles with labels } X^n, \text{ and a diamond at the right end.} \end{array} = \text{RHS}. \quad (\text{VI.101})$$

Here, the first equality follows from

$$\begin{array}{c} \xrightarrow{\quad} \bullet \xleftarrow{\quad} \bullet \xrightarrow{\quad} X^{-n} \xleftarrow{\quad} X^n \xrightarrow{\quad} \\ = \end{array} \quad \begin{array}{c} \xrightarrow{\quad} \bullet \xleftarrow{\quad} X^n \xrightarrow{\quad} \\ = \end{array}, \quad \begin{array}{c} \xrightarrow{\quad} X^{-n} \xleftarrow{\quad} \bullet \xrightarrow{\quad} X^n \xrightarrow{\quad} \\ = \end{array} \quad \begin{array}{c} \xrightarrow{\quad} \bullet \xleftarrow{\quad} \\ = \end{array}, \quad \begin{array}{c} \xrightarrow{\quad} S \xleftarrow{\quad} X^n \xrightarrow{\quad} \\ = \end{array} \quad \begin{array}{c} \xrightarrow{\quad} X^{-n} \xleftarrow{\quad} S \xrightarrow{\quad} \\ = \end{array}, \quad (\text{VI.102})$$

while the second equality follows from

$$\begin{array}{c} \xrightarrow{\quad} \bullet \xleftarrow{\quad} \bullet \xrightarrow{\quad} S \xleftarrow{\quad} \bullet \xrightarrow{\quad} \\ = \end{array} \quad \begin{array}{c} \xrightarrow{\quad} \bullet \xleftarrow{\quad} \bullet \xrightarrow{\quad} \bullet \xleftarrow{\quad} \bullet \xrightarrow{\quad} \\ = \end{array}, \quad \text{where } a \xrightarrow{\quad} \bullet \xleftarrow{\quad} b := \delta_{a,N-b} \quad \text{for } a, b = 0, 1, \dots, N-1. \quad (\text{VI.103})$$

Broken zipper condition. The fusion and splitting tensors defined by (VI.94) satisfy the broken zipper condition. More specifically, these tensors satisfy the zipper condition

$$\begin{array}{c} \mathcal{O}_{\text{KW}_N} \xrightarrow{\quad} \bullet \xleftarrow{\quad} \bullet \xrightarrow{\quad} \phi_{TU_n} \xleftarrow{\quad} \bullet \xrightarrow{\quad} \bullet \xrightarrow{\quad} \mathcal{O}_{TU_n} \xrightarrow{\quad} \\ = \end{array} \quad \begin{array}{c} \phi_{TU_n} \xrightarrow{\quad} \bullet \xleftarrow{\quad} \bullet \xrightarrow{\quad} \mathcal{O}_{TU_n} \xrightarrow{\quad} \\ = \end{array}, \quad \begin{array}{c} \bar{\phi}_{TU_n} \xrightarrow{\quad} \bullet \xleftarrow{\quad} \bullet \xrightarrow{\quad} \mathcal{O}_{\text{KW}_N} \xleftarrow{\quad} \bullet \xrightarrow{\quad} \bullet \xrightarrow{\quad} \mathcal{O}_{TU_n} \xrightarrow{\quad} \\ = \end{array} \quad \begin{array}{c} \mathcal{O}_{TU_n} \xrightarrow{\quad} \bullet \xleftarrow{\quad} \bullet \xrightarrow{\quad} \bar{\phi}_{TU_n} \xleftarrow{\quad} \bullet \xrightarrow{\quad} \\ = \end{array}, \quad (\text{VI.104})$$

which is stronger than the broken zipper condition. The above equation immediately follows from (VI.98).

Two-sided zipper condition. The fusion and splitting tensors defined by (VI.94) also satisfy the following two-sided zipper condition:

$$\begin{array}{c} \mathcal{O}_{\text{KW}_N}^\dagger \xrightarrow{\quad} \bullet \xleftarrow{\quad} \bullet \xrightarrow{\quad} \phi_{TU_n}^\dagger \xleftarrow{\quad} \bullet \xrightarrow{\quad} \bullet \xrightarrow{\quad} \mathcal{O}_{TU_n}^\dagger \xleftarrow{\quad} \bullet \xrightarrow{\quad} \\ = \end{array} \quad \begin{array}{c} \mathcal{O}_{TU_n}^\dagger \xrightarrow{\quad} \bullet \xleftarrow{\quad} \bullet \xrightarrow{\quad} \mathcal{O}_{\text{KW}_N}^\dagger \xleftarrow{\quad} \bullet \xrightarrow{\quad} \bullet \xrightarrow{\quad} \mathcal{O}_{\text{KW}_N}^\dagger \xleftarrow{\quad} \bullet \xrightarrow{\quad} \\ = \end{array}, \quad (\text{VI.105})$$

$$\begin{array}{c} \mathcal{O}_{\text{KW}_N} \xrightarrow{\quad} \bullet \xleftarrow{\quad} \bullet \xrightarrow{\quad} \phi_{TU_n} \xleftarrow{\quad} \bullet \xrightarrow{\quad} \bullet \xrightarrow{\quad} \mathcal{O}_{\text{KW}_N}^\dagger \xleftarrow{\quad} \bullet \xrightarrow{\quad} \\ = \end{array} \quad \begin{array}{c} \mathcal{O}_{TU_n} \xrightarrow{\quad} \bullet \xleftarrow{\quad} \bullet \xrightarrow{\quad} \mathcal{O}_{\text{KW}_N}^\dagger \xleftarrow{\quad} \bullet \xrightarrow{\quad} \bullet \xrightarrow{\quad} \mathcal{O}_{\text{KW}_N}^\dagger \xleftarrow{\quad} \bullet \xrightarrow{\quad} \\ = \end{array}, \quad (\text{VI.106})$$

The above equations immediately follow from the zipper condition (VI.104) together with the following equalities:

$$\begin{array}{c} \phi_{TU_n}^\dagger \xleftarrow{\quad} \bullet \xrightarrow{\quad} \bullet \xleftarrow{\quad} \phi_{TU_n} \xleftarrow{\quad} \bullet \xrightarrow{\quad} \\ = \end{array}, \quad \begin{array}{c} \bar{\phi}_{TU_n}^\dagger \xleftarrow{\quad} \bullet \xrightarrow{\quad} \bullet \xleftarrow{\quad} \bar{\phi}_{TU_n} \xleftarrow{\quad} \bullet \xrightarrow{\quad} \\ = \end{array}, \quad \begin{array}{c} \bullet \xleftarrow{\quad} \phi_{TU_n} \xrightarrow{\quad} \bullet \xleftarrow{\quad} \phi_{TU_n}^\dagger \xleftarrow{\quad} \bullet \xrightarrow{\quad} \\ = \end{array}, \quad \begin{array}{c} \bullet \xleftarrow{\quad} \bar{\phi}_{TU_n} \xrightarrow{\quad} \bullet \xleftarrow{\quad} \bar{\phi}_{TU_n}^\dagger \xleftarrow{\quad} \bullet \xrightarrow{\quad} \\ = \end{array}. \quad (\text{VI.107})$$

Lattice quantum dimension and index. The lattice quantum dimension and the index of the \mathbb{Z}_N Kramers-Wannier MPO $\mathcal{O}_{\text{KW}_N}$ can be computed in the same way as in the case of $N = 2$.

Concretely, one can compute the left and right dimensions of $\mathcal{O}_{\text{KW}_N}$ as

$$\text{ldim}(\mathcal{O}_{\text{KW}_N}) = N, \quad \text{rdim}(\mathcal{O}_{\text{KW}_N}) = 1. \quad (\text{VI.108})$$

Thus, the lattice quantum dimension and the index of $\mathcal{O}_{\text{KW}_N}$ are given by

$$\text{qdim}_{\text{lat}}(\mathcal{O}_{\text{KW}_N}) = \sqrt{N}, \quad \text{ind}(\mathcal{O}_{\text{KW}_N}) = \sqrt{N}. \quad (\text{VI.109})$$

We note that the lattice quantum dimension of $\mathcal{O}_{\text{KW}_N}$ agrees with the quantum dimension of the unique non-invertible simple object of a \mathbb{Z}_N Tambara-Yamagami category [80]. The index of $\mathcal{O}_{\text{KW}_N}$ computed above agrees with the index of the \mathbb{Z}_N Kramers-Wannier duality operator viewed as a QCA on the algebra of \mathbb{Z}_N -symmetric local operators [49] or a QCA on a fusion spin chain [48].

VII. SUMMARY AND OUTLOOK

In this paper, we studied general structures of non-invertible symmetries on a tensor product Hilbert space in 1+1 dimensions using two complementary approaches: one is an axiomatic approach based on physical assumptions, and the other is a more concrete approach based on tensor networks. In particular, we defined an index of non-invertible symmetry operators in 1+1d and discussed its role in constraining possible fusion rules of symmetry operators on a tensor product Hilbert space. In what follows, we provide a more detailed summary of the results.

Axiomatic approach. Assuming the existence of defect Hilbert spaces satisfying Assumptions 1–4, we showed that the fusion rules of a unitary fusion category \mathcal{C} can be realized by symmetry operators on a tensor product Hilbert space only when \mathcal{C} is integral, if we do not allow mixing with QCAs. This result agrees with the mathematical result recently proved in [26]. Furthermore, based on the same assumptions, we showed that if the fusion rules of \mathcal{C} are realized up to QCAs on a tensor product Hilbert space, then \mathcal{C} must be weakly integral as long as the index is homogeneous in the sense that all fusion channels of two indecomposable symmetry operators have the same index. This is consistent with the conjecture recently proposed in [32, 33], which states that a unitary fusion category symmetry realized on a tensor product Hilbert space must be weakly integral even if we allow mixing with spacetime symmetry. We emphasize that the homogeneity of the index has not been proven, and hence the conjecture in [32, 33] is still open.

Tensor network approach. We proposed a general class of tensor network operators, called topological injective MPOs, that describe symmetry operators on a tensor product Hilbert space in 1+1d. For these MPOs, we defined the corresponding defect Hilbert spaces and constructed local unitary operators that move the defects. We also showed that topological injective MPOs admit sequential quantum circuit representations, which is consistent with the recent proposal in [36].

The tensor network description allows us to study the properties of the index of non-invertible symmetry operators without relying on physical assumptions. In particular, within the framework of tensor networks, we can formulate the homogeneity of the index as a purely algebraic problem. Based on this formulation, we provided sufficient conditions for the homogeneity of the index of topological injective MPOs. More specifically, we showed that the index is homogeneous if every fusion channel of two topological injective MPOs has a pair of fusion and splitting tensors (cf. Definition V.1) that satisfy the broken zipper condition (cf. Definition V.2) and the two-sided

zipper condition (cf. Definition V.3). We provided various examples of topological injective MPOs whose fusion channels have fusion and splitting tensors satisfying the broken zipper condition and the two-sided zipper condition. However, the existence of such fusion and splitting tensors for general topological injective MPOs has not yet been proven.

Outlook. Given that all examples of topological injective MPOs discussed in this paper satisfy the sufficient conditions for the homogeneity of the index, it would be natural to ask whether the same holds for all topological injective MPOs. Namely, we would pose the following question:

Question 1. *For every fusion channel of topological injective MPOs, does there exist a pair of a fusion tensor and a splitting tensor that satisfy both the broken zipper condition and the two-sided zipper condition, if we block a sufficient number of physical sites?*

Combined with the results obtained in this paper, the above question leads to the following statement:

Corollary 1. *If the answer to Question 1 is affirmative, a unitary fusion category symmetry realized by topological injective MPOs must be weakly integral even if we allow mixing with non-trivial QCAs. More specifically, if there exists a finite set of topological injective MPOs whose fusion rules agree with those of a unitary fusion category \mathcal{C} up to QCAs, then \mathcal{C} must be weakly integral, as long as Question 1 is answered affirmatively.*

The above statement does not claim that any weakly integral unitary fusion category symmetry can be realized on a tensor product Hilbert space if we allow mixing with non-trivial QCAs.³¹ Nevertheless, it was recently shown in [29] that weakly integral fusion categories describing the self-dualities under gauging non-anomalous fusion category symmetries can be realized on a tensor product Hilbert space if we allow mixing with lattice translations. It would be interesting to construct concrete lattice models that realize more general weakly integral fusion category symmetries on a tensor product Hilbert space.³²

Another interesting direction is to consider different realizations of fusion category symmetries on a tensor product Hilbert space. Recently, it was found in [91, 92] that a symmetry with non-commutative fusion rules dictated by the Onsager algebra on the lattice can flow to a $U(1) \times U(1)$ symmetry with a mixed anomaly in the continuum. It would be interesting to study whether non-invertible symmetries also admit a similar realization on the lattice.

ACKNOWLEDGMENTS

The author thanks Christian Copetti, Kantaro Ohmori, and Shuhei Ohyama for helpful discussions. The author is supported in part by the EPSRC Open Fellowship EP/X01276X/1 and by the Leverhulme-Peierls Fellowship funded by the Leverhulme Trust. A part of this work was done while visiting the Okinawa Institute of Science and Technology (OIST) through the Theoretical Sciences Visiting Program (TSVP) Thematic Program on Generalized Symmetries in Quantum Matter (TP25QM).

³¹ We note that any unitary fusion category symmetry can be realized exactly on a Hilbert space with local constraints [23–25]. This does not contradict Corollary 1 because the projection to the constrained Hilbert space cannot be written as a topological injective MPO.

³² Typical examples of weakly integral fusion categories are weakly group-theoretical ones. To the best of the author’s knowledge, it is an open problem whether every weakly integral fusion category is weakly group-theoretical [90, Question 2].

Appendix A: Choice of Λ^l and Λ^r in Definition IV.1

In this appendix, we show that if there exist positive definite linear maps Λ^l and Λ^r that satisfy (IV.10), the fixed points of the transfer matrix $\mathsf{T}[\mathcal{O}]$ must also satisfy (IV.10). The same applies to (IV.11). Therefore, as long as we impose the positive definiteness of Λ^l and Λ^r in Definition IV.1, we can choose the fixed points of $\mathsf{T}[\mathcal{O}]$ as Λ^l and Λ^r without loss of generality. In what follows, we will show the above statement only for the right fixed point. The case of the left fixed point is similar.

To show the above statement, we suppose that there exists a positive definite linear map $\tilde{\Lambda}^r$ that satisfies the second equality of (IV.10), i.e.,

$$\begin{array}{c} \mathcal{O}^\dagger \uparrow \quad \mathcal{O}^\dagger \uparrow \\ \mathcal{O} \leftarrow \quad \mathcal{O} \leftarrow \\ \mathcal{O} \uparrow \quad \mathcal{O} \uparrow \end{array} = \begin{array}{c} \mathcal{O}^\dagger \uparrow \quad \mathcal{O}^\dagger \uparrow \\ \mathcal{O} \leftarrow \quad \mathcal{O} \leftarrow \\ \mathcal{O} \uparrow \quad \mathcal{O} \uparrow \end{array} \bullet \tilde{\Lambda}^r \quad (A.1)$$

If we take the trace over both physical legs, the above equation reduces to

$$\mathsf{T}[\mathcal{O}] \mathsf{T}[\mathcal{O}] \tilde{\Lambda}^r = \dim(\mathcal{H}_o) \mathsf{T}[\mathcal{O}] \tilde{\Lambda}^r, \quad (A.2)$$

where $\mathsf{T}[\mathcal{O}]$ is the transfer matrix of \mathcal{O} . Equation (A.2) shows that $\mathsf{T}[\mathcal{O}] \tilde{\Lambda}^r$ is an eigenvector of $\mathsf{T}[\mathcal{O}]$ with eigenvalue $\dim(\mathcal{H}_o)$. On the other hand, $\mathsf{T}[\mathcal{O}] \tilde{\Lambda}^r$ is positive definite because the transfer matrix of an injective MPO tensor preserves the positive definiteness; see, e.g., [66, Section V]. Since a positive definite eigenvector of $\mathsf{T}[\mathcal{O}]$ is unique and is given by the fixed point due to [73, Theorem 2.4], we find that $\mathsf{T}[\mathcal{O}] \tilde{\Lambda}^r$ is the right fixed point of $\mathsf{T}[\mathcal{O}]$. Therefore, $\tilde{\Lambda}^r$ can be written as

$$\tilde{\Lambda}^r = \Lambda^r + \Delta, \quad (A.3)$$

where Λ^r is the right fixed point of $\mathsf{T}[\mathcal{O}]$ and Δ is an eigenvector of $\mathsf{T}[\mathcal{O}]$ with eigenvalue zero. Now, we plug (A.3) into (A.1) and write down equations for Λ^r and Δ . To this end, we use the decomposition

$$\tilde{\mathsf{T}}[\mathcal{O}] := \begin{array}{c} \mathcal{O}^\dagger \uparrow \\ \mathcal{O} \leftarrow \\ \mathcal{O} \uparrow \end{array} = \frac{1}{\dim(\mathcal{H}_o)} \mathsf{T}[\mathcal{O}] \otimes \text{id}_{\mathcal{H}_o} + \sum_{\alpha} S_{\alpha} \otimes \sigma_{\alpha}, \quad (A.4)$$

where σ_{α} 's are linearly independent traceless operators acting on the physical leg and S_{α} 's are operators acting on the pair of the top and bottom virtual bonds. Using the above decomposition, we can compute the left-hand side and the right-hand side of (A.1) as follows:

$$\text{LHS} = \tilde{\mathsf{T}}[\mathcal{O}]^{(1)} \Lambda^r \otimes \text{id}_{\mathcal{H}_o}^{(2)} + \tilde{\mathsf{T}}[\mathcal{O}]^{(1)} \sum_{\alpha} S_{\alpha} (\Lambda^r + \Delta) \otimes \sigma_{\alpha}^{(2)}, \quad (A.5)$$

$$\text{RHS} = \tilde{\mathsf{T}}[\mathcal{O}]^{(1)} \Lambda^r \otimes \text{id}_{\mathcal{H}_o}^{(2)} + \sum_{\alpha} S_{\alpha} \Delta \otimes \sigma_{\alpha}^{(1)} \otimes \text{id}_{\mathcal{H}_o}^{(2)}. \quad (A.6)$$

Here, the operators with superscripts 1 and 2 act on the left and right physical legs, respectively. Due to the above equations, the condition (A.1) reduces to

$$\tilde{\mathsf{T}}[\mathcal{O}]^{(1)} \sum_{\alpha} S_{\alpha} (\Lambda^r + \Delta) \otimes \sigma_{\alpha}^{(2)} = \sum_{\alpha} S_{\alpha} \Delta \otimes \sigma_{\alpha}^{(1)} \otimes \text{id}_{\mathcal{H}_o}^{(2)}. \quad (A.7)$$

Since σ_α 's are linearly independent traceless operators, the above equation is equivalent to

$$S_\alpha \Delta = 0, \quad \tilde{\mathcal{T}}[\mathcal{O}] S_\alpha \Lambda^r = 0, \quad \forall \alpha. \quad (\text{A.8})$$

In particular, if there exists a pair (Λ^r, Δ) that satisfies the above equation, the pair $(\Lambda^r, 0)$ also satisfies the same equation. Recalling that $\tilde{\Lambda}^r$ is defined by (A.3), we conclude that if there exists a positive definite $\tilde{\Lambda}^r$ that satisfies (A.1), the fixed point Λ^r also satisfies the same equation.

Appendix B: Equivalence of Definitions IV.1 and IV.2

In Section IV B, we provided two definitions of a topological injective MPO, namely, Definitions IV.1 and IV.2. In this appendix, we show that these definitions are equivalent. More specifically, we show that (IV.11) and (IV.12) are equivalent given that the injective MPO tensor \mathcal{O} satisfies (IV.10). As shown in Section IV C, equation (IV.11) together with (IV.10) implies (IV.12). Thus, in what follows, it suffices to show that equation (IV.12) together with (IV.10) implies (IV.11).

To show (IV.11), we recall that \mathcal{O} can be decomposed into two three-leg tensors as in (IV.53). Using this decomposition, we can write the zigzag relations in (IV.12) as

$$\Lambda^l \circ \begin{array}{|c|} \hline A_l \\ \hline B_l \\ \hline B_l^\dagger \\ \hline A_l^\dagger \\ \hline \end{array} = \delta_l(\mathcal{O}) \quad \text{and} \quad \Lambda^r \circ \begin{array}{|c|} \hline A_r \\ \hline B_r \\ \hline B_r^\dagger \\ \hline A_r^\dagger \\ \hline \end{array} = \delta_r(\mathcal{O}), \quad (\text{B.1})$$

where we used (IV.56). Since A_l and A_r have left inverses and B_l and B_r have right inverses by construction, the above equation implies

$$\Lambda^l \circ \begin{array}{|c|} \hline A_l \\ \hline B_l \\ \hline B_l^\dagger \\ \hline A_l^\dagger \\ \hline \end{array} = \delta_l(\mathcal{O}) \quad \text{and} \quad \Lambda^r \circ \begin{array}{|c|} \hline A_r \\ \hline B_r \\ \hline B_r^\dagger \\ \hline A_r^\dagger \\ \hline \end{array} = \delta_r(\mathcal{O}), \quad (\text{B.2})$$

Using this equation, we can show the first equality of (IV.11) by a direct computation as follows:

$$\Lambda^l \circ \begin{array}{|c|} \hline \mathcal{O} \\ \hline \mathcal{O}^\dagger \\ \hline \mathcal{O} \\ \hline \mathcal{O}^\dagger \\ \hline \end{array} = \delta_l(\mathcal{O}) \quad \text{and} \quad \Lambda^l \circ \begin{array}{|c|} \hline A_l \\ \hline w_l \\ \hline w_l^\dagger \\ \hline A_l \\ \hline \end{array} = \delta_l(\mathcal{O}) \quad \text{and} \quad \Lambda^l \circ \begin{array}{|c|} \hline A_l \\ \hline A_l^\dagger \\ \hline A_l^\dagger \\ \hline A_l \\ \hline \end{array} = \Lambda^l \circ \begin{array}{|c|} \hline \mathcal{O} \\ \hline \mathcal{O}^\dagger \\ \hline \mathcal{O} \\ \hline \mathcal{O}^\dagger \\ \hline \end{array}. \quad (\text{B.3})$$

Here, w_l is defined by (IV.58) and we used the fact that it is unitary (IV.62).³³ A similar computation also shows the second equality of (IV.11). Thus, we find that Definitions IV.1 and IV.2 are equivalent.

³³ We note that the derivation of the unitarity of w_l does not rely on (IV.11): it follows only from (IV.10).

Appendix C: Determination of $\delta_l(\mathcal{O})$ and $\delta_r(\mathcal{O})$ in Definition IV.2

In this appendix, following the proof of [53, Proposition 1], we show that $\delta_l(\mathcal{O})$ and $\delta_r(\mathcal{O})$ in the zigzag equation (IV.12) are uniquely given by the positive real numbers defined by (IV.31). To this end, we recall that the three-leg tensors B_l and B_r in the decomposition (IV.53) satisfy (B.2). By taking the trace of both sides of this equation, we obtain

$$\delta_l(\mathcal{O}) = \frac{1}{\text{rank}_l(\mathcal{O})} \text{tr} \left(\Lambda^l \circ \begin{array}{c} \text{square loop} \\ \text{red vertical line} \\ B_l \\ B_l^\dagger \end{array} \right) = \frac{1}{\text{rank}_l(\mathcal{O})} \text{tr} \left(\Lambda^l \circ \begin{array}{c} \text{square loop} \\ \text{red vertical line} \\ B_l^\dagger \\ B_l \end{array} \right), \quad (\text{C.1})$$

$$\delta_r(\mathcal{O}) = \frac{1}{\text{rank}_r(\mathcal{O})} \text{tr} \left(\begin{array}{c} B_r \\ B_r^\dagger \end{array} \circ \begin{array}{c} \text{square loop} \\ \text{blue vertical line} \\ \bullet \Lambda^r \end{array} \right) = \frac{1}{\text{rank}_r(\mathcal{O})} \text{tr} \left(\begin{array}{c} B_r^\dagger \\ B_r \end{array} \circ \begin{array}{c} \text{square loop} \\ \text{blue vertical line} \\ \bullet \Lambda^r \end{array} \right). \quad (\text{C.2})$$

On the other hand, equation (IV.28) together with (IV.56) implies that B_l and B_r satisfy

$$\Lambda^l \circ \begin{array}{c} \text{square loop} \\ \text{red vertical line} \\ B_l \\ B_l^\dagger \end{array} = \gamma \uparrow = \begin{array}{c} \text{square loop} \\ \text{blue vertical line} \\ B_r^\dagger \\ B_r \end{array} \circ \bullet \Lambda^r. \quad (\text{C.3})$$

By plugging this into (C.1) and (C.2), we obtain

$$\delta_l(\mathcal{O}) = \frac{\gamma}{\text{ldim}(\mathcal{O})}, \quad \delta_r(\mathcal{O}) = \frac{\gamma}{\text{rdim}(\mathcal{O})}, \quad (\text{C.4})$$

which shows (IV.31).

Appendix D: Derivation of (VI.28)

In this appendix, we show that the MPO tensor (VI.25) labeled by a finite dimensional $*$ -representation (V, ρ) of a finite dimensional semisimple Hopf $*$ -algebra A satisfies (VI.28). Equivalently, we show

$$\begin{array}{c} \Delta^\dagger \\ \uparrow \\ \text{square loop} \\ \uparrow \\ \rho^\dagger \end{array} = \begin{array}{c} \Delta \\ \uparrow \\ \text{square loop} \\ \uparrow \\ S \bullet \text{orange dot} \\ \uparrow \\ \rho \end{array}, \quad \text{i.e.,} \quad (\text{D.1})$$

$$(\Delta^\dagger \otimes \text{id}_V) \circ (\text{id}_A \otimes \rho^\dagger) = (\text{id}_A \otimes \rho) \circ (\text{id}_A \otimes S \otimes \text{id}_V) \circ (\Delta \otimes \text{id}_V),$$

where the Hermitian conjugate is defined with respect to the inner product (VI.21). In the above equation, the representation map ρ is regarded as a linear map from $A \otimes V$ to V . The same linear map regarded as a map from A to $\text{End}(V)$ via the canonical isomorphism $\text{Hom}(A \otimes V, V) \cong \text{Hom}(A, \text{End}(V))$ will be denoted by ϱ .³⁴ We note that ρ and ϱ are related by $\rho(a \otimes v) = \varrho(a)(v)$ for all $a \in A$ and $v \in V$. In what follows, the inner product on a Hilbert space X is denoted by $\langle x|y \rangle_X$ for $x, y \in X$, where X is either A , V , $A \otimes A$, or $A \otimes V$. Furthermore, orthonormal bases of A and V are denoted by $\{a_i \mid i = 1, 2, \dots, \dim(A)\}$ and $\{v_\mu \mid \mu = 1, 2, \dots, \dim(V)\}$, respectively.

³⁴ In Section VIB, both ρ and ϱ are denoted by ρ by abuse of notation.

To show (D.1), we compute the components of the linear maps on both sides. On the one hand, the components of the linear map on the left-hand side can be computed as

$$\begin{aligned}
& \langle a_i \otimes v_\mu | (\Delta^\dagger \otimes \text{id}_V) \circ (\text{id}_A \otimes \rho^\dagger)(a_j \otimes v_\nu) \rangle_{A \otimes V} \\
&= \sum_{k=1}^{\dim(A)} \langle a_i | \Delta^\dagger(a_j \otimes a_k) \rangle_A \langle a_k \otimes v_\mu | \rho^\dagger(v_\nu) \rangle_{A \otimes V} = \sum_{k=1}^{\dim(A)} \langle \Delta(a_i) | a_j \otimes a_k \rangle_{A \otimes A} \langle \rho(a_k \otimes v_\mu) | v_\nu \rangle_V \\
&= \sum_{k=1}^{\dim(A)} \langle \Delta(a_i) | a_j \otimes a_k \rangle_{A \otimes A} \langle v_\mu | \rho(a_k)^\dagger(v_\nu) \rangle_V = \sum_{k=1}^{\dim(A)} \langle \Delta(a_i) | a_j \otimes a_k \rangle_{A \otimes A} \langle v_\mu | \rho(a_k^*)(v_\nu) \rangle_V,
\end{aligned} \tag{D.2}$$

where the last equality follows from the fact that (V, ρ) is a $*$ -representation. On the other hand, the component of the linear map on the right-hand side can be computed as

$$\begin{aligned}
& \langle a_i \otimes v_\mu | (\text{id}_A \otimes \rho) \circ (\text{id}_A \otimes S \otimes \text{id}_V) \circ (\Delta \otimes \text{id}_V)(a_j \otimes v_\nu) \rangle_{A \otimes V} \\
&= \sum_{k=1}^{\dim(A)} \langle a_i \otimes a_k | (\text{id}_A \otimes S) \circ \Delta(a_j) \rangle_{A \otimes A} \langle v_\mu | \rho(a_k)(v_\nu) \rangle_V.
\end{aligned} \tag{D.3}$$

The above equations imply that (D.1) holds if we have

$$\langle \Delta(a_i) | a_j \otimes a_k \rangle_{A \otimes A} = \langle a_i \otimes a_k | (\text{id}_A \otimes S) \circ \Delta(a_j) \rangle_{A \otimes A}, \quad \forall i, j, k, \tag{D.4}$$

in a basis where $a_i^* = a_i$ for all $i = 1, 2, \dots, \dim(A)$.³⁵ In what follows, we will show that (D.4) holds in any orthonormal basis of A .

To show (D.4), we note that the left-hand side of (D.4) can be written as

$$\langle \Delta(a_i) | a_j \otimes a_k \rangle_{A \otimes A} = \langle (\text{id}_A \otimes a^k) \circ \Delta(a_i) | a_j \rangle_A = \langle \widehat{\Delta}(a^k)(a_i) | a_j \rangle_A, \tag{D.5}$$

where $\{a^k \mid k = 1, 2, \dots, \dim(A)\}$ is the dual basis of $\{a_k \mid k = 1, 2, \dots, \dim(A)\}$, and $\widehat{\Delta} : A^* \rightarrow \text{End}(A)$ is defined by

$$\widehat{\Delta}(\phi) := (\text{id}_A \otimes \phi) \circ \Delta, \quad \forall \phi \in A^*. \tag{D.6}$$

One can show that $(A, \widehat{\Delta})$ is a $*$ -representation of the dual Hopf $*$ -algebra A^* ,³⁶ where the $*$ -operation on A^* is defined by $\phi^* := \phi \circ S$ for all $\phi \in A^*$. Therefore, it follows that

$$\langle \widehat{\Delta}(a^k)(a_i) | a_j \rangle_A = \langle a_i | \widehat{\Delta}((a^k)^*)(a_j) \rangle_A = \langle a_i \otimes a_k | (\text{id}_A \otimes S) \circ \Delta(a_j) \rangle_A. \tag{D.7}$$

Equations (D.5) and (D.7) show (D.4). Thus, we find that (D.1) holds.

[1] J. McGreevy, ‘‘Generalized Symmetries in Condensed Matter,’’ [Ann. Rev. Condensed Matter Phys. 14 \(2023\) 57–82, arXiv:2204.03045 \[cond-mat.str-el\]](#).

³⁵ Such a basis always exists. Indeed, since A is semisimple, it is isomorphic to a direct sum of endomorphism algebras $\bigoplus \text{End}(V_X)$, where the direct sum is taken over all (isomorphism classes of) irreducible $*$ -representations $(V_X, \rho_X) \in \text{Rep}(A)$. The $*$ -operation and the inner product on $\bigoplus \text{End}(V_X)$ are given by the Hermitian conjugation and the Hilbert-Schmidt inner product, respectively. We can then take $\{a_i \mid i = 1, 2, \dots, \dim(A)\}$ to be a Hermitian orthonormal basis of $\bigoplus \text{End}(V_X)$.

³⁶ This immediately follows from Example 3.1.6 and Proposition 3.1.7 of [67].

- [2] C. Córdova, T. T. Dumitrescu, K. Intriligator, and S.-H. Shao, “Snowmass White Paper: Generalized Symmetries in Quantum Field Theory and Beyond,” in Snowmass 2021. 5, 2022. [arXiv:2205.09545 \[hep-th\]](https://arxiv.org/abs/2205.09545).
- [3] S. Schäfer-Nameki, “ICTP lectures on (non-)invertible generalized symmetries,” Phys. Rept. **1063** (2024) 1–55, [arXiv:2305.18296 \[hep-th\]](https://arxiv.org/abs/2305.18296).
- [4] T. D. Brennan and S. Hong, “Introduction to Generalized Global Symmetries in QFT and Particle Physics,” [arXiv:2306.00912 \[hep-ph\]](https://arxiv.org/abs/2306.00912).
- [5] S.-H. Shao, “What’s Done Cannot Be Undone: TASI Lectures on Non-Invertible Symmetries,” [arXiv:2308.00747 \[hep-th\]](https://arxiv.org/abs/2308.00747).
- [6] N. Carqueville, M. Del Zotto, and I. Runkel, “Topological defects,” 11, 2023. [arXiv:2311.02449 \[math-ph\]](https://arxiv.org/abs/2311.02449).
- [7] N. Iqbal, “Jena lectures on generalized global symmetries: principles and applications,” 7, 2024. [arXiv:2407.20815 \[hep-th\]](https://arxiv.org/abs/2407.20815).
- [8] D. Costa et al., “Simons Lectures on Categorical Symmetries,” 11, 2024. [arXiv:2411.09082 \[math-ph\]](https://arxiv.org/abs/2411.09082).
- [9] D. Gaiotto, A. Kapustin, N. Seiberg, and B. Willett, “Generalized Global Symmetries,” JHEP **02** (2015) 172, [arXiv:1412.5148 \[hep-th\]](https://arxiv.org/abs/1412.5148).
- [10] L. Bhardwaj and Y. Tachikawa, “On finite symmetries and their gauging in two dimensions,” JHEP **03** (2018) 189, [arXiv:1704.02330 \[hep-th\]](https://arxiv.org/abs/1704.02330).
- [11] C.-M. Chang, Y.-H. Lin, S.-H. Shao, Y. Wang, and X. Yin, “Topological Defect Lines and Renormalization Group Flows in Two Dimensions,” JHEP **01** (2019) 026, [arXiv:1802.04445 \[hep-th\]](https://arxiv.org/abs/1802.04445).
- [12] R. Thorngren and Y. Wang, “Fusion category symmetry. Part I. Anomaly in-flow and gapped phases,” JHEP **04** (2024) 132, [arXiv:1912.02817 \[hep-th\]](https://arxiv.org/abs/1912.02817).
- [13] R. Thorngren and Y. Wang, “Fusion category symmetry. Part II. Categoriosities at $c = 1$ and beyond,” JHEP **07** (2024) 051, [arXiv:2106.12577 \[hep-th\]](https://arxiv.org/abs/2106.12577).
- [14] E. P. Verlinde, “Fusion Rules and Modular Transformations in 2D Conformal Field Theory,” Nucl. Phys. B **300** (1988) 360–376.
- [15] V. B. Petkova and J. B. Zuber, “Generalized twisted partition functions,” Phys. Lett. B **504** (2001) 157–164, [arXiv:hep-th/0011021](https://arxiv.org/abs/hep-th/0011021).
- [16] J. Fuchs, I. Runkel, and C. Schweigert, “TFT construction of RCFT correlators 1. Partition functions,” Nucl. Phys. B **646** (2002) 353–497, [arXiv:hep-th/0204148](https://arxiv.org/abs/hep-th/0204148).
- [17] J. Fröhlich, J. Fuchs, I. Runkel, and C. Schweigert, “Kramers-Wannier duality from conformal defects,” Phys. Rev. Lett. **93** (2004) 070601, [arXiv:cond-mat/0404051](https://arxiv.org/abs/cond-mat/0404051).
- [18] J. Fröhlich, J. Fuchs, I. Runkel, and C. Schweigert, “Duality and defects in rational conformal field theory,” Nucl. Phys. B **763** (2007) 354–430, [arXiv:hep-th/0607247](https://arxiv.org/abs/hep-th/0607247).
- [19] J. Fuchs, M. R. Gaberdiel, I. Runkel, and C. Schweigert, “Topological defects for the free boson CFT,” J. Phys. A **40** (2007) 11403, [arXiv:0705.3129 \[hep-th\]](https://arxiv.org/abs/0705.3129).
- [20] Z. Komargodski, K. Ohmori, K. Roumpedakis, and S. Seifnashri, “Symmetries and strings of adjoint QCD_2 ,” JHEP **03** (2021) 103, [arXiv:2008.07567 \[hep-th\]](https://arxiv.org/abs/2008.07567).
- [21] T.-C. Huang, Y.-H. Lin, and S. Seifnashri, “Construction of two-dimensional topological field theories with non-invertible symmetries,” JHEP **12** (2021) 028, [arXiv:2110.02958 \[hep-th\]](https://arxiv.org/abs/2110.02958).
- [22] K. Inamura, “On lattice models of gapped phases with fusion category symmetries,” JHEP **03** (2022) 036, [arXiv:2110.12882 \[cond-mat.str-el\]](https://arxiv.org/abs/2110.12882).
- [23] A. Feiguin, S. Trebst, A. W. W. Ludwig, M. Troyer, A. Kitaev, Z. Wang, and M. H. Freedman, “Interacting anyons in topological quantum liquids: The golden chain,” Phys. Rev. Lett. **98** (2007) 160409, [arXiv:cond-mat/0612341](https://arxiv.org/abs/cond-mat/0612341).
- [24] M. Buican and A. Gromov, “Anyonic Chains, Topological Defects, and Conformal Field Theory,” Commun. Math. Phys. **356** no. 3, (2017) 1017–1056, [arXiv:1701.02800 \[hep-th\]](https://arxiv.org/abs/1701.02800).
- [25] D. Aasen, P. Fendley, and R. S. K. Mong, “Topological Defects on the Lattice: Dualities and Degeneracies,” [arXiv:2008.08598 \[cond-mat.stat-mech\]](https://arxiv.org/abs/2008.08598).
- [26] D. E. Evans and C. Jones, “An operator algebraic approach to fusion category symmetry on the

lattice,” [arXiv:2507.05185 \[math-ph\]](https://arxiv.org/abs/2507.05185).

[27] N. Seiberg and S.-H. Shao, “Majorana chain and Ising model - (non-invertible) translations, anomalies, and emanant symmetries,” [SciPost Phys.](https://doi.org/10.21468/SciPostPhys.16.064) **16** no. 3, (2024) 064, [arXiv:2307.02534 \[cond-mat.str-el\]](https://arxiv.org/abs/2307.02534).

[28] N. Seiberg, S. Seifnashri, and S.-H. Shao, “Non-invertible symmetries and LSM-type constraints on a tensor product Hilbert space,” [SciPost Phys.](https://doi.org/10.21468/SciPostPhys.16.054) **16** (2024) 154, [arXiv:2401.12281 \[cond-mat.str-el\]](https://arxiv.org/abs/2401.12281).

[29] D.-C. Lu, A. Chatterjee, and N. Tantivasadakarn, “Generalized Kramers-Wannier Self-Duality in Hopf-Ising Models,” [arXiv:2602.10183 \[cond-mat.str-el\]](https://arxiv.org/abs/2602.10183).

[30] T. Farrelly, “A review of Quantum Cellular Automata,” [Quantum](https://doi.org/10.22331/q-2020-368) **4** (2020) 368, [arXiv:1904.13318 \[quant-ph\]](https://arxiv.org/abs/1904.13318).

[31] P. Arrighi, “An overview of quantum cellular automata,” [Natural Comput.](https://doi.org/10.1007/s11089-019-0944-2) **18** no. 4, (2019) 885–899, [arXiv:1904.12956 \[quant-ph\]](https://arxiv.org/abs/1904.12956).

[32] A. Antinucci, C. Delaney, T. Johnson-Freyd, H. T. Lam, N. Tantivasadakarn, and C. Zhang, “Open Problems: Views from High Energy Physics, Condensed Matter/QI and Mathematics,” 2025. <https://online.kitp.ucsb.edu/online/gensym25/openproblems/>. Talk at Kavli Institute for Theoretical Physics.

[33] N. Tantivasadakarn, “Non-invertible self-duality symmetries on a tensor product Hilbert space,” 2025. <https://www.youtube.com/watch?v=hRwBSGUbjf0>. Talk at Isaac Newton Institute for Mathematical Sciences.

[34] P. Etingof, S. Gelaki, D. Nikshych, and V. Ostrik, [Tensor Categories](https://www.math.mit.edu/~etingof/egnobookfinal.pdf), vol. 205 of [Mathematical Surveys and Monographs](https://www.math.mit.edu/~etingof/egnobookfinal.pdf). American Mathematical Society, Providence, RI, 2015. [http://www.math.mit.edu/~etingof/egnobookfinal.pdf](https://www.math.mit.edu/~etingof/egnobookfinal.pdf).

[35] M. Okada and Y. Tachikawa, “Noninvertible Symmetries Act Locally by Quantum Operations,” [Phys. Rev. Lett.](https://doi.org/10.1103/PhysRevLett.133.191602) **133** no. 19, (2024) 191602, [arXiv:2403.20062 \[hep-th\]](https://arxiv.org/abs/2403.20062).

[36] N. Tantivasadakarn, X. Liu, and X. Chen, “Sequential Circuit as Generalized Symmetry on Lattice,” [arXiv:2507.22394 \[cond-mat.str-el\]](https://arxiv.org/abs/2507.22394).

[37] L. Lootens, C. Delcamp, D. Williamson, and F. Verstraete, “Low-Depth Unitary Quantum Circuits for Dualities in One-Dimensional Quantum Lattice Models,” [Phys. Rev. Lett.](https://doi.org/10.1103/PhysRevLett.134.130403) **134** no. 13, (2025) 130403, [arXiv:2311.01439 \[quant-ph\]](https://arxiv.org/abs/2311.01439).

[38] G. Ortiz, C. Giridhar, P. Vojta, A. H. Nevidomskyy, and Z. Nussinov, “Generalized Wigner theorem for non-invertible symmetries,” [arXiv:2509.25327 \[quant-ph\]](https://arxiv.org/abs/2509.25327).

[39] T. Bartsch, Y. Gai, and S. Schafer-Nameki, “Beyond Wigner: Non-Invertible Symmetries Preserve Probabilities,” [arXiv:2602.07110 \[quant-ph\]](https://arxiv.org/abs/2602.07110).

[40] D. Gross, V. Nesme, H. Vogts, and R. F. Werner, “Index Theory of One Dimensional Quantum Walks and Cellular Automata,” [Commun. Math. Phys.](https://doi.org/10.1007/s00180-012-0544-4) **310** no. 2, (2012) 419–454, [arXiv:0910.3675 \[quant-ph\]](https://arxiv.org/abs/0910.3675).

[41] A. Molnar, A. R. de Alarcón, J. Garre-Rubio, N. Schuch, J. I. Cirac, and D. Pérez-García, “Matrix product operator algebras I: representations of weak Hopf algebras and projected entangled pair states,” [arXiv:2204.05940 \[quant-ph\]](https://arxiv.org/abs/2204.05940).

[42] L. Lootens, C. Delcamp, G. Ortiz, and F. Verstraete, “Dualities in One-Dimensional Quantum Lattice Models: Symmetric Hamiltonians and Matrix Product Operator Intertwiners,” [PRX Quantum](https://doi.org/10.1103/PRXQuantum.4.020357) **4** no. 2, (2023) 020357, [arXiv:2112.09091 \[quant-ph\]](https://arxiv.org/abs/2112.09091).

[43] L. Lootens, C. Delcamp, and F. Verstraete, “Dualities in One-Dimensional Quantum Lattice Models: Topological Sectors,” [PRX Quantum](https://doi.org/10.1103/PRXQuantum.5.010338) **5** no. 1, (2024) 010338, [arXiv:2211.03777 \[quant-ph\]](https://arxiv.org/abs/2211.03777).

[44] B. Vancraeynest-De Cuiper, W. Wiesiolek, and F. Verstraete, “Les Houches Lecture Notes on Tensor Networks,” [arXiv:2512.24390 \[cond-mat.str-el\]](https://arxiv.org/abs/2512.24390).

[45] S. Seifnashri, “Lieb-Schultz-Mattis anomalies as obstructions to gauging (non-on-site) symmetries,” [SciPost Phys.](https://doi.org/10.21468/SciPostPhys.16.098) **16** no. 4, (2024) 098, [arXiv:2308.05151 \[cond-mat.str-el\]](https://arxiv.org/abs/2308.05151).

[46] D. A. Marcus, [Number Fields](https://doi.org/10.1007/978-3-030-38902-0). Universitext. Springer Cham, Second ed., 2018.

[47] Z. Jia, “Generalized cluster states from Hopf algebras: non-invertible symmetry and Hopf tensor network representation,” [JHEP](https://doi.org/10.1007/jhep09(2024)147) **09** (2024) 147, [arXiv:2405.09277 \[quant-ph\]](https://arxiv.org/abs/2405.09277).

[48] C. Jones and J. Lim, “An Index for Quantum Cellular Automata on Fusion Spin Chains,” [Annales](https://doi.org/10.1007/s00180-024-05207-0)

Henri Poincare **25** no. 10, (2024) 4399–4422, [arXiv:2309.10961](https://arxiv.org/abs/2309.10961) [math.OA].

[49] R. Ma, Y. Li, and M. Cheng, “Quantum Cellular Automata on Symmetric Subalgebras,” [arXiv:2411.19280](https://arxiv.org/abs/2411.19280) [quant-ph].

[50] L. Bhardwaj, L. E. Bottini, S. Schafer-Nameki, and A. Tiwari, “Lattice Models for Phases and Transitions with Non-Invertible Symmetries,” [arXiv:2405.05964](https://arxiv.org/abs/2405.05964) [cond-mat.str-el].

[51] J. I. Cirac, D. Perez-Garcia, N. Schuch, and F. Verstraete, “Matrix product unitaries: structure, symmetries, and topological invariants,” *J. Phys. A* **2017** no. 8, (2017) 083105, [arXiv:1703.09188](https://arxiv.org/abs/1703.09188) [cond-mat.str-el].

[52] M. B. Şahinoğlu, S. K. Shukla, F. Bi, and X. Chen, “Matrix Product Representation of Locality Preserving Unitaries,” *Phys. Rev. B* **98** (2018) 245122, [arXiv:1704.01943](https://arxiv.org/abs/1704.01943) [quant-ph].

[53] A. Franco-Rubio, A. Bochniak, and J. I. Cirac, “Symmetry defects and gauging for quantum states with matrix product unitary symmetries,” [arXiv:2502.20257](https://arxiv.org/abs/2502.20257) [quant-ph].

[54] J. I. Cirac, D. Pérez-García, N. Schuch, and F. Verstraete, “Matrix product states and projected entangled pair states: Concepts, symmetries, theorems,” *Rev. Mod. Phys.* **93** no. 4, (2021) 045003, [arXiv:2011.12127](https://arxiv.org/abs/2011.12127) [quant-ph].

[55] D. Pérez-García, F. Verstraete, M. M. Wolf, and J. I. Cirac, “Matrix product state representations,” *Quant. Inf. Comput.* **7** no. 5-6, (2007) 401–430, [arXiv:quant-ph/0608197](https://arxiv.org/abs/quant-ph/0608197).

[56] J. I. Cirac, D. Perez-Garcia, N. Schuch, and F. Verstraete, “Matrix Product Density Operators: Renormalization Fixed Points and Boundary Theories,” *Annals Phys.* **378** (2017) 100, [arXiv:1606.00608](https://arxiv.org/abs/1606.00608) [quant-ph].

[57] M. Fannes, B. Nachtergaele, and R. F. Werner, “Finitely correlated states on quantum spin chains,” *Communications in Mathematical Physics* **144** no. 3, (Mar, 1992) 443–490.

[58] S. Seifnashri, S.-H. Shao, and X. Yang, “Gauging non-invertible symmetries on the lattice,” *SciPost Phys.* **19** no. 2, (2025) 063, [arXiv:2503.02925](https://arxiv.org/abs/2503.02925) [cond-mat.str-el].

[59] X. Chen, A. Dua, M. Hermele, D. T. Stephen, N. Tantivasadakarn, R. Vanhove, and J.-Y. Zhao, “Sequential quantum circuits as maps between gapped phases,” *Phys. Rev. B* **109** no. 7, (2024) 075116, [arXiv:2307.01267](https://arxiv.org/abs/2307.01267) [cond-mat.str-el].

[60] N. Bultinck, M. Mariën, D. J. Williamson, M. B. Şahinoğlu, J. Haegeman, and F. Verstraete, “Anyons and matrix product operator algebras,” *Annals Phys.* **378** (2017) 183–233, [arXiv:1511.08090](https://arxiv.org/abs/1511.08090) [cond-mat.str-el].

[61] L. Lootens, J. Fuchs, J. Haegeman, C. Schweigert, and F. Verstraete, “Matrix product operator symmetries and intertwiners in string-nets with domain walls,” *SciPost Phys.* **10** no. 3, (2021) 053, [arXiv:2008.11187](https://arxiv.org/abs/2008.11187) [quant-ph].

[62] J. Garre-Rubio, L. Lootens, and A. Molnár, “Classifying phases protected by matrix product operator symmetries using matrix product states,” *Quantum* **7** (2023) 927, [arXiv:2203.12563](https://arxiv.org/abs/2203.12563) [cond-mat.str-el].

[63] K. Inamura and S. Ohyama, “1+1d SPT phases with fusion category symmetry: interface modes and non-abelian Thouless pump,” [arXiv:2408.15960](https://arxiv.org/abs/2408.15960) [cond-mat.str-el].

[64] D.-C. Lu, F. Xu, and Y.-Z. You, “Strange correlator and string order parameter for non-invertible symmetry protected topological phases in 1+1d,” [arXiv:2505.00673](https://arxiv.org/abs/2505.00673) [cond-mat.str-el].

[65] S. Ohyama and S. Ryu, “Higher Berry phase from projected entangled pair states in (2+1) dimensions,” *Phys. Rev. B* **111** no. 4, (2025) 045112, [arXiv:2405.05325](https://arxiv.org/abs/2405.05325) [cond-mat.str-el].

[66] A. Molnar, Y. Ge, N. Schuch, and J. I. Cirac, “A generalization of the injectivity condition for Projected Entangled Pair States,” *J. Math. Phys.* **59** (2018) 021902, [arXiv:1706.07329](https://arxiv.org/abs/1706.07329) [cond-mat.str-el].

[67] T. Timmermann, *An Invitation to Quantum Groups and Duality. From Hopf Algebras to Multiplicative Unitaries and Beyond*. EMS Textb. Math. Zürich: European Mathematical Society, 2008.

[68] R. G. Larson and M. Sweedler, “An Associative Orthogonal Bilinear Form for Hopf Algebras,” *American Journal of Mathematics* **91** (1969) 75–94.

[69] D. E. Radford, “The Order of the Antipode of a Finite Dimensional Hopf Algebra is Finite,” *American Journal of Mathematics* **98** (1969) 333–355.

[70] R. G. Larson and D. E. Radford, “Semisimple Cosemisimple Hopf Algebras,” *American Journal of Mathematics* **110** (1988) 187–195.

[71] S. Neshveyev and L. Tuset, *Compact Quantum Groups and Their Representation Categories*, vol. 20 of *Cours Spéc. (Paris)*. Paris: Société Mathématique de France (SMF), 2013. <https://smf.emath.fr/publications/compact-quantum-groups-and-their-representation-categories>.

[72] C. Meng, X. Yang, T. Lan, and Z. Gu, “Non-invertible SPTs: an on-site realization of (1+1)d anomaly-free fusion category symmetry,” [arXiv:2412.20546](https://arxiv.org/abs/2412.20546) [cond-mat.str-el].

[73] D. E. Evans and R. Høegh-Krohn, “Spectral Properties of Positive Maps on C^* -Algebras,” *Journal of the London Mathematical Society* **s2-17** no. 2, (1978) 345–355.

[74] H. A. Kramers and G. H. Wannier, “Statistics of the Two-Dimensional Ferromagnet. Part I,” *Phys. Rev.* **60** (Aug, 1941) 252–262.

[75] D. Aasen, R. S. K. Mong, and P. Fendley, “Topological Defects on the Lattice I: The Ising model,” *J. Phys. A* **49** no. 35, (2016) 354001, [arXiv:1601.07185](https://arxiv.org/abs/1601.07185) [cond-mat.stat-mech].

[76] N. Tantivasadakarn, R. Thorngren, A. Vishwanath, and R. Verresen, “Long-Range Entanglement from Measuring Symmetry-Protected Topological Phases,” *Phys. Rev. X* **14** no. 2, (2024) 021040, [arXiv:2112.01519](https://arxiv.org/abs/2112.01519) [cond-mat.str-el].

[77] L. Li, M. Oshikawa, and Y. Zheng, “Noninvertible duality transformation between symmetry-protected topological and spontaneous symmetry breaking phases,” *Phys. Rev. B* **108** no. 21, (2023) 214429, [arXiv:2301.07899](https://arxiv.org/abs/2301.07899) [cond-mat.str-el].

[78] P. Gorantla, S.-H. Shao, and N. Tantivasadakarn, “Tensor Networks for Noninvertible Symmetries in 3+1D and Beyond,” *Phys. Rev. X* **15** no. 4, (2025) 041006, [arXiv:2406.12978](https://arxiv.org/abs/2406.12978) [quant-ph].

[79] W. Cao, L. Li, and M. Yamazaki, “Generating lattice non-invertible symmetries,” *SciPost Phys.* **17** no. 4, (2024) 104, [arXiv:2406.05454](https://arxiv.org/abs/2406.05454) [cond-mat.str-el].

[80] D. Tambara and S. Yamagami, “Tensor Categories with Fusion Rules of Self-Duality for Finite Abelian Groups,” *Journal of Algebra* **209** no. 2, (1998) 692 – 707.

[81] G. Schutz, “‘Duality twisted’ boundary conditions in n-state Potts models,” *J. Phys. A* **26** (1993) 4555–4564.

[82] U. Grimm and G. M. Schutz, “The Spin 1/2 XXZ Heisenberg chain, the quantum algebra $U(q)[sl(2)]$, and duality transformations for minimal models,” *J. Statist. Phys.* **71** (1993) 921–964, [arXiv:hep-th/0111083](https://arxiv.org/abs/hep-th/0111083).

[83] U. Grimm, “Spectrum of a duality twisted Ising quantum chain,” *J. Phys. A* **35** (2002) L25–L30, [arXiv:hep-th/0111157](https://arxiv.org/abs/hep-th/0111157).

[84] M. Oshikawa and I. Affleck, “Boundary conformal field theory approach to the critical two-dimensional Ising model with a defect line,” *Nucl. Phys. B* **495** (1997) 533–582, [arXiv:cond-mat/9612187](https://arxiv.org/abs/cond-mat/9612187).

[85] W. W. Ho, L. Cincio, H. Moradi, D. Gaiotto, and G. Vidal, “Edge-entanglement spectrum correspondence in a nonchiral topological phase and Kramers-Wannier duality,” *Phys. Rev. B* **91** no. 12, (2015) 125119, [arXiv:1411.6932](https://arxiv.org/abs/1411.6932) [cond-mat.str-el].

[86] M. Hauru, G. Evenbly, W. W. Ho, D. Gaiotto, and G. Vidal, “Topological conformal defects with tensor networks,” *Phys. Rev. B* **94** no. 11, (2016) 115125, [arXiv:1512.03846](https://arxiv.org/abs/1512.03846) [cond-mat.str-el].

[87] N. Tantivasadakarn, A. Vishwanath, and R. Verresen, “Hierarchy of Topological Order From Finite-Depth Unitaries, Measurement, and Feedforward,” *PRX Quantum* **4** no. 2, (2023) 020339, [arXiv:2209.06202](https://arxiv.org/abs/2209.06202) [quant-ph].

[88] A. Parayil Mana, Y. Li, H. Sukeno, and T.-C. Wei, “Kennedy-Tasaki transformation and noninvertible symmetry in lattice models beyond one dimension,” *Phys. Rev. B* **109** no. 24, (2024) 245129, [arXiv:2402.09520](https://arxiv.org/abs/2402.09520) [cond-mat.str-el].

[89] Y. Wang, Z. Hu, B. C. Sanders, and S. Kais, “Qudits and High-Dimensional Quantum Computing,” *Front. in Phys.* **8** (2020) 589504, [arXiv:2008.00959](https://arxiv.org/abs/2008.00959) [quant-ph].

[90] P. Etingof, D. Nikshych, and V. Ostrik, “Weakly group-theoretical and solvable fusion categories,” *Advances in Mathematics* **226** no. 1, (2011) 176–205, [arXiv:0809.3031](https://arxiv.org/abs/0809.3031) [math.QA].

[91] A. Chatterjee, S. D. Pace, and S.-H. Shao, “Quantized Axial Charge of Staggered Fermions and the Chiral Anomaly,” *Phys. Rev. Lett.* **134** no. 2, (2025) 021601, [arXiv:2409.12220](https://arxiv.org/abs/2409.12220) [hep-th].

[92] S. D. Pace, A. Chatterjee, and S.-H. Shao, “Lattice T-duality from non-invertible symmetries in

quantum spin chains,” [SciPost Phys. 18](#) no. 4, (2025) 121, [arXiv:2412.18606 \[cond-mat.str-el\]](#).